

**Terrain and climate effects mediate change in surface water across the western Canadian  
Arctic and Subarctic**  
by

Hana Travers-Smith

B.Sc. University of Victoria, 2019

A Thesis Submitted in Partial Fulfillment  
of the Requirements for the Degree of  
MASTER OF SCIENCE  
in the School of Environmental Studies

© Hana Travers-Smith, 2021  
University of Victoria

All rights reserved. This thesis may not be reproduced in whole or in part, by photocopy  
or other means, without the permission of the author.

## **Supervisory Committee**

Terrain and climate effects mediating change in surface water across the western Canadian  
Arctic and Subarctic

by

Hana Travers-Smith  
B.Sc., University of Victoria, 2019

### **Supervisory Committee**

Dr. Trevor C. Lantz, School of Environmental Studies  
**Supervisor**

Dr. Robert H. Fraser, Canada Centre for Remote Sensing  
**Committee Member**

## **Abstract**

### **Supervisory Committee**

Dr. Trevor C. Lantz, School of Environmental Studies  
**Supervisor**

Dr. Robert H. Fraser, Canada Centre for Remote Sensing  
**Committee Member**

Rising temperature and precipitation are driving widespread changes in the area of surface water across the Arctic and sub-Arctic. Previous work suggests that broad-scale increases in surface water area are occurring in the zone of continuous permafrost, while decreases are occurring in the zone of discontinuous permafrost. However, there are still uncertainties surrounding regional change and fine-scale terrain factors that may mediate the effects of temperature and precipitation. In my MSc research I examine terrain and climatic drivers of change in the area of lakes and ponds across the western Canadian Arctic and Sub-Arctic. In the first part of my thesis I use the Landsat satellite image archive to map change in lake area within the Lower Mackenzie Plain, NWT. I found that overall lake area has largely decreased since 1985, due to the drainage of large lakes. I also found that lakes located in fire scars were more likely to show persistent decreases in area, likely due to interactions with surrounding permafrost conditions. In the second part of my thesis, I used the Global Surface Water dataset developed by the GLAD research group to model changes in total permanent water across the Northwest Territories and the Yukon. I used a Random Forest model to analyze the effects of terrain and climate variables on the direction of change in permanent water. My observations show that surface water area has generally increased, and that the response of surface water to climate change largely depends on regional geology. Increases in permanent water were more likely to occur in wetter regions underlain by bedrock or fine-colluvium while decreases were more likely to occur in warmer

regions and areas underlain till blanket. I also used methods developed in the first part of my thesis to compare regional changes in surface water across six distinct study areas. I observed increases in surface water across five of the six study areas and consistent decreases in lake area associated with wildfire. This research shows that changes in surface water are complex and depend on interactions between climate variables and fine-scale terrain factors. My research also demonstrates the importance of wildfire in driving permafrost and lake dynamics.

## Table of Contents

Supervisory Committee .....	ii
Abstract .....	iii
Table of Contents .....	v
List of Tables .....	vii
List of Figures .....	viii
Acknowledgements.....	xi
1. Introduction.....	1
1.1 Study Rational .....	1
1.2 Critical Context .....	3
1.2.1 Climate change impacts in the Arctic.....	3
1.2.2 Northern lake geomorphology and lake drainage.....	5
1.2.3 Landsat based methods for surface water mapping.....	8
Bibliography .....	11
2. Surface water dynamics and rapid lake drainage in the Lower Mackenzie Plain, NWT .....	21
2.1 Introduction .....	22
2.2 Methods .....	24
2.2.1 Study Area .....	24
2.2.2 Climate Data .....	26
2.2.3 Landsat Image Processing .....	29
2.2.4 Changes in Lake Area.....	30
2.2.5 Climate Models and Terrain Factors .....	32
2.3 Results .....	33
2.3.1 Overall Change in Lake Area .....	33
2.3.2 Identifying Lake Drainage .....	34
2.3.3 Effect of Fire on Lake Area.....	35
2.3.4 Climate Models.....	39
2.3.5 Chi-Square .....	39
2.4 Discussion .....	41
Bibliography.....	44
Appendix 1: Sub-pixel water faction method .....	49

Appendix 2: Lake area trend classification.....	51
3. Drivers of surface water change across the western Canadian Arctic and Sub-Arctic.....	52
3.1 Introduction.....	53
3.2 Methods.....	55
3.2.1 Study Domain.....	55
3.2.2 Net Change in Surface Water.....	58
3.2.3 Regional Change in Surface Water.....	61
3.2.4 Landsat Processing.....	62
3.2.5 Mapping Trends in Lake Area.....	63
3.2.6 Rapid Lake Drainage and Wildfire.....	64
3.3 Results.....	65
3.3.1 Random Forests.....	65
3.3.2 Regional Lake Change.....	67
3.2.3 Rapid Drainage.....	70
3.4 Discussion.....	73
Bibliography.....	76
Appendix 3: Regional Study Areas.....	89
A. Tuktoyaktuk Coastal Plain.....	89
B. Lower Mackenzie Plain.....	89
C. Eagle Plains.....	89
D. Central Mackenzie Valley.....	90
E. Bulmer Plain.....	90
F. Great Slave Upland.....	90
Appendix 4: Change in permanent surface water.....	91
Appendix 5: Rapid Lake Drainage.....	92
4. Conclusion.....	93
4.1 Study Synthesis.....	93
4.2 Limitations and Future Research Opportunities.....	95
Bibliography.....	99

## List of Tables

Table 2.1 Percent of lakes in the study area belonging to classes assigned based on a Mann Kendall trend test to determine the direction of change (increasing, decreasing or non-trended) and a Generalized Additive Model to determine the nature of change (linear or non-linear). .....	34
Table 2.2 Parameter estimates from GAM models of total lake area as a function of month, lake size and May and July climate variables. Estimates of parametric coefficients represent the change in total lake area in km <sup>2</sup> per unit increase in each explanatory variable. The effect of acquisition month represents the mean difference in lake area between July and August acquisitions. The effective degrees of freedom (EDF) of the smooth term represents the number of knots in the smoothed parameter, where values close to 1 indicate that the parameter was modelled as a linear effect. Asterisks denote statistically significant results at the p<0.1 (*), p<0.05 (**) and p <0.01 (***) level. ....	40
Table 2.3 Standardized residuals from Chi-square tests comparing lake area trends and lake/terrain characteristics (ecoregion, fire presence, lake area and geology). Values with an asterisk (*) indicate a significant deviation from expected counts with positive values indicating more lakes than expected in that category and a negative values indicating fewer lakes than expected. ....	41
Table 3.1: Climate normals (1981-2010) across the study domain in the western Canadian arctic. Data is from ECCC and can be found at: <a href="https://climate.weather.gc.ca/climate_normals/index_e.html">https://climate.weather.gc.ca/climate_normals/index_e.html</a> .....	57
Table 3.2: Explanatory variables used in the Random Forests classifier to predict increasing and decreasing change in total permanent water within 10x10km grid cells. ....	60
Table 3.3: Summary table showing the physical parameters within the six regional study areas.	62
Table 3.4: Absolute and relative change in total lake area in each study area. Absolute change in area was calculated as the difference between total lake area in the first and last five years of the time series and relative change was calculated as absolute change divided by total area in the first time period. ....	69
Table 3.5: Proportion of lakes showing non-trended and significant increasing and decreasing patterns in each study area. ....	69
Table 3.6: The number of rapid drainage events per study site and the lake area losses associated with these events. The last column in the table shows the percent of the absolute change in lake area attributable to rapid drainage.....	71
Table 3.7: Standardized residuals from Chi-square tests comparing lake area trends and the presence of fire. Standardized residuals were calculated as: observed count – expected count / sqrt(expected count). Residuals with an asterisk (*) indicate a significant deviation (p<0.01) from expected counts with positive values indicating more lakes than expected in that category and negative values indicating fewer lakes than expected. ....	72

## List of Figures

Figure 2.1 Study area map of the Lower Mackenzie Plains, NWT. The black outline shows the extent of the study region. The brown shaded area shows the Arctic Red Plain ecoregion and the green shaded area represents the Travaillant Uplands ecoregion. The red outline shows the boundary of a 1999 fire scar. The inset map in the upper left shows the location of the study region within western Canada. ....	25
Figure 2.2 Maps showing surficial geology (A) and fire history (B) within the study area (black box in Figure 2.2). Surficial geology data is from Aylsworth et al., (2000) and fire history data is from the NWT Centre for Geomatics (2019). Dates show the timing of fires within the study region. Points in B represent lake centroids and the color of the points indicate whether lake area showed significant increasing or decreasing trends. ....	26
Figure 2.3 Theil-Sen trends of the deviation from (left) average seasonal temperatures (°C) between 1985 and 1990, and (right) total precipitation (mm). Data was recorded at the Fort McPherson airport and is available from ECCC at: <a href="https://climate.weather.gc.ca/historical_data/search_historic_data_e.html">https://climate.weather.gc.ca/historical_data/search_historic_data_e.html</a> .....	28
Figure 2.4 Number of spring and summer days with over 16mm of rain measured at the Fort McPherson airport between 1985 and 2014 (Environment Canada, 2020). ....	28
Figure 2.5 Change in lake area relative to average area between 1985 and 1990 by lake size (left) and total lake area (right). Data in the time series represents a 5-point moving average. Total lake area shows a decline of approximately 1%. ....	34
Figure 2.6 Large and medium sized lakes (>0.05km <sup>2</sup> ) showing rapid drainage. The left panel shows the time series of change in lake area relative to average area between 1985 and 1990. The black line shows 30% change for reference. Lakes B and C were both impacted by the 1999 fire and drained rapidly between 2000 and 2001. The right panel shows the drainage of lake B following a 1999 fire. Landsat imagery are displayed in false colour (SWIR1/NIR/Green) using images from the Landsat time series explorer. ....	35
Figure 2.7 Trends in lake area within the boundaries of a large fire that burned in 1999. Note the cluster of lakes with decreasing trends inside the extent of the 1999 fire. The extent of the fire within the entire study area is shown in Figure 2.1. ....	37
Figure 2.8 Boxplots comparing the median change in lake area relative to the average area between 1985 and 1990 for lakes within a fire scar, lakes up to 0.1-2km away from the fire and lakes 2-10km away the fire. The extent of the box shows the interquartile range and the whiskers show the 10 <sup>th</sup> and 90 <sup>th</sup> percentiles. Landsat imagery from 1999 was captured prior to the fire. The dashed vertical line shows the year after the fire. ....	38
Figure 2.9 Comparison of the frequency of breakpoints in the time series of lake area for lakes within a large burned area (top, n=836) and lakes within 10km of the fire scar (bottom, n=752). Note that no data was available for 1996, 1997 and 2008. The solid black line shows the year of the fire and the dashed horizontal line shows the average proportion of lakes with a breakpoint for all lakes in the study area. ....	38

Figure A.1: Relative error in lake area calculated as: $(Area_{SWF} - Area_{AF})/Area_{AF}$ . The x-axis is displayed on a logarithmic scale and the shaded area around the fitted line represents the 95% confidence interval for the slope parameter.....	50
Figure A.2: Example times series showing the categories used to classify changes in lake area depending on the direction of change and whether change over time was linear or non-linear. Plots A-C show different linear trends and plots D-F show different non-linear patterns. The blue line shows the fitted model using Ordinary Least Squares (OLS) regression for the linear class and a Generalized Additive Model (GAM) with a smooth term for time for the non-linear class. Note that the range of the y-axis varies among plots.....	51
Figure 3.1: Map of the study domain in the western Canadian Arctic showing the major ecozones and elevation from Arctic DEM (Porter et al., 2018). Study areas used to explore regional controls of surface water are shown with red boxes: A) Tuktoyaktuk Coastal Plain, B) Lower Mackenzie Plain, C) Eagle Plains, D) Central Mackenzie Valley, E) Bulmer Plain and F) Great Slave Upland. The inset map in the upper left shows the location of the study domain within Canada.....	57
Figure 3.2: Map of the study domain showing proportional change in total permanent water between 1999 and 2020 derived from the GLAD Global Surface Water Dataset (Pickens et al., 2020). Only cells with over 5km of total permanent water are shown. Study areas used to explore regional controls of surface water are shown with red boxes: A) Tuktoyaktuk Coastal Plain, B) Lower Mackenzie Plain, C) Eagle Plains, D) Central Mackenzie Valley, E) Bulmer Plain and F) Great Slave Upland. The dashed line shows the boundary between continuous and discontinuous permafrost (O'Neil, 2019) and the grey boxes show the extent of the fire boundaries shown in Figure 3.7.....	61
Figure 3.3: Variable importance plot from the Random Forests Model of lake-trend type (increasing, decreasing, stable). Unscaled variable importance shows the mean decrease in model accuracy if that variable is removed. ....	66
Figure 3.4: Partial dependence plots showing the probability of observing increasing surface water area as a function of the four most important independent variables in the random forests model: (A) precipitation, (B) temperature (C) ground ice content (ranked on a 5 point scale, with 5 representing high ice content) and (D) surficial geology. Negative probability values indicate that increases in area were less likely at that value of the independent variable. Note that the x-axis has been scaled to avoid plotting partial dependence at levels not characteristic of the study domain. Rug marks show the deciles of the precipitation and temperature data. The blue line in A and B shows the smoothed trend. ....	66
Figure 3.5: Partial dependence plots showing the probability of observing decreasing surface water area as a function of the four most important independent variables in the random forests model: (A) precipitation, (B) temperature and (C) ground ice content (ranked on a 5 point scale, with 5 representing high ice content) and (D) surficial geology. Negative probability values indicate that decreases in area were less likely at that value of the independent variable. Note that the x-axis has been scaled to avoid plotting partial dependence at levels not characteristic of the study domain. Rug marks show the deciles of the precipitation and temperature data. The blue line in A and B shows the smoothed trend. ....	67

Figure 3.6: Changes in lake area in the six study areas relative to the average area in the first time period ( $t_1$ ). The left panel of each plot shows the change in lake area grouped by lake size and the right panel shows change in total lake area across all lakes. Each point represents the average relative area for a rolling 5-point period and the shaded area represents a 95% confidence interval. ....	70
Figure 3.7: Lake area trends and fire history in A) Lower Mackenzie Plain, B) Bulmer Plain, C) Great Slave Upland and D) Central Mackenzie Valley study areas. Fire history data is from the NWT Centre for Geomatics (2019). Dates indicate the timing of each fire within the study area and points show lake centroids, with green points showing lakes with increasing trends in area and red points showing decreasing trends. The extent of the fires within each study area are shown in Figure 3.....	72
Figure 3.8: Boxplots showing change in the relative area of lakes within fire affected areas and outside fires (within 10km of fire boundaries) for the four study sites in forested study areas. The dashed red lines show the year the fire occurred. Note that the x-axis is not continuous because it does not show years with missing data. ....	73
Figure A.4: Histogram of net change in permanent surface water within 10x10km grid cells. Increasing and decreasing classes were defined using the median absolute percent change in surface water area. Thresholds for increasing and decreasing classes are shown as red dashed lines. ....	91
Figure A.5: Examples of annual lake area time series showing gradual drainage followed by expansion (ie bi-directional change shown in A and B) and rapid permanent drainage (C). The horizontal line shows a 30% decrease in lake area relative to average lake area between 1985 and 1990.....	92

## Acknowledgements

This work was made possible by financial support from the University of Victoria, the Natural Resources and Engineering Council of Canada, the W. Garfield Weston Foundation and the Northern Studies Training Program.

Thank you to the Environmental Studies cohort (“Cocoa” cohort) for the lunchtime frisbee and productive coffee break sessions! Special thanks to past and present members of the Arctic Landscape Ecology Lab (Angel Chen, Nicola Shipman, Jordan Seider, Zander Chila, Tait Overeem, Melody Fraser, Grant Francis, Mike Newton) for all your encouragement and snacks.

Many thanks to my committee member Rob Fraser for your excellent feedback and guidance.

Big thangs to Trevor Lantz for introducing me to the Arctic and for many hours of mentorship!

The majority of this thesis was written during the COVID-19 pandemic and I am forever grateful to my parents, Edward and Laurel, and my cats/office-mates Pickles and Tigger for their unwavering support and optimism.

# 1. Introduction

## 1.1 Study Rational

Across the circumpolar Arctic surface air temperatures are warming at twice the global average (ACIA, 2004; Serreze et al., 2009), and several lines of evidence show that these changes are accelerating the rate and extent of permafrost thaw (Biskaborn et al., 2019; Farquharson et al., 2019; Nitze et al., 2018). Permafrost underlies half of Canada's land surface and these changes impact infrastructure, surface hydrology, ground temperature and carbon storage (Grosse et al., 2013; Hinkel et al., 2003; Hjort et al., 2018; Jorgenson & Shur, 2007; Kokelj et al., 2009). The processes and landforms associated with the thawing of ice-rich permafrost are defined as thermokarst (French, 2007). Thermokarst processes produce a range of distinctive landforms, including thermokarst lakes, drained lake basins, retrogressive thaw slumps, ice-wedge polygons, and thermokarst bogs and fens (Kokelj & Jorgenson, 2013). Studies across the circumpolar show that climate warming is accelerating the rate of thermokarst development, resulting in increasing thaw slump activity (Kokelj et al., 2017; Segal et al., 2016), ice-wedge melt (Fraser et al., 2018; Steedman et al., 2017), expanding thermokarst bogs and fens (Haynes et al., 2019; Osterkamp et al., 2000) and widespread changes in lakes (Jones et al., 2020; Lantz & Turner, 2015; Nitze et al., 2017, 2020; Olthof et al., 2015; Roach et al., 2013; Swanson, 2019). Long-term monitoring of these landforms is important to understanding the magnitude and extent of change to permafrost landscapes.

Changes in the number and area of thermokarst lakes are among the most widespread impacts of shifting permafrost conditions (Kokelj & Jorgenson., 2013). Lakes are common in low-lying

areas underlain by fine-grained and ice-rich sediments. In ice-rich permafrost, lakes can expand gradually into surrounding permafrost as a result of thermal and mechanical erosion, however continued thaw can also lead to bank overtopping or the formation of a drainage outlet, resulting in rapid permanent lake drainage (Jones & Arp, 2015; Jorgenson & Shur, 2007; Mackay, 1988). Monitoring trends in lake expansion and drainage is important because lake area can exceed 40% of land cover, representing a significant contribution to the climate and carbon cycles (Grosse et al., 2013; Hinkel et al., 2003; Schuur et al., 2015; Tarnocai et al., 2009). At a regional scale, lakes also provide a source of freshwater and are habitat for a range of culturally and ecologically significant species including beavers, lake fish and muskrats (Greenland & Walker-Larsen, 2001; Tape et al., 2018; Turner et al., 2018).

The objectives of my MSc research are to characterize lake dynamics across the western Canadian Arctic and Subarctic and identify environmental and climatic factors driving lake expansion and drainage. To accomplish this, I completed the two distinct but complimentary research projects presented in Chapters 2 and 3 of this thesis. In Chapter 2, I investigated regional drivers of change in the Lower Mackenzie Plains by using Generalized Additive Models to explore the relationship between climate variables and interannual lake area, and Chi-Square tests to identify terrain and lake factors associated with change. In Chapter 3, I used the methods developed in Chapter 2 to compare the regional drivers of change at six sites across the Arctic and Boreal regions of the NWT and Yukon. I also used Random Forests models to investigate broad-scale terrain and climate factors associated with net increases and decreases in surface water area across the Northwest Territories and Yukon. In the remainder of this chapter I provide background on several topics that are not detailed in the introduction of the individual data chapters.

## 1.2 Critical Context

### 1.2.1 Climate change impacts in the Arctic

Over the past century anthropogenic greenhouse gas emissions have driven unprecedented changes in the global climate system (IPCC, 2014). Changes in temperature and precipitation are having profound impacts on both human and natural systems around the world (IPCC, 2014). In particular, the Arctic has experienced climate warming at twice the rate of lower latitudes (Cohen et al., 2014; Serreze et al., 2009). This phenomenon, known as Arctic amplification, results from the increased absorption of solar energy associated with declines in snow and ice cover, and global circulation patterns that transfer warm air from southern latitudes (Graversen et al., 2008; Serreze et al., 2009). While rising air temperatures have been reported in all seasons, warming has been most pronounced in the winter months (Box et al., 2019; Hinzman et al., 2005). In Alaska and Canada, winter temperatures have increased by approximately 3-4°C in the past 50 years (ACIA, 2004). In parallel with warming temperatures, several lines of evidence show that precipitation in the Arctic is also increasing (Box et al., 2019; Hinzman et al., 2005). Between 1970 and 2017 Box et al. (2019) reported a 6.8% increase in precipitation during the cold season (October to May) and a 4.7% increase in the warm season (June to September). Shifts in temperature and precipitation are driving a range of ecological changes in marine and terrestrial environments (ACIA, 2004).

Permafrost thaw is one of the most widespread terrestrial impacts of climate change at high latitudes (ACIA, 2004). Permafrost covers approximately one quarter of the Northern Hemisphere and is broadly defined as ground that remains below 0°C for at least two years (French, 2007). Rising air temperatures and increased precipitation across the Arctic are

expected to drive substantial thaw of permafrost over the next century (Chadburn et al., 2017; Slater & Lawrence, 2013). Chadburn et al. (2017) estimate that 40% of global permafrost area could be lost if the climate warms to 2°C above pre-industrial levels. This is particularly concerning because permafrost thaw may release large amounts of carbon to the atmosphere (Schuur et al., 2015; Tarnocai et al., 2009). Northern soils contain approximately 1672Pg of organic carbon, representing 50% of global soil carbon storage (Tarnocai et al., 2009). Following permafrost thaw, previously frozen organic material can decompose into carbon dioxide and methane, potentially amplifying ongoing climate warming (Schuur et al., 2015; Tarnocai et al., 2009). Recent modeling suggests that the permafrost-carbon feedback could contribute to temperature increases of 0.13-0.27°C by 2100 (Schuur et al., 2015).

In addition to acting as a positive feedback to climate warming, permafrost thaw also has a significant impact on regional infrastructure and livelihoods. Hjort et al. (2018) estimate that 4 million people currently live in areas at high risk of permafrost thaw. Ground subsidence and slumping can damage critical infrastructure in northern communities including roads, buildings, water supplies and sanitation pipelines (French, 1975; Hjort et al., 2018). Permafrost thaw also destabilizes soil slopes, increasing the frequency of hazardous thaw slumps and permafrost slope failures (ACIA, 2004). Loss of permafrost also has significant implications for surface hydrology and freshwater resources (Jorgenson et al., 2010; Osterkamp et al., 2000; Schuur & Mack, 2018). Slumping along the margins of lakes and streams can lead to increased sediment load and decreased water quality (Kokelj et al., 2009). In some regions, increased connectivity to groundwater and a thicker active layer can also drive drying in shallow streams, ponds and wetlands (Roach et al., 2013; Woo & Guan, 2006). Changes in water levels and flow regimes can reduce access to important fishing and trapping areas (Medeiros et al., 2017). For example, the

Qairngirmiut in Nunavut describe how drying streams have blocked routes to traditional caribou hunting grounds (Medeiros et al., 2017), and Gwich'in communities in the Northwest Territories report permafrost thaw and landslides as a significant concern in accessing fish (Gwich'in Tribal Council Department of Cultural Heritage et al., 2020).

### **1.2.2 Northern lake geomorphology and lake drainage**

Lakes and ponds are ubiquitous at high latitudes and approximately 25% of all lakes are located at high latitudes (Lehner & Döll, 2004). The abundance and distribution of northern lakes depends on a range of terrain factors including surficial geology, landscape position, glacial history, permafrost distribution and ground ice content (French, 2007; Grosse et al., 2013; Olefeldt et al., 2016; Smith et al., 2007). At a continental scale, lake density is greatest in regions that have been previously glaciated, and decreases sharply in the absence of permafrost (Smith et al., 2007). Many lakes in the Canadian Arctic including Great Slave Lake and Great Bear Lake formed after the retreat of the Laurentide ice sheet during the Pleistocene-Holocene transition beginning approximately 18,000 years ago (Rampton, 1987; Wolfe et al., 2017). Permafrost is an especially important control on lake distribution as it limits the connectivity between lakes and groundwater, and facilitates lake expansion and drainage through thermokarst processes (Roach et al., 2013). Permafrost thaw throughout the Holocene also resulted in the formation of thousands of smaller lakes and ponds (Rampton, 1987).

Thermokarst lakes are broadly defined as lakes that form as a result of ground-ice degradation and the accumulation of water in thaw depressions (Hopkins & Karlstrom, 1955). They are abundant in low-lying regions underlain by fine-grained, ice-rich sediments, but can also form in poorly consolidated bedrock with high ground ice content (French, 2007). It is worth noting that

not all northern lakes are thermokarst in origin; lakes can also form in the absence of thaw subsidence when water accumulates in low-lying regions (Jorgenson & Shur, 2007). Jorgenson and Shur (2007) propose a model of lake formation and development involving six stages: 1) lake formation via flooding of surface depressions, 2) basin expansion through thermal and mechanical erosion of surrounding permafrost, 3) lake drainage, 4) ice aggradation in the drained basin, 5) infilling and the formation of secondary thaw lakes in the drained basin and, 6) basin stabilization. They suggest that drained basins and secondary thaw lakes form permanent topographic features, unlike previous models which assumed that ice aggradation and heave following lake drainage eventually returned the landscape to original conditions (Billings & Peterson, 1980; Hopkins, 1949).

The hydrology of northern lakes is primarily controlled by inputs from snowmelt and rainfall, and water losses through evaporation (Marsh & Bigras, 1988; Pohl et al., 2007, 2009; Woo & Guan, 2006). Unlike lakes at lower latitudes, water fluxes in northern lakes are limited to the short spring and summer seasons. The presence of permafrost can also limit interactions between lakes and ground water storage (Woo & Guan, 2006). Hydrologic dynamics in northern lakes are predicted to change with ongoing climate warming. Projected increases in temperature and precipitation suggest that spring snowmelt will occur earlier in the year, and water losses in the spring and summer could also increase due to increased evaporation and a deeper active layer (Pohl et al., 2007; Woo & Guan, 2006). Several recent remote sensing studies have also linked changes in lake area to changes in climate conditions (Campbell et al., 2018; Lantz & Turner, 2015; Plug et al., 2008; Smol & Douglas, 2007; Swanson, 2019). In the high-Arctic rising air temperatures have been associated with evaporative drying in small ponds (Campbell et al.,

2018; Smol & Douglas, 2007). In other regions, interannual variability in lake area has been associated with shifts in precipitation (Lantz & Turner, 2015; Plug et al., 2008; Swanson, 2019).

Winter conditions and the formation of lake ice are also important factors in lake development. The maximum ice thickness in northern lakes ranges from 1-2m (Jeffries et al., 1994) and lake depth largely determines whether a lake will completely freeze to the lake bed, or retain liquid water beneath a layer of ice (Weeks et al., 1981; Weeks & Sellman, 1977). The presence of liquid water throughout the winter has a significant effect on ground temperatures and the stability of surrounding permafrost (Ling & Zhang, 2003). Data from Burn (2005) show that winter lake bottom temperatures can range from  $-2^{\circ}\text{C}$  beneath the shallow lake shores and up to  $3^{\circ}\text{C}$  beneath the deeper central pool. Lakes that don't freeze to the bottom can develop taliks (an unfrozen pocket within the surrounding permafrost), which impacts surrounding permafrost temperatures (Burn, 2002, 2005).

Lake expansion and drainage in ice-rich sediments is particularly important because these processes can indicate underlying permafrost degradation (Kokelj & Jorgenson, 2013). Lakes can expand laterally via thermal and mechanical erosion at rates between  $0.3\text{-}0.8\text{m yr}^{-1}$  (Grosse et al., 2013). Partial or complete drainage can follow lake expansion if the lake encounters a drainage pathway such as an adjacent ice-wedge network, river or another lake (Mackay, 1988; Marsh & Neumann, 2001). Lake drainage can also occur after intense precipitation or snowmelt, as increased water levels can lead to the formation of outlet channels through bank overtopping or erosion (Jones & Arp, 2015; Pohl et al., 2009). Marsh and Neumann (2001) also describe how cold winter temperatures can create cracks along ice-wedges and provide pathways for lake drainage in the ice-free season. Complete lake drainage through the formation of an outlet channel can occur rapidly within hours or days (Jones & Arp, 2015; Mackay, 1981), and due to

the intensity of these drainage events, they are commonly referred to as ‘catastrophic’ (Hinkel et al., 2007; Jones & Arp, 2015; Lantz & Turner, 2015; Mackay, 1981, 1988). Drained lake basins can occupy a significant portion of the land surface, sometimes exceeding the area of existing lakes (Grosse et al., 2013; Hinkel et al., 2003). Annual rates of catastrophic lake drainage vary spatially and temporally (Jones et al., 2020; Lantz & Turner, 2015; Nitze et al., 2020). Lantz and Turner (2015) reported an increase in the rate of catastrophic lake drainage events in the Old Crow Flats, Yukon, while Jones et al. (2020) reported a decreases in drainage rates in the Arctic Coastal Plain of Alaska. Compared to previous estimates, the rate of lake drainage increased by a factor of 10 in northwestern Alaska, following a particularly warm and wet winter in 2017/2018 (Nitze et al., 2020). Monitoring the rate of lake drainage is important because drained lake basins impact vegetation coverage and wildlife habitat (Cooley et al., 2020; Lantz, 2017), carbon storage (Hinkel et al., 2003) and permafrost development (Mackay & Burn, 2002). Long-term monitoring of northern lakes is important because the trajectory of change will impact a range of ecological functions at varying spatial scales (Hinkel et al., 2003; Lantz, 2017; Roach et al., 2013; Roach & Griffith, 2015).

### **1.2.3 Landsat based methods for surface water mapping**

Satellite remote sensing methods can be used to monitor a range of landscape features in northern regions, including changes in snow characteristics, thaw subsidence, vegetation distribution, wildfire and surface water dynamics (Jorgenson & Grosse, 2016). The emergence of open access data and powerful image processing tools such as Google Earth Engine, has facilitated large-scale analyses of geospatial data (Gorelick et al., 2017). A range of earth observation systems provide data at different spatial and temporal resolutions, spectral characteristics and wavelength combinations. One of the most commonly used datasets is the

Landsat satellite image archive, created and maintained by the United States Geological Survey (USGS) and the National Aeronautics and Space Administration (NASA) (Wulder et al., 2012).

The Landsat series of satellite missions has been operational since 1972, and the entire image archive was made freely available to the public in 2008 (Wulder et al., 2012). The 30m pixel resolution, 16-day revisit time and relatively long mission duration (1972 to present) are well suited for long-term environmental monitoring (Wulder et al., 2012). In this project, I used the Landsat image archive to map changes in the area of lakes and ponds.

The spectral characteristics of shortwave infrared (SWIR) are particularly useful in separating land and water (Frazier & Page, 2000; Roach et al., 2012). Water strongly absorbs SWIR energy, thus reflectance measured by the satellite sensor from open water is low compared to dry land.

The Landsat SWIR-1 band (1.57-1.65 $\mu$ m) is sensitive to variation in soil and vegetation moisture content and has been used in several studies to map the extent of northern water bodies (Campbell et al., 2018; Olthof et al., 2015; Roach et al., 2012, 2013; Swanson, 2019). Roach et al. (2012) show that a simple threshold in SWIR reflectance is effective in classifying land and water pixels in a boreal environment. However, Landsat pixels are 900m<sup>2</sup> (30x30m) and may contain a combination of land and water. Olthof et al. (2015) show that binary land and water classifications tends to overestimate water area, because pixels classified as water along lake margins often contain both water and land. To capture the contribution of mixed pixels Olthof et al. (2015) proposed the histogram breakpoint method, which can be used to estimate the fraction of a pixel covered by water.

Other Landsat-based methods to map surface water use multiple bands and other remote sensing indices. For example, the Normalized Difference Water Index (NDWI) uses the SWIR-1 and near-infrared (NIR) bands to measure moisture content in vegetation and soil (Gao, 1996).

Several studies have used NDWI in combination with the Normalized Difference Vegetation Index (NDVI), the Normalized Difference Moisture Index (NDMI), Tasseled Cap transformations, and individual Landsat bands to classify surface water (Carroll & Loboda, 2017; Lindgren et al., 2021; Nitze et al., 2017; Plug et al., 2008). Multi-variate approaches that combine information from indices and individual bands into a classification algorithm have also been used to distinguish different land cover classes. For example, Nitze et al. (2017) used per-pixel trends in a range of multi-spectral indices to train a Random Forests classifier to identify stable water, stable land and transitions between the two classes.

In Chapters 2 and 3, I use the histogram breakpoint method developed by Olthof et al. (2015) to map the area of lakes and ponds. This method was selected because it was previously validated for a tundra environment and was shown to best represent fractional water cover within a Landsat pixel (Olthof et al., 2015). Furthermore, it provides a direct estimate of water area, where spectral indices such as NDWI and NDMI provide a measure of “wetness”, but do not translate directly to water area. Regardless of the method used, the Landsat satellite archive provides one of the most accessible datasets for examining long-term trends in surface water across regional or global scales (Pekel et al., 2016; Pickens et al., 2020).

## Bibliography

- ACIA. (2004). *Impacts of a Warming Arctic: Arctic Climate Impact Assessment*. Cambridge University Press.
- Billings, W. D., & Peterson, K. M. (1980). Vegetational change and ice-wedge polygons through the thaw lake cycle in Arctic Alaska. *Arctic and Alpine Research*, *12*, 413–432.
- Biskaborn, B. K., Smith, S. L., Noetzli, J., Matthes, H., Vieira, G., Streletskiy, D. A., Schoeneich, P., Romanovsky, V. E., Lewkowicz, A. G., Abramov, A., Allard, M., Boike, J., Cable, W. L., Christiansen, H. H., Delaloye, R., Diekmann, B., Drozdov, D., Etzelmüller, B., Grosse, G., ... Lantuit, H. (2019). Permafrost is warming at a global scale. *Nature Communications*, *10*(1), 1–11. <https://doi.org/10.1038/s41467-018-08240-4>
- Box, J. E., Colgan, W. T., Christensen, T. R., Schmidt, N. M., Lund, M., Parmentier, F.-J. W., Brown, R., Bhatt, U. S., Euskirchen, E. S., Romanovsky, V. E., Walsh, J. E., Overland, J. E., Wang, M., Corell, R. W., Meier, W. N., Wouters, B., Mernild, S., Mård, J., Pawlak, J., & Olsen, M. S. (2019). Key indicators of Arctic climate change: 1971–2017. *Environmental Research Letters*, *14*(4), 045010. <https://doi.org/10.1088/1748-9326/aafc1b>
- Burn, C. R. (2002). Tundra lakes and permafrost, Richards Island, western Arctic coast, Canada. *Journal of Earth Sciences*, *39*, 1281–1298.
- Burn, C. R. (2005). Lake-bottom thermal regimes, western Arctic coast, Canada. *Permafrost and Periglacial Processes*, *16*(4), 355–367. <https://doi.org/10.1002/ppp.542>
- Campbell, T. K. F., Lantz, T. C., & Fraser, R. H. (2018). Impacts of Climate Change and Intensive Lesser Snow Goose (*Chen caerulescens caerulescens*) Activity on Surface Water in High Arctic Pond Complexes. *Remote Sensing*, *10*(12), 1892. <https://doi.org/10.3390/rs10121892>
- Carroll, M. L., & Loboda, T. V. (2017). Multi-Decadal Surface Water Dynamics in North American Tundra. *Remote Sensing*, *9*(5), 497. <https://doi.org/10.3390/rs9050497>
- Chadburn, S. E., Burke, E. J., Cox, P. M., Friedlingstein, P., Hugelius, G., & Westermann, S. (2017). An observation-based constraint on permafrost loss as a function of global warming. *Nature Climate Change*, *7*(5), 340–344. <https://doi.org/10.1038/nclimate3262>
- Cohen, J., Screen, J. A., Furtado, J. C., Barlow, M., Whittleston, D., Coumou, D., Francis, J., Dethloff, K., Entekhabi, D., Overland, J., & Jones, J. (2014). Recent Arctic amplification and extreme mid-latitude weather. *Nature Geoscience*, *7*(9), 627–637. <https://doi.org/10.1038/ngeo2234>
- Cooley, D., Clarke, H., Graupe, S., Landry-Cuerrier, M., Lantz, T., Milligan, H., Pretzlaw, T., Larocque, G., & Humphries, M. M. (2020). THE SEASONALITY OF A MIGRATORY MOOSE POPULATION IN NORTHERN YUKON. *Alces: A Journal Devoted to the Biology and Management of Moose*, *55*(0), 105–130.

- Farquharson, L. M., Romanovsky, V. E., Cable, W. L., Walker, D. A., Kokelj, S. V., & Nicolsky, D. (2019). Climate Change Drives Widespread and Rapid Thermokarst Development in Very Cold Permafrost in the Canadian High Arctic. *Geophysical Research Letters*, *46*(12), 6681–6689. <https://doi.org/10.1029/2019GL082187>
- Fraser, R., Kokelj, S., Lantz, T., McFarlane-Winchester, M., Olthof, I., & Lacelle, D. (2018). Climate Sensitivity of High Arctic Permafrost Terrain Demonstrated by Widespread Ice-Wedge Thermokarst on Banks Island. *Remote Sensing*, *10*(6), 954. <https://doi.org/10.3390/rs10060954>
- Frazier, P. S., & Page, K. J. (2000). Water Body Detection and Delineation with Landsat TM Data. *PHOTOGRAMMETRIC ENGINEERING*, *7*.
- French, H. M. (1975). Man-Induced Thermokarst, Sachs Harbour Airstrip, Banks Island, Northwest Territories. *Canadian Journal of Earth Sciences*, *12*(2), 132–144. <https://doi.org/10.1139/e75-014>
- French, H. M. (2007). *The Periglacial Environment* (3rd ed.). John Wiley & Sons, Ltd.
- Gao, B. (1996). NDWI—A normalized difference water index for remote sensing of vegetation liquid water from space. *Remote Sensing of Environment*, *58*(3), 257–266. [https://doi.org/10.1016/S0034-4257\(96\)00067-3](https://doi.org/10.1016/S0034-4257(96)00067-3)
- Gorelick, N., Hancher, M., Dixon, M., Ilyushchenko, S., Thau, D., & Moore, R. (2017). Google Earth Engine: Planetary-scale geospatial analysis for everyone. *Remote Sensing of Environment*, *202*, 18–27. <https://doi.org/10.1016/j.rse.2017.06.031>
- Graversen, R. G., Mauritsen, T., Tjernström, M., Källén, E., & Svensson, G. (2008). Vertical structure of recent Arctic warming. *Nature*, *451*(7174), 53–56. <https://doi.org/10.1038/nature06502>
- Greenland, B., J., & Walker-Larsen, J. (2001). *Community Concerns and Knowledge about Broad Whitefish (Coregonus nasus) in the Gwich'in Settlement Area* (No. 01–08). Gwich'in Renewable Resource Board.
- Grosse, G., Jones, B. M., & Arp, C. D. (2013). Thermokarst lakes, drainage, and drained basins. In J. F. Shroder (Ed.), *Treatise on Geomorphology*. 8. (pp. 325–353). Academic Press, San Diego, CA. <https://doi.org/10.1016/B978-0-12-374739-6.00216-5>
- Gwich'in Tribal Council Department of Cultural Heritage, Proverbs, T. A., Lantz, T. C., Lord, S. I., Amos, A., & Ban, N. C. (2020). Social-Ecological Determinants of Access to Fish and Well-Being in Four Gwich'in Communities in Canada's Northwest Territories. *Human Ecology*, *48*(2), 155–171. <https://doi.org/10.1007/s10745-020-00131-x>
- Haynes, K. M., Connon, R. F., & Quinton, W. L. (2019). Hydrometeorological measurements in peatland-dominated, discontinuous permafrost at Scotty Creek, Northwest Territories, Canada. *Geoscience Data Journal*, *6*(2), 85–96. <https://doi.org/10.1002/gdj3.69>
- Hinkel, K. M., Eisner, W. R., Bockheim, J. G., Nelson, F. E., Peterson, K. M., & Dai, X. (2003). Spatial Extent, Age, and Carbon Stocks in Drained Thaw Lake Basins on the Barrow Peninsula,

Alaska. *Arctic, Antarctic, and Alpine Research*, 35(3), 291–300. [https://doi.org/10.1657/1523-0430\(2003\)035\[0291:SEAACS\]2.0.CO;2](https://doi.org/10.1657/1523-0430(2003)035[0291:SEAACS]2.0.CO;2)

Hinkel, K. M., Jones, B. M., Eisner, W. R., Cuomo, C. J., Beck, R. A., & Frohn, R. (2007). Methods to assess natural and anthropogenic thaw lake drainage on the western Arctic coastal plain of northern Alaska. *Journal of Geophysical Research: Earth Surface*, 112(F2). <https://doi.org/10.1029/2006JF000584>

Hinzman, L. D., Bettez, N. D., Bolton, W. R., Chapin, F. S., Dyurgerov, M. B., Fastie, C. L., Griffith, B., Hollister, R. D., Hope, A., Huntington, H. P., Jensen, A. M., Jia, G. J., Jorgenson, T., Kane, D. L., Klein, D. R., Kofinas, G., Lynch, A. H., Lloyd, A. H., McGuire, A. D., ... Yoshikawa, K. (2005). Evidence and Implications of Recent Climate Change in Northern Alaska and Other Arctic Regions. *Climatic Change*, 72(3), 251–298. <https://doi.org/10.1007/s10584-005-5352-2>

Hjort, J., Karjalainen, O., Aalto, J., Westermann, S., Romanovsky, V. E., Nelson, F. E., Eitzelmüller, B., & Luoto, M. (2018). Degrading permafrost puts Arctic infrastructure at risk by mid-century. *Nature Communications*, 9(1), 5147. <https://doi.org/10.1038/s41467-018-07557-4>

Hopkins, D. M. (1949). Thaw Lakes and Thaw Sinks in the Imuruk Lake Area, Seward Peninsula, Alaska. *The Journal of Geology*, 57(2), 119–131. <https://doi.org/10.1086/625591>

Hopkins, D. M., & Karlstrom, T. N. V. (1955). *Permafrost and Ground Water in Alaska*. 69.

IPCC. (2014). *Climate Change 2014: Synthesis Report. Contribution of Working Groups I, II and III to the Fifth Assessment Report of the Intergovernmental Panel on Climate Change* (p. 151 pp). IPCC.

ACIA. (2004). *Impacts of a Warming Arctic: Arctic Climate Impact Assessment*. Cambridge University Press.

Billings, W. D., & Peterson, K. M. (1980). Vegetational change and ice-wedge polygons through the thaw lake cycle in Arctic Alaska. *Arctic and Alpine Research*, 12, 413–432.

Biskaborn, B. K., Smith, S. L., Noetzli, J., Matthes, H., Vieira, G., Streletskiy, D. A., Schoeneich, P., Romanovsky, V. E., Lewkowicz, A. G., Abramov, A., Allard, M., Boike, J., Cable, W. L., Christiansen, H. H., Delaloye, R., Diekmann, B., Drozdov, D., Eitzelmüller, B., Grosse, G., ... Lantuit, H. (2019). Permafrost is warming at a global scale. *Nature Communications*, 10(1), 1–11. <https://doi.org/10.1038/s41467-018-08240-4>

Box, J. E., Colgan, W. T., Christensen, T. R., Schmidt, N. M., Lund, M., Parmentier, F.-J. W., Brown, R., Bhatt, U. S., Euskirchen, E. S., Romanovsky, V. E., Walsh, J. E., Overland, J. E., Wang, M., Corell, R. W., Meier, W. N., Wouters, B., Mernild, S., Mård, J., Pawlak, J., & Olsen, M. S. (2019). Key indicators of Arctic climate change: 1971–2017. *Environmental Research Letters*, 14(4), 045010. <https://doi.org/10.1088/1748-9326/aafc1b>

Burn, C. R. (2002). Tundra lakes and permafrost, Richards Island, western Arctic coast, Canada. *Journal of Earth Sciences*, 39, 1281–1298.

- Burn, C. R. (2005). Lake-bottom thermal regimes, western Arctic coast, Canada. *Permafrost and Periglacial Processes*, 16(4), 355–367. <https://doi.org/10.1002/ppp.542>
- Campbell, T. K. F., Lantz, T. C., & Fraser, R. H. (2018). Impacts of Climate Change and Intensive Lesser Snow Goose (*Chen caerulescens caerulescens*) Activity on Surface Water in High Arctic Pond Complexes. *Remote Sensing*, 10(12), 1892. <https://doi.org/10.3390/rs10121892>
- Carroll, M. L., & Loboda, T. V. (2017). Multi-Decadal Surface Water Dynamics in North American Tundra. *Remote Sensing*, 9(5), 497. <https://doi.org/10.3390/rs9050497>
- Chadburn, S. E., Burke, E. J., Cox, P. M., Friedlingstein, P., Hugelius, G., & Westermann, S. (2017). An observation-based constraint on permafrost loss as a function of global warming. *Nature Climate Change*, 7(5), 340–344. <https://doi.org/10.1038/nclimate3262>
- Cohen, J., Screen, J. A., Furtado, J. C., Barlow, M., Whittleston, D., Coumou, D., Francis, J., Dethloff, K., Entekhabi, D., Overland, J., & Jones, J. (2014). Recent Arctic amplification and extreme mid-latitude weather. *Nature Geoscience*, 7(9), 627–637. <https://doi.org/10.1038/ngeo2234>
- Cooley, D., Clarke, H., Graupe, S., Landry-Cuerrier, M., Lantz, T., Milligan, H., Pretzlaw, T., Larocque, G., & Humphries, M. M. (2020). THE SEASONALITY OF A MIGRATORY MOOSE POPULATION IN NORTHERN YUKON. *Alces: A Journal Devoted to the Biology and Management of Moose*, 55(0), 105–130.
- Farquharson, L. M., Romanovsky, V. E., Cable, W. L., Walker, D. A., Kokelj, S. V., & Nicolsky, D. (2019). Climate Change Drives Widespread and Rapid Thermokarst Development in Very Cold Permafrost in the Canadian High Arctic. *Geophysical Research Letters*, 46(12), 6681–6689. <https://doi.org/10.1029/2019GL082187>
- Fraser, R., Kokelj, S., Lantz, T., McFarlane-Winchester, M., Olthof, I., & Lacelle, D. (2018). Climate Sensitivity of High Arctic Permafrost Terrain Demonstrated by Widespread Ice-Wedge Thermokarst on Banks Island. *Remote Sensing*, 10(6), 954. <https://doi.org/10.3390/rs10060954>
- Frazier, P. S., & Page, K. J. (2000). Water Body Detection and Delineation with Landsat TM Data. *PHOTOGRAMMETRIC ENGINEERING*, 7.
- French, H. M. (1975). Man-Induced Thermokarst, Sachs Harbour Airstrip, Banks Island, Northwest Territories. *Canadian Journal of Earth Sciences*, 12(2), 132–144. <https://doi.org/10.1139/e75-014>
- French, H. M. (2007). *The Periglacial Environment* (3rd ed.). John Wiley & Sons, Ltd.
- Gao, B. (1996). NDWI—A normalized difference water index for remote sensing of vegetation liquid water from space. *Remote Sensing of Environment*, 58(3), 257–266. [https://doi.org/10.1016/S0034-4257\(96\)00067-3](https://doi.org/10.1016/S0034-4257(96)00067-3)
- Gorelick, N., Hancher, M., Dixon, M., Ilyushchenko, S., Thau, D., & Moore, R. (2017). Google Earth Engine: Planetary-scale geospatial analysis for everyone. *Remote Sensing of Environment*, 202, 18–27. <https://doi.org/10.1016/j.rse.2017.06.031>

- Graversen, R. G., Mauritsen, T., Tjernström, M., Källén, E., & Svensson, G. (2008). Vertical structure of recent Arctic warming. *Nature*, *451*(7174), 53–56. <https://doi.org/10.1038/nature06502>
- Greenland, B. J., & Walker-Larsen, J. (2001). *Community Concerns and Knowledge about Broad Whitefish (Coregonus nasus) in the Gwich'in Settlement Area* (No. 01–08). Gwich'in Renewable Resource Board.
- Grosse, G., Jones, B. M., & Arp, C. D. (2013). Thermokarst lakes, drainage, and drained basins. In J. F. Shroder (Ed.), *Treatise on Geomorphology*. 8. (pp. 325–353). Academic Press, San Diego, CA. <https://doi.org/10.1016/B978-0-12-374739-6.00216-5>
- Gwich'in Tribal Council Department of Cultural Heritage, Proverbs, T. A., Lantz, T. C., Lord, S. I., Amos, A., & Ban, N. C. (2020). Social-Ecological Determinants of Access to Fish and Well-Being in Four Gwich'in Communities in Canada's Northwest Territories. *Human Ecology*, *48*(2), 155–171. <https://doi.org/10.1007/s10745-020-00131-x>
- Haynes, K. M., Connon, R. F., & Quinton, W. L. (2019). Hydrometeorological measurements in peatland-dominated, discontinuous permafrost at Scotty Creek, Northwest Territories, Canada. *Geoscience Data Journal*, *6*(2), 85–96. <https://doi.org/10.1002/gdj3.69>
- Hinkel, K. M., Eisner, W. R., Bockheim, J. G., Nelson, F. E., Peterson, K. M., & Dai, X. (2003). Spatial Extent, Age, and Carbon Stocks in Drained Thaw Lake Basins on the Barrow Peninsula, Alaska. *Arctic, Antarctic, and Alpine Research*, *35*(3), 291–300. [https://doi.org/10.1657/1523-0430\(2003\)035\[0291:SEAACS\]2.0.CO;2](https://doi.org/10.1657/1523-0430(2003)035[0291:SEAACS]2.0.CO;2)
- Hinkel, K. M., Jones, B. M., Eisner, W. R., Cuomo, C. J., Beck, R. A., & Frohn, R. (2007). Methods to assess natural and anthropogenic thaw lake drainage on the western Arctic coastal plain of northern Alaska. *Journal of Geophysical Research: Earth Surface*, *112*(F2). <https://doi.org/10.1029/2006JF000584>
- Hinzman, L. D., Bettez, N. D., Bolton, W. R., Chapin, F. S., Dyurgerov, M. B., Fastie, C. L., Griffith, B., Hollister, R. D., Hope, A., Huntington, H. P., Jensen, A. M., Jia, G. J., Jorgenson, T., Kane, D. L., Klein, D. R., Kofinas, G., Lynch, A. H., Lloyd, A. H., McGuire, A. D., ... Yoshikawa, K. (2005). Evidence and Implications of Recent Climate Change in Northern Alaska and Other Arctic Regions. *Climatic Change*, *72*(3), 251–298. <https://doi.org/10.1007/s10584-005-5352-2>
- Hjort, J., Karjalainen, O., Aalto, J., Westermann, S., Romanovsky, V. E., Nelson, F. E., Etzelmüller, B., & Luoto, M. (2018). Degrading permafrost puts Arctic infrastructure at risk by mid-century. *Nature Communications*, *9*(1), 5147. <https://doi.org/10.1038/s41467-018-07557-4>
- Hopkins, D. M. (1949). Thaw Lakes and Thaw Sinks in the Imuruk Lake Area, Seward Peninsula, Alaska. *The Journal of Geology*, *57*(2), 119–131. <https://doi.org/10.1086/625591>
- Hopkins, D. M., & Karlstrom, T. N. V. (1955). *Permafrost and Ground Water in Alaska*. 69.

- IPCC. (2014). *Climate Change 2014: Synthesis Report. Contribution of Working Groups I, II and III to the Fifth Assessment Report of the Intergovernmental Panel on Climate Change* (p. 151 pp). IPCC.
- Jeffries, M. O., Morris, K., & Liston, G. E. (1994). Method to determine lake depth and water availability on the north slope of Alaska with spaceborne imaging radar and numerical ice growth modelling. *Arctic*, 49(4), 5.
- Jones, B. M., & Arp, C. D. (2015). Observing a Catastrophic Thermokarst Lake Drainage in Northern Alaska. *Permafrost and Periglacial Processes*, 26(2), 119–128. <https://doi.org/10.1002/ppp.1842>
- Jones, B. M., Arp, C. D., Grosse, G., Nitze, I., Lara, M. J., Whitman, M. S., Farquharson, L. M., Kanevskiy, M., Parsekian, A. D., Breen, A. L., Ohara, N., Rangel, R. C., & Hinkel, K. M. (2020). Identifying historical and future potential lake drainage events on the western Arctic coastal plain of Alaska. *Permafrost and Periglacial Processes*, 31(1), 110–127. <https://doi.org/10.1002/ppp.2038>
- Jorgenson, M. T., Romanovsky, V., Harden, J., Shur, Y., O'Donnell, J., Schuur, E. A. G., Kanevskiy, M., & Marchenko, S. (2010). Resilience and vulnerability of permafrost to climate change. *Canadian Journal of Forest Research*, 40(7), 1219–1236.
- Jorgenson, M. T., & Shur, Y. (2007). Evolution of lakes and basins in northern Alaska and discussion of the thaw lake cycle. *Journal of Geophysical Research: Earth Surface*, 112(F2). <https://doi.org/10.1029/2006JF000531>
- Kokelj, S., Palmer, M., Lantz, T., & Burn, C. (2017). Ground Temperatures and Permafrost Warming from Forest to Tundra, Tuktoyaktuk Coastlands and Anderson Plain, NWT, Canada: Permafrost temperatures across tree line northwestern Canada. *Permafrost and Periglacial Processes*. <https://doi.org/10.1002/ppp.1934>
- Kokelj, S. V., & Jorgenson, M. T. (2013). Advances in Thermokarst Research. *Permafrost and Periglacial Processes*, 24(2), 108–119. <https://doi.org/10.1002/ppp.1779>
- Kokelj, S. V., Zajdlik, B., & Thompson, M. S. (2009). The impacts of thawing permafrost on the chemistry of lakes across the subarctic boreal-tundra transition, Mackenzie Delta region, Canada. *Permafrost and Periglacial Processes*, 20(2), 185–199. <https://doi.org/10.1002/ppp.641>
- Lantz, T. C. (2017). Vegetation Succession and Environmental Conditions following Catastrophic Lake Drainage in Old Crow Flats, Yukon. *ARCTIC*, 70(2), 177. <https://doi.org/10.14430/arctic4646>
- Lantz, T. C., & Turner, K. W. (2015). Changes in lake area in response to thermokarst processes and climate in Old Crow Flats, Yukon. *Journal of Geophysical Research: Biogeosciences*, 120(3), 513–524. <https://doi.org/10.1002/2014JG002744>
- Lehner, B., & Döll, P. (2004). Development and validation of a global database of lakes, reservoirs and wetlands. *Journal of Hydrology*, 296, 1–22.

- Lindgren, P. R., Farquharson, L. M., Romanovsky, V. E., & Grosse, G. (2021). Landsat-based lake distribution and changes in western Alaska permafrost regions between the 1970s and 2010s. *Environmental Research Letters*, *16*(2), 025006. <https://doi.org/10.1088/1748-9326/abd270>
- Ling, F., & Zhang, T. (2003). Numerical simulation of permafrost thermal regime and talik development under shallow thaw lakes on the Alaskan Arctic Coastal Plain. *Journal of Geophysical Research: Atmospheres*, *108*(D16). <https://doi.org/10.1029/2002JD003014>
- Mackay, J. R. (1981). *An experiment in lake drainage, Richards Island, Northwest Territories: A progress report*. (Paper 81-1A; Current Research, Part A., pp. 63–68). Geological Survey of Canada.
- Mackay, J. R. (1988). Catastrophic lake drainage, Tuktoyaktuk Peninsula area, District of Mackenzie. *Geological Survey of Canada*, *88-1D*.
- Mackay, J. R., & Burn, C. R. (2002). The first 20 years (1978–1979 to 1998–1999) of ice-wedge growth at the Illisarvik drained lake site, western Arctic coast, Canada. *Canadian Journal of Earth Sciences*, *39*, 95–111.
- Marsh, P., & Bigras, S. C. (1988). Evaporation from Mackenzie Delta Lakes, N.W.T., Canada. *Arctic and Alpine Research*, *20*(2), 220–229. <https://doi.org/10.2307/1551500>
- Marsh, P., & Neumann, N. N. (2001). Processes controlling the rapid drainage of two ice-rich permafrost-dammed lakes in NW Canada. *Hydrological Processes*, *15*(18), 3433–3446. <https://doi.org/10.1002/hyp.1035>
- Medeiros, A. S., Wood, P., Wesche, S. D., Bakaic, M., & Peters, J. F. (2017). Water security for northern peoples: Review of threats to Arctic freshwater systems in Nunavut, Canada. *Regional Environmental Change*, *17*(3), 635–647. <https://doi.org/10.1007/s10113-016-1084-2>
- Nitze, I., Cooley, S., Duguay, C., Jones, B. M., & Grosse, G. (2020). The catastrophic thermokarst lake drainage events of 2018 in northwestern Alaska: Fast-forward into the future. *The Cryosphere Discussions*, 1–33. <https://doi.org/10.5194/tc-2020-106>
- Nitze, I., Grosse, G., Jones, B., Arp, C., Ulrich, M., Fedorov, A., & Veremeeva, A. (2017). Landsat-Based Trend Analysis of Lake Dynamics across Northern Permafrost Regions. *Remote Sensing*, *9*(7), 640. <https://doi.org/10.3390/rs9070640>
- Nitze, I., Grosse, G., Jones, B. M., Romanovsky, V. E., & Boike, J. (2018). Remote sensing quantifies widespread abundance of permafrost region disturbances across the Arctic and Subarctic. *Nature Communications*, *9*(1), 1–11. <https://doi.org/10.1038/s41467-018-07663-3>
- Olefeldt, D., Goswami, S., Grosse, G., Hayes, D., Hugelius, G., Kuhry, P., McGuire, A. D., Romanovsky, V. E., Sannel, A. B. K., Schuur, E. a. G., & Turetsky, M. R. (2016). Circumpolar distribution and carbon storage of thermokarst landscapes. *Nature Communications*, *7*(1), 13043. <https://doi.org/10.1038/ncomms13043>

- Olthof, I., Fraser, R. H., & Schmitt, C. (2015). Landsat-based mapping of thermokarst lake dynamics on the Tuktoyaktuk Coastal Plain, Northwest Territories, Canada since 1985. *Remote Sensing of Environment*, *168*, 194–204. <https://doi.org/10.1016/j.rse.2015.07.001>
- Osterkamp, T. E., Viereck, L., Shur, Y., Jorgenson, M. T., Racine, C., Doyle, A., & Boone, R. D. (2000). Observations of Thermokarst and Its Impact on Boreal Forests in Alaska, U.S.A. *Arctic, Antarctic, and Alpine Research*, *32*(3), 303–315. <https://doi.org/10.1080/15230430.2000.12003368>
- Pekel, J.-F., Cottam, A., Gorelick, N., & Belward, A. S. (2016). High-resolution mapping of global surface water and its long-term changes. *Nature*, *540*(7633), 418–422. <https://doi.org/10.1038/nature20584>
- Pickens, A. H., Hansen, M. C., Hancher, M., Stehman, S. V., Tyukavina, A., Potapov, P., Marroquin, B., & Sherani, Z. (2020). Mapping and sampling to characterize global inland water dynamics from 1999 to 2018 with full Landsat time-series. *Remote Sensing of Environment*, *243*, 111792. <https://doi.org/10.1016/j.rse.2020.111792>
- Plug, L. J., Walls, C., & Scott, B. M. (2008). Tundra lake changes from 1978 to 2001 on the Tuktoyaktuk Peninsula, western Canadian Arctic. *Geophysical Research Letters*, *35*(3). <https://doi.org/10.1029/2007GL032303>
- Pohl, S., Marsh, P., & Bonsal, B. R. (2007). Modeling the Impact of Climate Change on Runoff and Annual Water Balance of an Arctic Headwater Basin. *Arctic*, *60*(2), 173–186.
- Pohl, S., Marsh, P., Onclin, C., & Russell, M. (2009). The summer hydrology of a small upland tundra thaw lake: Implications to lake drainage. *Hydrological Processes*, *23*(17), 2536–2546. <https://doi.org/10.1002/hyp.7238>
- Rampton, V. N. (1987). *Surficial geology, Tuktoyaktuk Coastlands, District of Mackenzie, Northwest Territories. Geological Survey of Canada, Map 1647A, scale 1:500,000, 1 sheet* [Map]. doi:10.4095/125160
- Roach, J. K., & Griffith, B. (2015). Climate-induced lake drying causes heterogeneous reductions in waterfowl species richness. *Landscape Ecology*, *30*(6), 1005–1022. <https://doi.org/10.1007/s10980-015-0207-3>
- Roach, J. K., Griffith, B., & Verbyla, D. (2012). Comparison of three methods for long-term monitoring of boreal lake area using Landsat TM and ETM+ imagery. *Canadian Journal of Remote Sensing*, *38*(4), 427–440. <https://doi.org/10.5589/m12-035>
- Roach, J. K., Griffith, B., & Verbyla, D. (2013). Landscape influences on climate-related lake shrinkage at high latitudes. *Global Change Biology*, *19*(7), 2276–2284. <https://doi.org/10.1111/gcb.12196>
- Schuur, E. A. G., & Mack, M. C. (2018). Ecological Response to Permafrost Thaw and Consequences for Local and Global Ecosystem Services. *Annual Review of Ecology, Evolution, and Systematics*, *49*(1), 279–301. <https://doi.org/10.1146/annurev-ecolsys-121415-032349>

- Schuur, E. a. G., McGuire, A. D., Schädel, C., Grosse, G., Harden, J. W., Hayes, D. J., Hugelius, G., Koven, C. D., Kuhry, P., Lawrence, D. M., Natali, S. M., Olefeldt, D., Romanovsky, V. E., Schaefer, K., Turetsky, M. R., Treat, C. C., & Vonk, J. E. (2015). Climate change and the permafrost carbon feedback. *Nature*, *520*(7546), 171–179. <https://doi.org/10.1038/nature14338>
- Segal, R. A., Lantz, T. C., & Kokelj, S. V. (2016). Acceleration of thaw slump activity in glaciated landscapes of the Western Canadian Arctic. *Environmental Research Letters*, *11*(3), 034025. <https://doi.org/10.1088/1748-9326/11/3/034025>
- Serreze, M. C., Barrett, A. P., Stroeve, J. C., Kindig, D. N., & Holland, M. M. (2009). The emergence of surface-based Arctic amplification. *The Cryosphere*, *9*.
- Slater, A. G., & Lawrence, D. M. (2013). Diagnosing Present and Future Permafrost from Climate Models. *Journal of Climate*, *26*(15), 5608–5623. <https://doi.org/10.1175/JCLI-D-12-00341.1>
- Smith, L. C., Sheng, Y., & MacDonald, G. M. (2007). A first pan-Arctic assessment of the influence of glaciation, permafrost, topography and peatlands on northern hemisphere lake distribution. *Permafrost and Periglacial Processes*, *18*(2), 201–208. <https://doi.org/10.1002/ppp.581>
- Smol, J. P., & Douglas, M. S. V. (2007). Crossing the final ecological threshold in high Arctic ponds. *Proceedings of the National Academy of Sciences*, *104*(30), 12395–12397. <https://doi.org/10.1073/pnas.0702777104>
- Steedman, A. E., Lantz, T. C., & Kokelj, S. V. (2017). Spatio-Temporal Variation in High-Centre Polygons and Ice-Wedge Melt Ponds, Tuktoyaktuk Coastlands, Northwest Territories: Variation in High-Centre Polygons and Ice-Wedge Melt Ponds, NWT. *Permafrost and Periglacial Processes*, *28*(1), 66–78. <https://doi.org/10.1002/ppp.1880>
- Swanson, D. K. (2019). Thermokarst and precipitation drive changes in the area of lakes and ponds in the National Parks of northwestern Alaska, 1984–2018. *Arctic, Antarctic, and Alpine Research*, *51*(1), 265–279. <https://doi.org/10.1080/15230430.2019.1629222>
- Tape, K. D., Jones, B. M., Arp, C. D., Nitze, I., & Grosse, G. (2018). Tundra be dammed: Beaver colonization of the Arctic. *Global Change Biology*, *24*(10), 4478–4488. <https://doi.org/10.1111/gcb.14332>
- Tarnocai, C., Canadell, J. G., Schuur, E. a. G., Kuhry, P., Mazhitova, G., & Zimov, S. (2009). Soil organic carbon pools in the northern circumpolar permafrost region. *Global Biogeochemical Cycles*, *23*(2). <https://doi.org/10.1029/2008GB003327>
- Turner, C. K., Lantz, T. C., & Gwich'in Tribal Council Department of Cultural Heritage. (2018). Springtime in the Delta: The Socio-Cultural Importance of Muskrats to Gwich'in and Inuvialuit Trappers through Periods of Ecological and Socioeconomic Change. *Human Ecology*, *46*(4), 601–611. <https://doi.org/10.1007/s10745-018-0014-y>

Weeks, W. F., Gow, A. J., & Schertler, R. J. (1981). *Ground-Truth Observations of Ice-Covered North Slope Lakes Imaged by Radar*. 24.

Weeks, W. F., & Sellman, P. (1977). Interesting Features Of Radar Imagery Of Ice-Covered North Slope Lakes. *Journal of Glaciology*, 18(78), 129–136.

Wolfe, S. A., Morse, P. D., Kokelj, S. V., & Gaanderse, A. J. (2017). Great Slave Lowland: The Legacy of Glacial Lake McConnell. In O. Slaymaker (Ed.), *Landscapes and Landforms of Western Canada* (pp. 87–96). Springer International Publishing. [https://doi.org/10.1007/978-3-319-44595-3\\_5](https://doi.org/10.1007/978-3-319-44595-3_5)

Woo, M.-K., & Guan, X. J. (2006). Hydrological connectivity and seasonal storage change of tundra ponds in a polar oasis environment, Canadian High Arctic. *Permafrost and Periglacial Processes*, 17(4), 309–323. <https://doi.org/10.1002/ppp.565>

Wulder, M. A., Masek, J. G., Cohen, W. B., Loveland, T. R., & Woodcock, C. E. (2012). Opening the archive: How free data has enabled the science and monitoring promise of Landsat. *Remote Sensing of Environment*, 122, 2–10. <https://doi.org/10.1016/j.rse.2012.01.010>

## **2. Surface water dynamics and rapid lake drainage in the Lower Mackenzie Plain, NWT**

Hana Travers-Smith<sup>1</sup>, Trevor C. Lantz<sup>1</sup>, Robert H. Fraser<sup>2</sup>

1. School of Environmental Studies, University of Victoria

2. Canada Centre of Remote Sensing

## 2.1 Introduction

Across the circumpolar north, rising air temperatures and variable precipitation patterns are driving changes in the distribution and abundance of surface water (Nitze et al., 2017; Pastick et al., 2019; Serreze et al., 2009; Smol & Douglas, 2007; Watts et al., 2012). Previous work shows that the magnitude and direction of change varies with both terrain and climate (Nitze et al., 2017; Pastick et al., 2019). In the western Canadian Arctic surface water has shown net declines in some areas (Campbell et al., 2018; Lantz & Turner, 2015), but has been stable or increasing in others (Olthof et al., 2015; Plug et al., 2008). Understanding the rate and spatial pattern of these changes is important because wetlands, lakes and small ponds play an important role in global climate and carbon cycles (Hinkel et al., 2003; Schuur et al., 2015; Anthony et al., 2018). At a regional scale, water bodies are also a source of freshwater and provide habitat for a range of culturally and ecologically significant species (Arp et al., 2016; GRRB, 2018).

Several lines of evidence show that interactions between climate and terrain characteristics influence the magnitude and direction of changes in the area of Arctic surface water at varying spatial scales (Arp et al., 2012; Marsh et al., 2009; Pohl et al., 2009; Yoshikawa & Hinzman, 2003). In some regions, declines in surface water are associated with rising air temperatures (Campbell et al., 2018; Smith et al., 2005; Smol & Douglas, 2007), but in other areas variability in precipitation is a stronger driver of interannual change (Plug et al., 2008; Lantz & Turner 2015). Some studies have found little correlation between climate variables and surface water dynamics, suggesting that the effects of climate are mediated by terrain factors (Carroll & Loboda, 2018). Terrain characteristics likely to influence surface water dynamics include landscape position (Nitze et al., 2017; Roach et al., 2013), ground ice content (Jones et al., 2020; Swanson, 2019; Yoshikawa & Hinzman, 2003), vegetation (Turner et al., 2014), and surficial

geology (Carroll & Loboda, 2018; Nitze et al., 2017; Roach et al., 2013; Wang et al., 2018; Yoshikawa & Hinzman, 2003). These terrain characteristics also strongly influence the prevalence of thermokarst processes, which can drive both lake expansion and drainage (S. V. Kokelj & Jorgenson, 2013). Rising air temperatures, changes in the intensity of precipitation, and more frequent wildfire are also increasing the frequency of thermokarst processes across the circumpolar arctic (Becker & Pollard, 2016; Gibson et al., 2018; Jones et al., 2015; Narita et al., 2015). Roach et al., (2013) found that lakes in areas affected by boreal wildfire were 1.5x more likely to show a decreasing trend in area. Recent evidence that thermokarst disturbances and fire are increasing in frequency and intensity highlights the need to better understand interactions between climate change, fire, permafrost conditions and surface water dynamics (Jones et al., 2015; Kasischke & Turetsky, 2006; Nitze et al., 2020).

To understand changes in the area of surface water, previous remote sensing studies have relied on differencing techniques across two to four time-periods (Jones et al., 2011; Lantz & Turner, 2015; Lindgren et al., 2021; Marsh et al., 2009; Plug et al., 2008). Unfortunately, high variation at interannual and seasonal scales, particularly in small water bodies, means that this approach is not sensitive to the full range of changes in surface water (Carroll & Loboda, 2018; S. W. Cooley et al., 2019). Recent analyses address these challenges using temporally dense image stacks to capture per-pixel trends in water coverage over large areas (Campbell et al., 2018; Nitze et al., 2017; Pastick et al., 2019; Swanson, 2019). However, inferring mechanisms of lake-level changes using conventional approaches in trend detection may mask rapid non-linear trends common in northern regions (Jones & Arp, 2015; Mackay, 1988; Nitze et al., 2020). In areas of ice-rich permafrost, non-linear surface water dynamics can also be driven by thermokarst

processes that may not be well represented by linear per-pixel trends in water coverage (Jones & Arp, 2015; Nitze et al., 2020).

In this study, we examined changes in the area of 5,328 lakes and ponds within the Lower Mackenzie Plains, NWT from 1985 to 2020 using 32 scenes from the Landsat satellite image archive. Our goal was to quantify the overall direction and magnitude of surface water gains and losses, and to investigate how climate and terrain attributes influenced observed changes. To accomplish this, we used a statistical approach to classify lakes based on the direction (+/-) and nature (linear/non-linear) of trends in surface water area. Generalized Additive Models were used to compare the effects of spring and summer temperature and precipitation on change in the area of large and small lakes. Chi-Square tests were used to associate increase and decreasing trends in lake area with several terrain variables. To assess the importance of non-linear changes in surface water, we also examined the timing of abrupt shifts in lake area following wildfire.

## **2.2 Methods**

### **2.2.1 Study Area**

The Lower Mackenzie Plain is located in the Northwest Territories, Canada, south of the Mackenzie Delta (Figure 2.1). This region is characterized by thousands of small lakes, peatlands and spruce forests (Ecosystem Classification Group, 2009). The region is within the Gwich'in Settlement Area and includes the Gwichya Gwich'in community of Tsiigehtchic (Heine et al., 2001). Surficial geology in this region is complex and is mainly comprised of a patchwork of morainal deposits, with silty fluvial deposits and peatlands adjacent to the Mackenzie River (Figure 2.2A). The Mackenzie River runs through the middle of the 14,631 km<sup>2</sup> study area and divides two distinct ecoregions: the Arctic Red Plains and the Travaillant Uplands (Ecosystem Classification Group, 2009). The Arctic Red Plain is located at lower elevations adjacent to the

Mackenzie River and contains black spruce forest and upright shrublands interspersed with extensive peatlands (Ecosystem Classification Group, 2009). The Travailliant Uplands are located at higher elevations and are characterized by white spruce forests and underlain by bedrock with thin veneer of glacial till (Ecosystem Classification Group, 2009). Wildfire is common across the study area, with 41% of it having been burned since 1965 (Figure 2.2B).

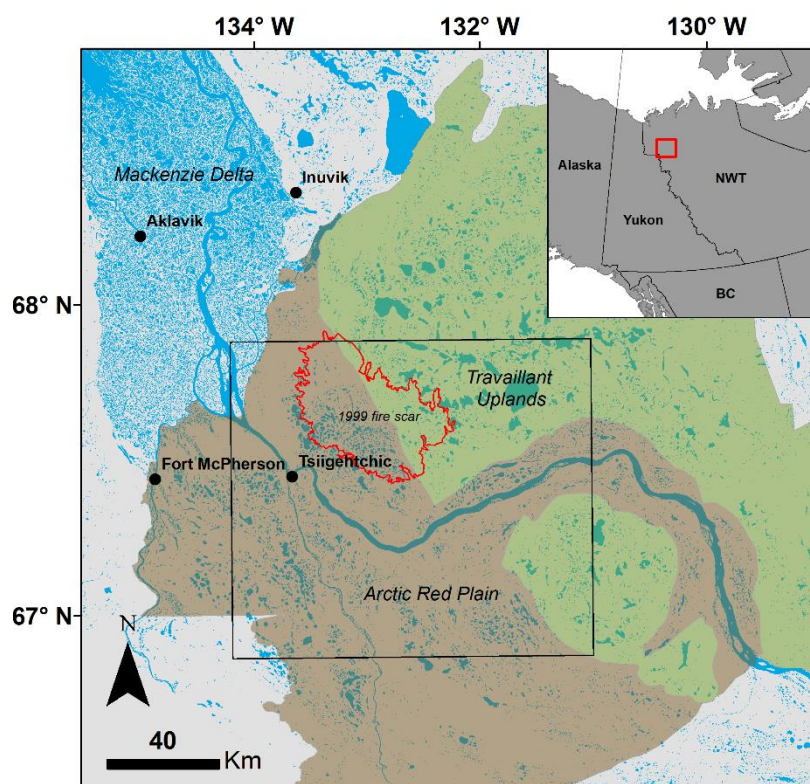


Figure 2.1 Study area map of the Lower Mackenzie Plains, NWT. The black outline shows the extent of the study region. The brown shaded area shows the Arctic Red Plain ecoregion and the green shaded area represents the Travailliant Uplands ecoregion. The red outline shows the boundary of a 1999 fire scar. The inset map in the upper left shows the location of the study region within western Canada.

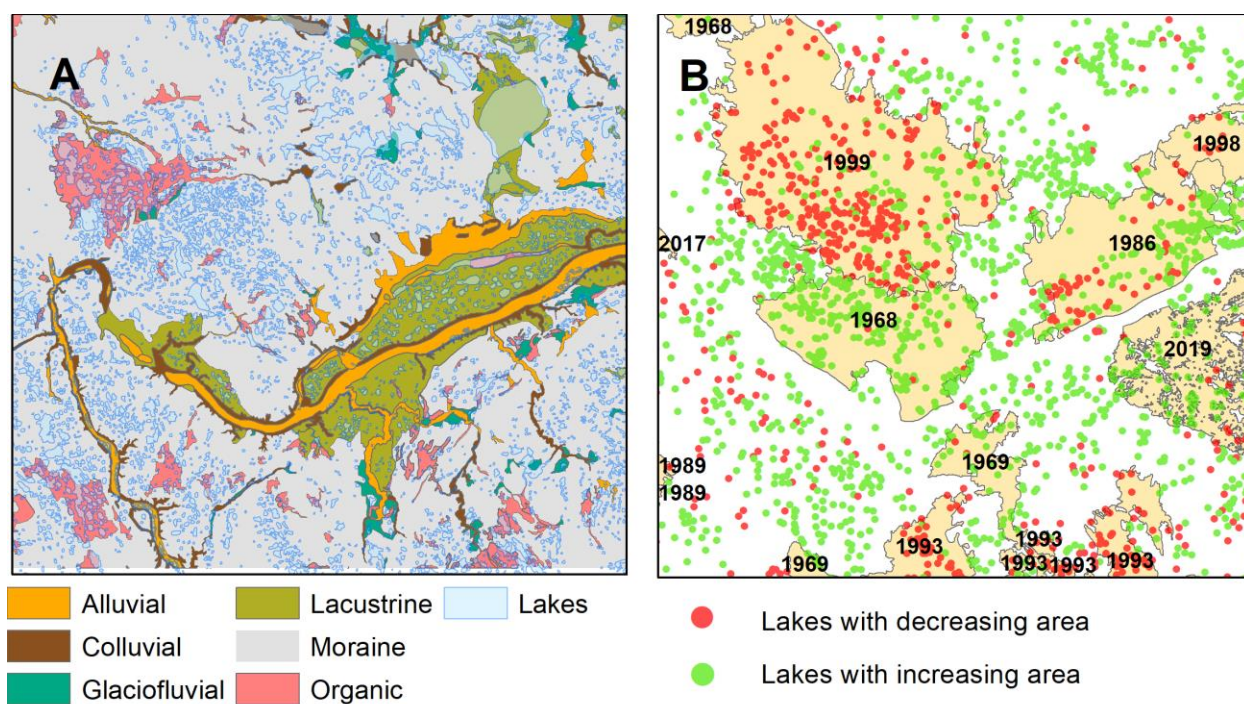


Figure 2.2 Maps showing surficial geology (A) and fire history (B) within the study area (black box in Figure 2.2). Surficial geology data is from Aylsworth et al. (2000) and fire history data is from the NWT Centre for Geomatics (2019). Dates show the timing of fires within the study region. Points in B represent lake centroids and the color of the points indicate whether lake area showed significant increasing or decreasing trends.

### 2.2.2 Climate Data

Monthly air temperature and precipitation data from 1985 to 2014 from the Fort McPherson airport (67°26'00N, 134°53'00W) were obtained from Environment Canada (Environment Canada, 2020). Monthly data were aggregated into seasons where July to August represented the summer, September represented the fall, June represented the spring, and October to May (of the following calendar year) represented the winter. Linear trends were calculated for each season using Thiel-Sen regression in the R package Kendall (McLeod, 2011). Seasons missing more than ten days of data were excluded from analysis. We also analyzed the frequency of large daily

spring and summer precipitation events, which we classified as a 24 hour window with 16mm or more of rain.

The climate of this region is cold, with a mean annual air temperature of  $-6.7^{\circ}\text{C}$  from 1985 to 2014. We calculated trends in seasonal climate variables using Thiel-Sen regression. Trends in mean seasonal air temperature show significant warming in the winter ( $p=0.034$ ) and spring ( $p=0.028$ , Figure 2.3) but summer ( $p=1$ ) and fall are not trended ( $p=0.89$ , Figure 2.3). Median total annual precipitation between 1985 and 2014 was 134.4mm per year, with a median of 104mm falling within the spring and summer months. Total precipitation has significantly increased across all seasons ( $p<0.05$ ) except winter, where it has decreased since the 1980's ( $p=0.001$ , Figure 3). The frequency of large precipitation events shows a non-significant increasing trend ( $p=0.08$ ). However, over this time period large rain events increased from an average of 0.8 times per year before 2000 to an average of 1.4 times after 2000 (Figure 2.4). The four years with the greatest number of large precipitation events all occur after 2000 (Figure 2.4).

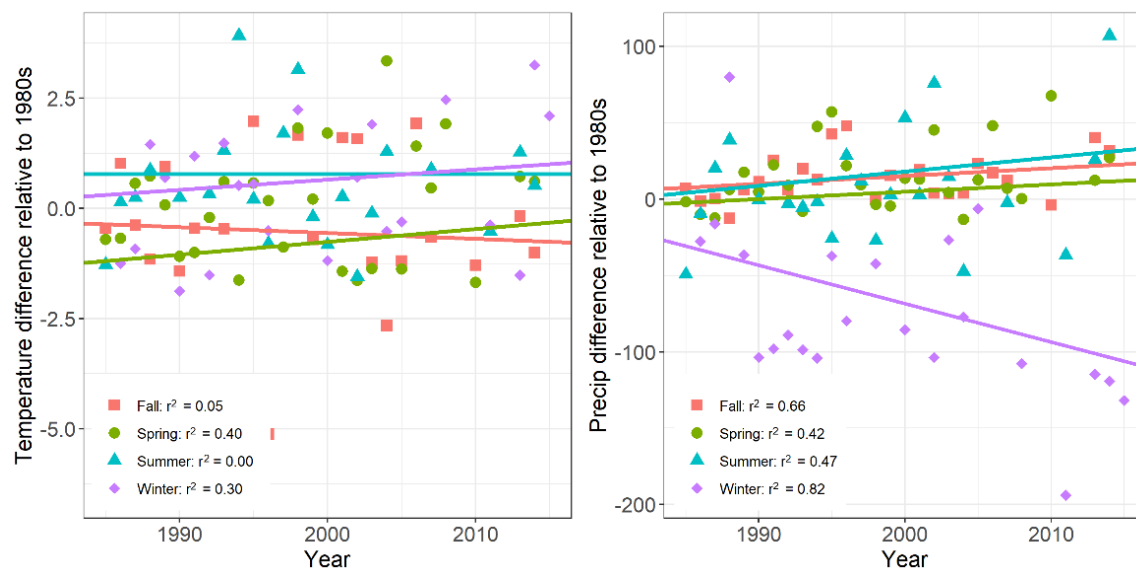


Figure 2.3 Theil-Sen trends of the deviation from (left) average seasonal temperatures ( $^{\circ}\text{C}$ ) between 1985 and 1990, and (right) total precipitation (mm). Data was recorded at the Fort McPherson airport and is available from ECCC at: [https://climate.weather.gc.ca/historical\\_data/search\\_historic\\_data\\_e.html](https://climate.weather.gc.ca/historical_data/search_historic_data_e.html)

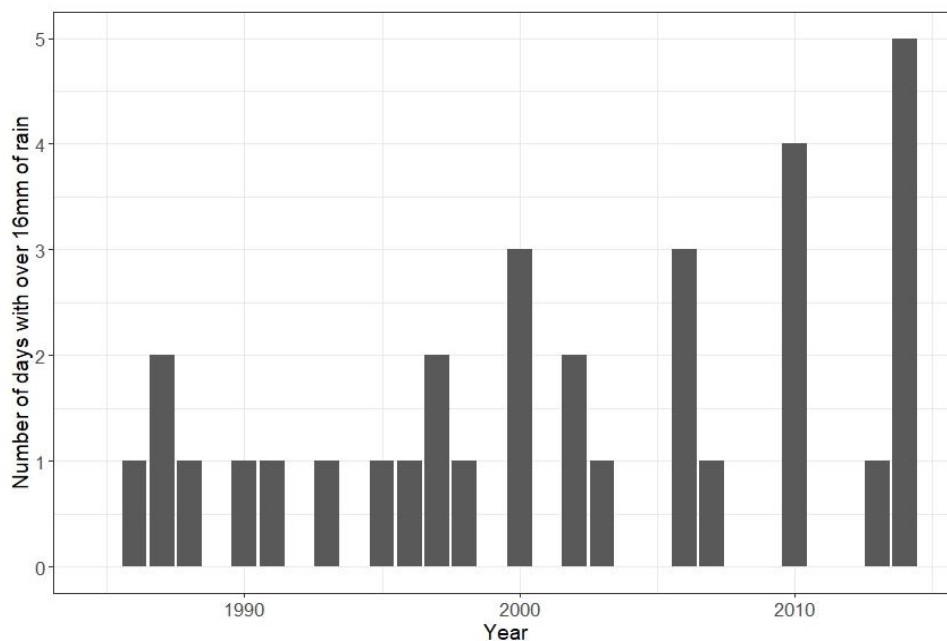


Figure 2.4 Number of spring and summer days with over 16mm of rain measured at the Fort McPherson airport between 1985 and 2014 (Environment Canada, 2020).

### 2.2.3 Landsat Image Processing

Data from Landsat Collection 1, which includes Landsat-5, Landsat-7, and Landsat-8, were used to quantify trends in surface water from 1985-2019 (Dwyer, 2019). We used Tier 1 Top-of-Atmosphere (TOA) scenes (n=32) which are geometrically and radiometrically calibrated for use in time-series analysis (Dwyer, 2019). We did not use Surface Reflectance data due to known issues with this product at high latitudes (Jenkerson, 2019). Scenes impacted by the Landsat-7 scan line corrector failure beginning in 2003 were also excluded from our analysis. To ensure snow-free conditions, consistency in seasonal water levels and atmospheric constituents across the time series, we filtered data to only include scenes from July and August. To minimize seasonal differences across the annual time-series we preferentially selected scenes within a one month window representing mid-summer conditions between July 15 and August 15, and 60% of scenes fell within this period. In each image, we masked pixels impacted by clouds and cloud shadows using the Quality Assessment Band. After removing clouds and cloud shadows, each scene was visually inspected and discarded if smoke or clouds remained in the study area. All Landsat image pre-processing steps were performed in Google Earth Engine.

To map annual surface water coverage, we used the histogram breakpoint method developed by Olthof et al. (2015). This method quantifies the proportion of a pixel covered by water (sub-pixel water fraction) by interpolating between thresholds in the shortwave infrared reflectance band (SWIR1) representing pixels containing pure land and pure water. For a detailed description and validation of the method, see Appendix 1. In the next part of the workflow, we created a mask representing the maximum area of all water bodies in the study area. Maximum area was defined using pixels where sub-pixel water fraction was greater than 50% in two or more years.

Subsequently, lake objects were created by transforming the maximal water area raster into

polygon features. We used an initial threshold of 30,000m<sup>2</sup> (0.03km<sup>2</sup>) equal to approximately 33 Landsat pixels, to filter out small ponds that were likely to have high mapping error, retaining 5328 water bodies in the study area.

#### 2.2.4 Changes in Lake Area

We assessed change in total lake area as well as changes within individual lakes. First we estimated total lake area using lakes with less than 10 missing observations across the time series (n=3164/5328). To estimate change in water area over time, we calculated a 5-point moving average for each lake. This process helped to fill gaps where lakes may have been covered by clouds or smoke in an individual Landsat scene. The resulting dataset was comprised of a moving average of lake area across five consecutive Landsat acquisitions. We calculated total lake area over time as the sum of lake area within time-periods. To ensure that the same population of lakes was represented in each period, we omitted periods with missing data resulting from lakes having no available data for five consecutive Landsat acquisitions. Changes in total lake area were also analyzed using the following size classes 1) large lakes (>0.5km<sup>2</sup>), medium lakes (0.05-0.5km<sup>2</sup>), and small lakes (<0.05km<sup>2</sup>) based on the average area between 1985 and 1990.

To assess changes in the area of individual lakes, we tested for trends over time and classified lakes using two criteria: 1) the direction of change and 2) whether changes were linear or non-linear over time. To test for trends, we used the Mann Kendall Trend Test to determine if lake area exhibited a monotonic increase, decrease or non-significant trend in area over time. We used the Kendall package in R to calculate the Kendall's Tau statistic and corresponding p-value for each lake (McLeod, 2011). Lakes with a p-value <0.1 were classified as either increasing or

decreasing depending on the sign of the Tau statistic, and lakes with p-value  $>0.1$  were classified as non-trended. Next, we used Generalized Additive Models (GAM) to classify trends as either linear or non-linear over time. We fit a GAM to the area of each lake over time and extracted the Estimated Degrees of Freedom (EDF) using the R package *mgcv* (Wood, 2017). The EDF indicates the number of knots in the smooth effect of time in the model, and provides a measure of the ‘wiggleness’ of the fitted model. Large values indicating a strong non-linear relationship over time and values close to one indicating a linear fit. Lakes with EDF greater than 1.1 were classified as non-linear and EDF less than 1.1 were classified as linear. The results of these two tests were combined to classify each lake into one of the six change classes representing the direction of change (increasing, decreasing or non-trended), and the nature of change (linear or non-linear). The six change classes are illustrated in Appendix 2.

To identify rapid drainage events in large and medium sized lakes we used breakpoint regression from the *strucchange* package in R (Zeileis, 2004). We did not identify rapid drainage events in small lakes as they represent a small (~6%) proportion of total lake area and potential for misclassification in the area of small lakes is greater. We selected lakes exhibiting one breakpoint, a decreasing trend in area, and change exceeding 30% relative to its initial area (average area between 1985 and 1990). We also examined the time-series of each lake to distinguish between lakes exhibiting rapid drainage from other drying processes (linear change, non-linear bi-directional). We considered lake drainage to be rapid if the lake lost at least 30% of its initial area within one year.

We also used breakpoint regression to examine the effect of a large fire that burned in 1999. The fire covered 1632 km<sup>2</sup> and 836 lakes were completely contained within the fire boundary. This fire was selected because its large size and timing allowed us to obtain a large sample of lakes

inside and outside the fire, and to assess change before and after the burn. To test the hypothesis that forest fires can initiate non-linear changes in lake area we calculated the frequency and timing of breakpoints in surface area time series for burned lakes and lakes within 10km of the fire scar. We also compared change in relative area over time between burned and unburned lakes.

### 2.2.5 Climate Models and Terrain Factors

We tested hypotheses relating the potential effects of spring and summer climate on changes in lake area using Generalized Additive Models and climate data from the Fort McPherson airport (Environment Canada, 2020). We used data from May and July as proxies for spring and summer conditions because data for these months comprised a nearly complete record over the period of study. In this analysis, we calculated lake area over time using a sample of large ( $n=17$ ) and small lakes ( $n=215$ ) and Landsat acquisitions ( $n=12$ ) with no missing data. Total lake area was aggregated by lake size and we fit Generalized Additive Models using the R package `mgcv` (Wood, 2011). We hypothesized that small lakes would be more responsive to variation in May and July climate conditions compared to large lakes, due to their greater surface area to volume ratios (Marsh & Bigras, 1988). We fit separate models for large and small lakes and compared the magnitude and significance of the climate parameters. In each model, total lake area ( $\text{km}^2$ ) was fit as the response variable and the number of days since the beginning of the time series was modelled as a non-linear smooth effect. To avoid overfitting on a small dataset we set a low basis dimension for the smoothed term ( $k=3$ ). Total May precipitation, mean May temperature, total July precipitation, mean July temperature and the month of the Landsat acquisition (July or August), were fit as linear effects. To account for temporal autocorrelation in the data we modelled a correlation structure by including a first order autoregressive term. To validate these

models we examined plots of model residuals and autocorrelation using the `acf` function in R (R Core Team, 2020). To determine if trends in lake area were significantly associated with surficial geology (Alysworth, 2000), ecoregion (Ecosystem Classification Group, 2009), fire history (NWT Centre for Geomatics, 2019) and lake size we used Chi-square tests of association. In this analysis, standardized Pearson residuals were used to determine whether trends in lake area (increasing, decreasing, non-trended) were over or underrepresented in specific terrain categories.

In addition to the R packages cited previously, figures throughout the paper were created using the `ggplot2` package (Wickham, 2016). A range of helper functions from the packages `dplyr` (Wickham & Henry, 2020) `tidyr` (Wickham et al., 2020), `data.table` (Dowle & Srinivasan, 2019), `gmodels` (Warnes et al., 2018) and `zoo` (Zeileis & Grothendieck, 2005) were also used to process and clean the data for analysis.

## **2.3 Results**

### **2.3.1 Overall Change in Lake Area**

Between 1985 and 2020, total lake area in the study region decreased by approximately 1%, representing a net change of 5.18km<sup>2</sup> (Figure 2.5). The total area of large and medium sized lakes both declined over time (Figure 2.5), while the total area of small lakes increased by approximately ~5%. Mann Kendall Trend tests show that the majority (57%) of lakes did not show a significant change in area over time. Approximately 29% of lakes showed a significant increasing trend and 13% showed a decreasing trend (Table 2.1). Lakes exhibiting significant changes in area tended to show primarily non-linear changes (Table 2.1).

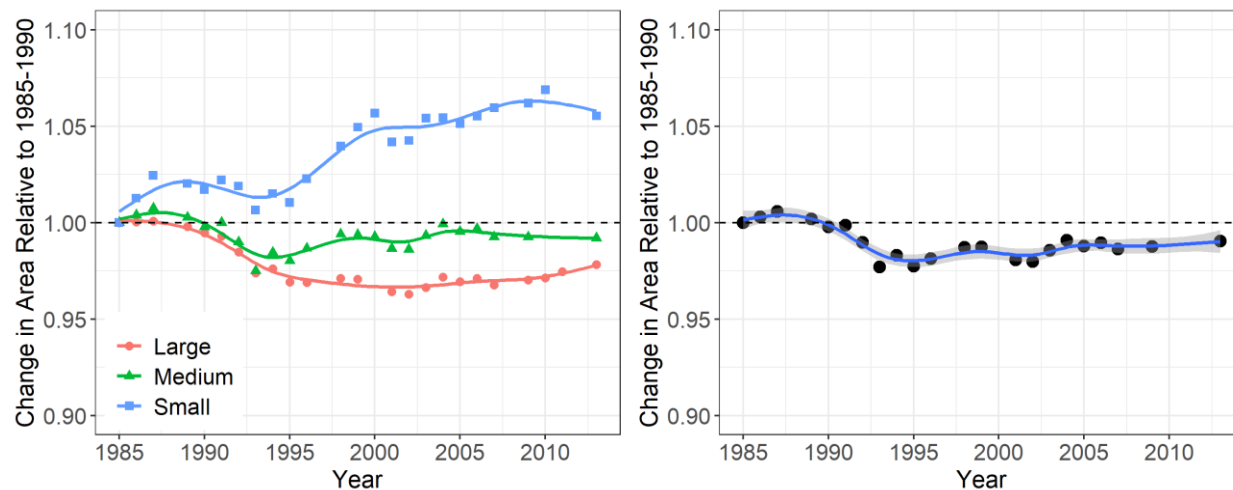


Figure 2.5 Change in lake area relative to average area between 1985 and 1990 by lake size (left) and total lake area (right). Data in the time series represents a 5-point moving average. Total lake area shows a decline of approximately 1%.

Table 2.1 Percent of lakes in the study area belonging to classes assigned based on a Mann Kendall trend test to determine the direction of change (increasing, decreasing or non-trended) and a Generalized Additive Model to determine the nature of change (linear or non-linear).

	<b>Increasing</b>	<b>Decreasing</b>	<b>Non-Trended</b>	<b>Total</b>
<b>Linear</b>	11%	4%	19%	<b>34%</b>
<b>Non-Linear</b>	18%	10%	38%	<b>66%</b>
<b>Total</b>	<b>29%</b>	<b>14%</b>	<b>57%</b>	<b>N=5328</b>

### 2.3.2 Identifying Lake Drainage

We identified 13 large lakes and 38 medium sized lakes exhibiting large non-linear decreases in area, indicative of catastrophic drainage. Inspection of each lake time series showed that the majority of these lakes exhibited bi-directional change and did not drain permanently. Based on patterns in the time-series we identified five lakes (two large and three medium sized lakes)

showing rapid drainage (Figure 6). This suggests that over the 35-year time series, the annual rate of rapid drainage events among lakes larger than  $0.05\text{km}^2$  was 0.14 lakes per year. The five lakes that drained over this period account for  $1.41\text{km}^2$  of surface water loss, or 27% of total surface water loss. Two of these lakes (accounting for 14% of total water loss) were located in the 1999 fire and drained rapidly within 3-years of the fire (Figure 2.6).

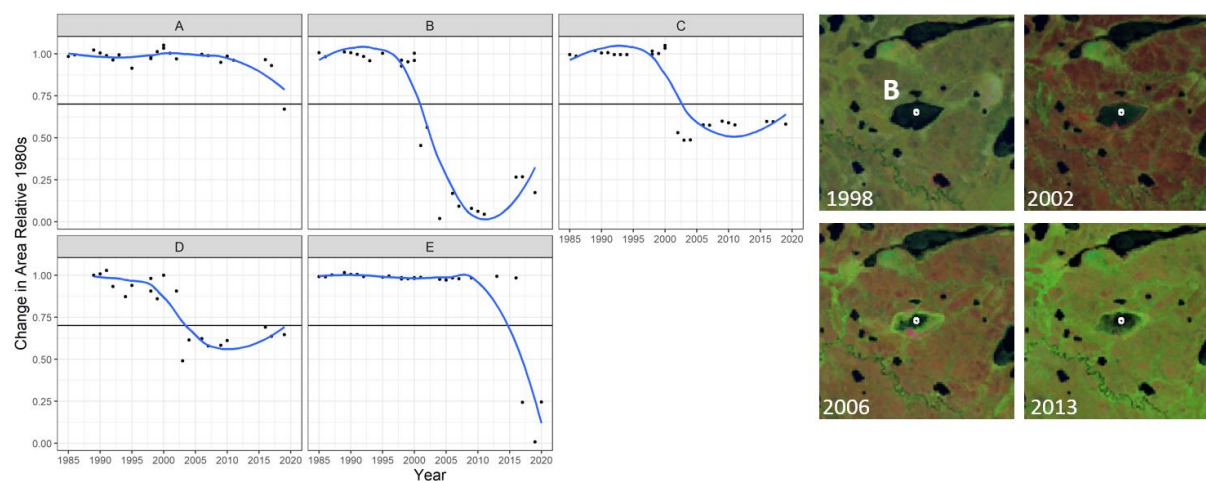


Figure 2.6 Large and medium sized lakes ( $>0.05\text{km}^2$ ) showing rapid drainage. The left panel shows the time series of change in lake area relative to average area between 1985 and 1990. The black line shows 30% change for reference. Lakes B and C were both impacted by the 1999 fire and drained rapidly between 2000 and 2001. The right panel shows the drainage of lake B following a 1999 fire. Landsat imagery are displayed in false colour (SWIR1/NIR/Green) using images from the Landsat time series explorer.

### 2.3.3 Effect of Fire on Lake Area

Our analysis shows that 33% of lakes inside the area burned by a 1999 fire exhibited a significant decrease in area compared to 5% of lakes within  $10\text{km}$  of the fire (Figure 2.7).

Boxplots of relative change in lake area show that lakes inside the burned areas experienced an

initial increase in area relative to unburned lakes, which was followed by declines between 2000 and 2002. The relative area of lakes within the fire remained lower than unburned lakes until 2019, twenty years after the fire (Figure 2.8). Breakpoint regression analysis shows that the frequency of breakpoints for lakes inside and outside the burned area was similar before the fire, but increased for lakes inside the burned area immediately after the fire (Figure 2.9). The largest difference in breakpoint frequency occurred in 2001, when 22% of burned lakes showed a breakpoint compared to only 2% of unburned lakes (Figure 2.9). After 2001, the difference in breakpoint frequency between burned and unburned lakes was less than 1% for all years except 2007 (6% difference).

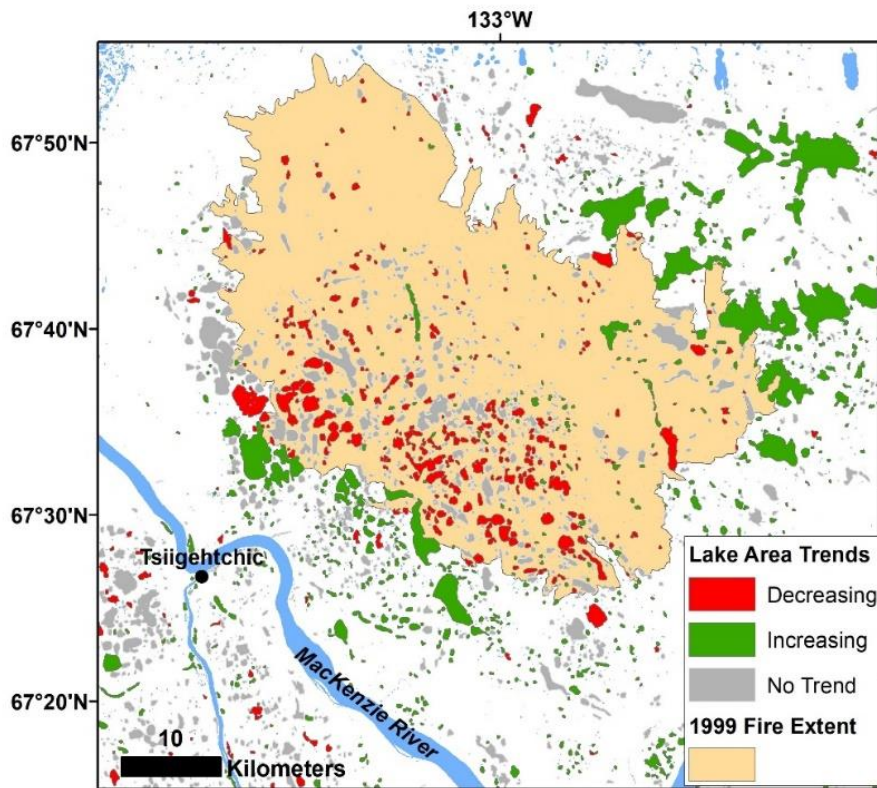


Figure 2.7 Trends in lake area within the boundaries of a large fire that burned in 1999. Note the cluster of lakes with decreasing trends inside the extent of the 1999 fire. The extent of the fire within the entire study area is shown in Figure 2.1.

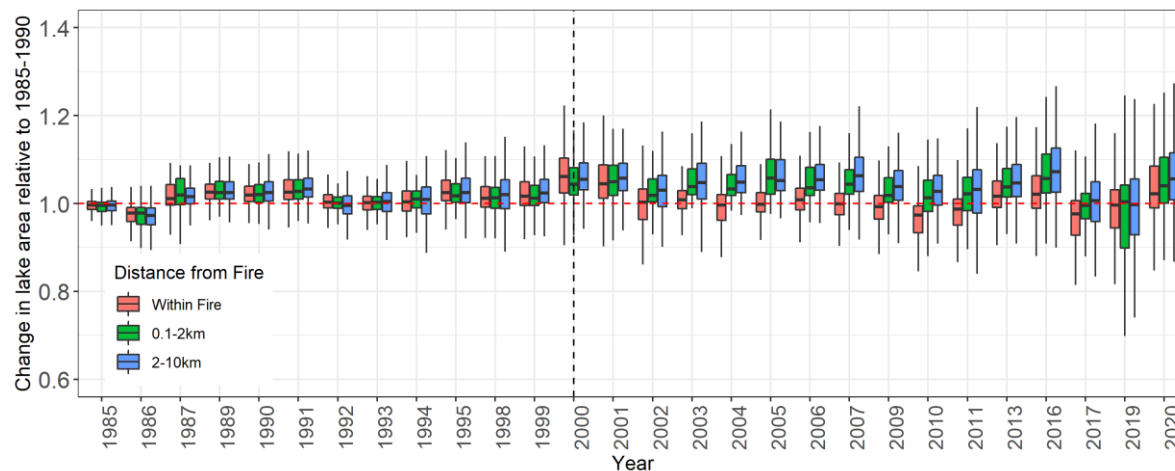


Figure 2.8 Boxplots comparing the median change in lake area relative to the average area between 1985 and 1990 for lakes within a fire scar, lakes up to 0.1-2km away from the fire and lakes 2-10km away from the fire. The extent of the box shows the interquartile range and the whiskers show the 10<sup>th</sup> and 90<sup>th</sup> percentiles. Landsat imagery from 1999 was captured prior to the fire. The dashed vertical line shows the year after the fire.

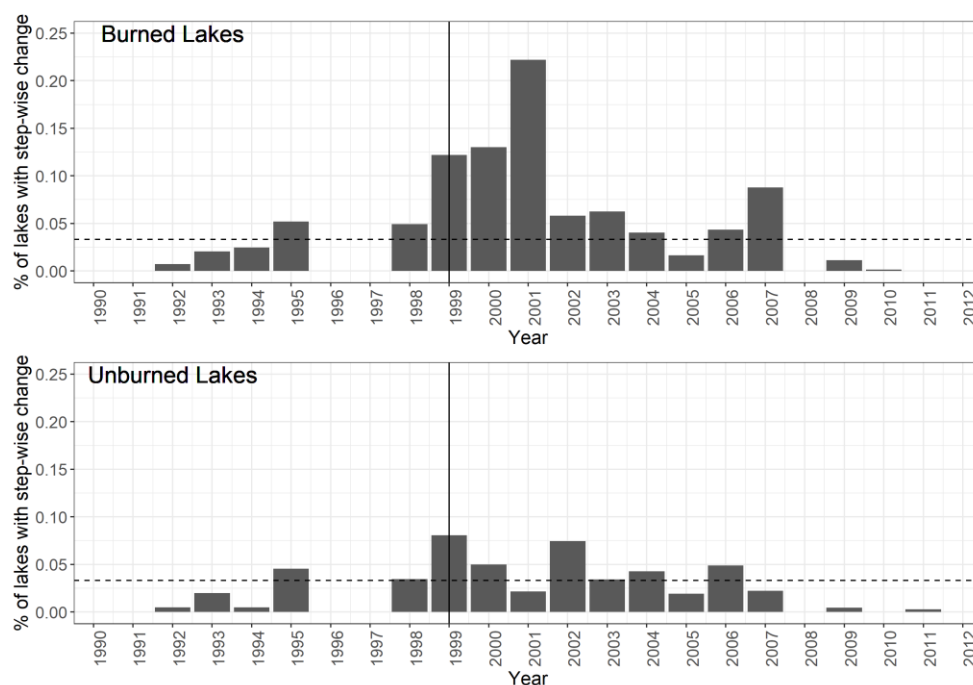


Figure 2.9 Comparison of the frequency of breakpoints in the time series of lake area for lakes within a large burned area (top, n=836) and lakes within 10km of the fire scar (bottom, n=752). Note that no data was available for 1996, 1997 and 2008. The solid black line shows the year of the fire and the dashed horizontal line shows the average proportion of lakes with a breakpoint for all lakes in the study area.

### **2.3.4 Climate Models**

Generalized additive models relating interannual variability in lake area with climate variables showed that the effects of May and July temperature and precipitation were similar for large and small lakes (Table 2.2). July precipitation had a significant positive effect on the total lake for both large and small lakes, but the effects of May and July temperature, and May precipitation were not significant in either model (Table 2.2). Plots showing the non-linear relationship between lake area and time indicate that the total area of large lakes generally decreased over time while the total area of small lakes generally increased over time. For large lakes, the effect of month was also significant, with lake area in August lower on average than lake area in July.

### **2.3.5 Chi-Square**

Chi-square tests also showed that lake area trends were significantly associated with terrain and lake characteristics (Table 2.3). The Arctic Red Plain contained more lakes with decreasing area than expected, while the Travaillant Uplands had more lakes with increasing area (Table 2.3). Lakes with decreasing area were also more frequently located inside fire scars, and less frequently found outside burned areas. Lakes in fine-grained lacustrine and alluvial sediments showed more increasing trends than expected and lakes in peatland-dominated areas exhibited fewer increasing lakes and more decreasing lakes than expected. Large lakes were more likely to show decreasing trends, while small lakes were more likely to show increases in surface area (Table 2.3).

Table 2.2 Parameter estimates from GAM models of total lake area as a function of month, lake size and May and July climate variables. Estimates of parametric coefficients represent the change in total lake area in km<sup>2</sup> per unit increase in each explanatory variable. The effect of acquisition month represents the mean difference in lake area between July and August acquisitions. The effective degrees of freedom (EDF) of the smooth term represents the number of knots in the smoothed parameter, where values close to 1 indicate that the parameter was modelled as a linear effect. Asterisks denote statistically significant results at the  $p < 0.1$  (\*),  $p < 0.05$  (\*\*) and  $p < 0.01$  (\*\*\*) level.

<b>Large Lakes</b>				
<b><math>r^2 = 0.874</math></b>				
<b>Parametric Coefficients</b>	<b>Estimate</b>	<b>Std.Error</b>	<b>t-value</b>	<b>p-value</b>
Intercept	13.770	0.905	15.220	0.000***
Acquisition month (Aug)	-1.076	0.200	-5.371	0.006***
May Precip (mm)	0.015	0.008	1.746	0.155
May Temp (°C)	0.057	0.05	1.139	0.318
July Temp (°C)	0.007	0.061	0.122	0.909
July Precip (mm)	0.020	0.004	4.508	0.012**
<b>Smooth term</b>	<b>edf</b>	<b>---</b>	<b>f-value</b>	<b>p-value</b>
Date	1.989	---	41.11	0.001***
<b>Small Lakes</b>				
<b><math>r^2 = 0.669</math></b>				
<b>Parametric Coefficients</b>	<b>Estimate</b>	<b>Std.Error</b>	<b>t-value</b>	<b>p-value</b>
Intercept	6.984	0.411	16.983	0.000***
Acquisition month (Aug)	-0.178	0.090	-1.973	0.118
May Precip (mm)	0.006	0.004	1.642	0.174
May Temp (°C)	0.016	0.023	0.722	0.509
July Temp (°C)	0.003	0.028	0.095	0.928
July Precip (mm)	0.008	0.002	4.087	0.014**
<b>Smooth term</b>	<b>edf</b>	<b>---</b>	<b>f-value</b>	<b>p-value</b>
Date	1.891	---	3.337	0.109

Table 2.3 Standardized residuals from Chi-square tests comparing lake area trends and lake/terrain characteristics (ecoregion, fire presence, lake area and geology). Values with an asterisk (\*) indicate a significant deviation from expected counts with positive values indicating more lakes than expected in that category and a negative values indicating fewer lakes than expected.

<b>Terrain Factor</b>		<b>Decreasing</b>	<b>Increasing</b>	<b>No Trend</b>
<b>Ecoregion</b>	Arctic Red Plain	3.260*	-1.761*	-0.338
	Travaillant Upland	-5.224*	2.823*	0.542
<b>Fire</b>	Within fire	9.923*	-3.615*	-2.277*
	Outside fire	-10.475*	3.816*	2.404*
<b>Lake Size</b>	Large	6.127*	-4.310*	0.079
	Medium	3.076*	-3.101*	0.708
	Small	-7.119*	6.200*	-0.941
<b>Geology</b>	Alluvial	-2.031*	3.545*	-1.656*
	Colluvial	-1.738	1.008	0.075
	Glaciofluvial	-1.711	2.921*	-1.346
	Lacustrine	-1.864*	8.783*	-5.591
	Moraine	0.448	-2.725*	1.796*
	Organic	3.325*	-5.455*	2.454*

## 2.4 Discussion

Our analysis shows that wildfire has a disproportionate influence on sub-Arctic surface water dynamics, but also shows that lake area is influenced by lake size, climate, and terrain factors. Drainage of two large lakes following a 1999 fire accounted for 14% of total water loss in the study area and the majority (79%) of lakes showing decreasing trends were located within burned areas. This is consistent with findings from Roach et al. (2013) who observed that lakes inside burned areas were 1.5 times more likely to decrease in area over time. Observed decreases in lake size within fire-impacted areas were likely caused by increased ground heat flux and active layer deepening following the combustion of vegetation and surface organics.

Observations at Arctic and sub-Arctic sites show that reduced organic layer depth, lower surface

albedo, and increased thermal conductivity following fire all contribute to long-term increases in active layer depth (Liljedahl et al., 2007; Yoshikawa et al., 2002; Zipper et al., 2018). Active layer deepening can drive decreases in lake area as soil water storage capacity and connectivity to ground water increase (Connon et al., 2014; Haynes et al., 2019; Jones, et al., 2020; Liljedahl et al., 2007; Roach et al., 2013). Further, fire may also induce the formation of sub-lake taliks which can lead to internal lake drainage (Yoshikawa et al., 2002; Yoshikawa & Hinzman, 2003). The rapid drainage of the two large lakes impacted by a 1999 fire may also reflect changes in near-surface ground ice conditions and the formation of new outlet channels (Yoshikawa et al., 2002). The initial increase in lake area we observed immediately following the 1999 fire likely resulted from unusually high rainfall in 2000 and decreased evapotranspiration following the removal of surface vegetation (Kang et al., 2006).

The strong relationship between interannual variation in lake area and July precipitation indicates that climate can also influence lake area. Despite the fact that summer precipitation and the number of large rainfall events have increased between 1985 and 2020, total surface water in the study area decreased by 1%, largely driven by declines in large and medium sized lakes (Figure 8). While the area of both large and small lakes showed a significant positive relationship with July precipitation, only small lakes experienced an overall increase in surface area (Figure 8). The greater sensitivity of small lakes to increased precipitation in the study region was likely driven by their greater surface area to volume ratios (Campbell et al., 2018; Marsh & Bigras, 1988). Greater sensitivity to climate change among small lakes and ponds has also been reported in the Arctic and sub-Arctic where decreases in lake area have been attributed to evaporative drying (Campbell et al., 2018; Carroll & Loboda, 2018; Smith et al., 2005; Smol & Douglas, 2007).

Our analyses suggest that decreases in lake area were also facilitated by differences in surficial materials across the study area. In our study region and elsewhere in the Arctic, decreases in the number and size of thermokarst lakes have been observed in areas with coarse soil texture and permeable sand deposits, while less permeable silt deposits have been associated with increasing lake area (Carroll & Loboda, 2018; Wang et al., 2018). Soil texture also influences ground-ice content, which may contribute to the frequency of thermokarst lake drainage (T. Jorgenson et al., 2008; O'Neill et al., 2019). Chi-square tests showed that lakes in more permeable organic deposits were more likely to show decreasing trends (Carroll & Loboda, 2018; Wang et al., 2018). Ecoregion classification also had a significant impact on the frequency of changes, likely because of the difference in soil texture between upland and lowland regions, which can impact the rate of drainage (Carroll & Loboda, 2018; Nitze et al., 2017). Lakes in the bedrock dominant areas Travaillant Uplands were more likely to show increasing trends in area, while lakes in the peatland regions of the Arctic Red Plain were more likely to show decrease in lake area.

Our data also shows that rapid lake drainage is an important process in our study area. Five rapid drainage events among lakes larger than  $0.05\text{km}^2$  accounted for 27% of total lake area loss. Rapid catastrophic lake drainage has been reported as a significant driver of change in many ice-rich permafrost environments (Mackay, 1988; Jones & Arp, 2015; Nitze et al., 2020; Lantz & Turner, 2015) Rapid lake drainage can occur through a range of thermokarst processes resulting in bank overtopping, head-ward erosion or the formation of a new outlet channel. We observed a rate of rapid drainage events of 0.14 lakes per year. This is lower than rates reported in studies focused on Alaska and the Tuktoyaktuk Coastal Plain where average drainage rates were 1.6 and 0.33 lakes per year over a similar time period (Jones et al., 2020; Marsh et al., 2009). Due to missing

data for some lakes we could not confirm if some drainage events occurred within a one-year period, thus our estimate of the rate of catastrophic drainage events is likely conservative.

### Bibliography

Anthony, K. M. W., Zimov, S. A., Grosse, G., Jones, M. C., Anthony, P. M., III, F. S. C., Finlay, J. C., Mack, M. C., Davydov, S., Frenzel, P., & Frolking, S. (2014). A shift of thermokarst lakes from carbon sources to sinks during the Holocene epoch. *Nature*, *511*(7510), 452. Gale OneFile: CPI.Q.

Arp, C. D., Jones, B. M., Grosse, G., Bondurant, A. C., Romanovsky, V. E., Hinkel, K. M., & Parsekian, A. D. (2016). Threshold sensitivity of shallow Arctic lakes and sublake permafrost to changing winter climate. *Geophysical Research Letters*, *43*(12), 6358–6365. <https://doi.org/10.1002/2016GL068506>

Arp, C. D., Jones, B. M., Lu, Z., & Whitman, M. S. (2012). Shifting balance of thermokarst lake ice regimes across the Arctic Coastal Plain of northern Alaska. *Geophysical Research Letters*, *39*(16). <https://doi.org/10.1029/2012GL052518>

Becker, M. S., & Pollard, W. H. (2016). Sixty-year legacy of human impacts on a high Arctic ecosystem. *Journal of Applied Ecology*, *53*(3), 876–884. <https://doi.org/10.1111/1365-2664.12603>

Campbell, T. K. F., Lantz, T. C., & Fraser, R. H. (2018). Impacts of Climate Change and Intensive Lesser Snow Goose (*Chen caerulescens caerulescens*) Activity on Surface Water in High Arctic Pond Complexes. *Remote Sensing*, *10*(12), 1892. <https://doi.org/10.3390/rs10121892>

Carroll, M. L., & Loboda, T. V. (2018). The sign, magnitude and potential drivers of change in surface water extent in Canadian tundra. *Environmental Research Letters*, *13*(4), 045009. <https://doi.org/10.1088/1748-9326/aab794>

Connon, R. F., Quinton, W. L., Craig, J. R., & Hayashi, M. (2014). Changing hydrologic connectivity due to permafrost thaw in the lower Liard River valley, NWT, Canada. *Hydrological Processes*, *28*(14), 4163–4178. <https://doi.org/10.1002/hyp.10206>

Cooley, S. W., Smith, L. C., Ryan, J. C., Pitcher, L. H., & Pavelsky, T. M. (2019). Arctic-Boreal Lake Dynamics Revealed Using CubeSat Imagery. *Geophysical Research Letters*, *46*(4), 2111–2120. <https://doi.org/10.1029/2018GL081584>

Ecosystem Classification Group. (2009). *Ecological Regions of the Northwest Territories – Taiga Plains*. (viii + 173 pp. + folded insert map.). Department of Environment and Natural Resources, Government of the Northwest Territories.

Environment Canada. (2020). *National Climate Data and Historical Information Archive*.  
<https://climate.weather.gc.ca/>

Gibson, C. M., Chasmer, L. E., Thompson, D. K., Quinton, W. L., Flannigan, M. D., & Olefeldt, D. (2018). Wildfire as a major driver of recent permafrost thaw in boreal peatlands. *Nature Communications*, 9(1), 3041. <https://doi.org/10.1038/s41467-018-05457-1>

GRRB. (2018). *Research and Management Interests for the GSA*.  
[http://www.grrb.nt.ca/pdf/Public%20registry/research/Research%20Interests\\_2018.pdf](http://www.grrb.nt.ca/pdf/Public%20registry/research/Research%20Interests_2018.pdf)

Haynes, K. M., Connon, R. F., & Quinton, W. L. (2019). Hydrometeorological measurements in peatland-dominated, discontinuous permafrost at Scotty Creek, Northwest Territories, Canada. *Geoscience Data Journal*, 6(2), 85–96. <https://doi.org/10.1002/gdj3.69>

Heine, M., Andre, A., Kritsch, I., & Cardinal, A. (2001). *Gwichya Gwich'in in Googwandak: The history and stories of the Gwichya Gwich'in ; as told by the Elders of Tsiigehtchic*. Gwich'in Social and Cultural Institute.

Hinkel, K. M., Eisner, W. R., Bockheim, J. G., Nelson, F. E., Peterson, K. M., & Dai, X. (2003). Spatial Extent, Age, and Carbon Stocks in Drained Thaw Lake Basins on the Barrow Peninsula, Alaska. *Arctic, Antarctic, and Alpine Research*, 35(3), 291–300. [https://doi.org/10.1657/1523-0430\(2003\)035\[0291:SEAACS\]2.0.CO;2](https://doi.org/10.1657/1523-0430(2003)035[0291:SEAACS]2.0.CO;2)

Jones, B. M., & Arp, C. D. (2015). Observing a Catastrophic Thermokarst Lake Drainage in Northern Alaska. *Permafrost and Periglacial Processes*, 26(2), 119–128.  
<https://doi.org/10.1002/ppp.1842>

Jones, B. M., Arp, C. D., Grosse, G., Nitze, I., Lara, M. J., Whitman, M. S., Farquharson, L. M., Kanevskiy, M., Parsekian, A. D., Breen, A. L., Ohara, N., Rangel, R. C., & Hinkel, K. M. (2020). Identifying historical and future potential lake drainage events on the western Arctic coastal plain of Alaska. *Permafrost and Periglacial Processes*, 31(1), 110–127.  
<https://doi.org/10.1002/ppp.2038>

Jones, B. M., Grosse, G., Arp, C. D., Jones, M. C., Anthony, K. M. W., & Romanovsky, V. E. (2011). Modern thermokarst lake dynamics in the continuous permafrost zone, northern Seward Peninsula, Alaska. *Journal of Geophysical Research: Biogeosciences*, 116(G2).  
<https://doi.org/10.1029/2011JG001666>

Jones, B. M., Grosse, G., Arp, C. D., Miller, E., Liu, L., Hayes, D. J., & Larsen, C. F. (2015). Recent Arctic tundra fire initiates widespread thermokarst development. *Scientific Reports*, 5.  
<https://doi.org/10.1038/srep15865>

Jorgenson, T., Yoshikawa, K., Kanevskiy, M., Shur, Y., Romanovsky, V., Marchenko, S., Grosse, G., Brown, J., & Jones, B. (2008). Permafrost Characteristics of Alaska. *Proceedings of the 9th International Conference on Permafrost*, 29, 121–122.

- Kang, S., Kimball, J. S., & Running, S. W. (2006). Simulating effects of fire disturbance and climate change on boreal forest productivity and evapotranspiration. *Science of The Total Environment*, 362(1), 85–102. <https://doi.org/10.1016/j.scitotenv.2005.11.014>
- Kasischke, E. S., & Turetsky, M. R. (2006). Recent changes in the fire regime across the North American boreal region—Spatial and temporal patterns of burning across Canada and Alaska. *Geophysical Research Letters*, 33(9). <https://doi.org/10.1029/2006GL025677>
- Kokelj, S. V., & Jorgenson, M. T. (2013). Advances in Thermokarst Research. *Permafrost and Periglacial Processes*, 24(2), 108–119. <https://doi.org/10.1002/ppp.1779>
- Lantz, T. C., & Turner, K. W. (2015). Changes in lake area in response to thermokarst processes and climate in Old Crow Flats, Yukon. *Journal of Geophysical Research: Biogeosciences*, 120(3), 513–524. <https://doi.org/10.1002/2014JG002744>
- Liljedahl, A., Hinzman, L., Busey, R., & Yoshikawa, K. (2007). Physical short-term changes after a tussock tundra fire, Seward Peninsula, Alaska. *Journal of Geophysical Research: Earth Surface*, 112(F2). <https://doi.org/10.1029/2006JF000554>
- Lindgren, P. R., Farquharson, L. M., Romanovsky, V. E., & Grosse, G. (2021). Landsat-based lake distribution and changes in western Alaska permafrost regions between the 1970s and 2010s. *Environmental Research Letters*, 16(2), 025006. <https://doi.org/10.1088/1748-9326/abd270>
- Mackay, J. R. (1988). Catastrophic lake drainage, Tuktoyaktuk Peninsula area, District of Mackenzie. *Geological Survey of Canada*, 88-1D.
- Marsh, P., & Bigras, S. C. (1988). Evaporation from Mackenzie Delta Lakes, N.W.T., Canada. *Arctic and Alpine Research*, 20(2), 220–229. <https://doi.org/10.2307/1551500>
- Marsh, P., Russell, M., Pohl, S., Haywood, H., & Onclin, C. (2009). Changes in thaw lake drainage in the Western Canadian Arctic from 1950 to 2000. *Hydrological Processes*, 23(1), 145–158. <https://doi.org/10.1002/hyp.7179>
- McLeod, A. I. (2011). *Kendall: Kendall rank correlation and Mann-Kendall trend test. R package version 2.2*. <https://CRAN.R-project.org/package=Kendall>
- Narita, K., Harada, K., Saito, K., Sawada, Y., Fukuda, M., & Tsuyuzaki, S. (2015). Vegetation and Permafrost Thaw Depth 10 Years after a Tundra Fire in 2002, Seward Peninsula, Alaska. *Arctic, Antarctic, and Alpine Research*, 47(3), 547–559. <https://doi.org/10.1657/AAAR0013-031>
- Nitze, I., Cooley, S., Duguay, C., Jones, B. M., & Grosse, G. (2020). The catastrophic thermokarst lake drainage events of 2018 in northwestern Alaska: Fast-forward into the future. *The Cryosphere Discussions*, 1–33. <https://doi.org/10.5194/tc-2020-106>

- Nitze, I., Grosse, G., Jones, B., Arp, C., Ulrich, M., Fedorov, A., & Veremeeva, A. (2017). Landsat-Based Trend Analysis of Lake Dynamics across Northern Permafrost Regions. *Remote Sensing*, 9(7), 640. <https://doi.org/10.3390/rs9070640>
- Olthof, I., Fraser, R. H., & Schmitt, C. (2015). Landsat-based mapping of thermokarst lake dynamics on the Tuktoyaktuk Coastal Plain, Northwest Territories, Canada since 1985. *Remote Sensing of Environment*, 168, 194–204. <https://doi.org/10.1016/j.rse.2015.07.001>
- O'Neill, H. B., Wolfe, S. A., & Duchesne, C. (2019). New ground ice maps for Canada using a paleogeographic modelling approach. *The Cryosphere*, 13(3), 753–773. <https://doi.org/10.5194/tc-13-753-2019>
- Pastick, N. J., Jorgenson, M. T., Goetz, S. J., Jones, B. M., Wylie, B. K., Minsley, B. J., Genet, H., Knight, J. F., Swanson, D. K., & Jorgenson, J. C. (2019). Spatiotemporal remote sensing of ecosystem change and causation across Alaska. *Global Change Biology*, 25(3), 1171–1189. <https://doi.org/10.1111/gcb.14279>
- Plug, L. J., Walls, C., & Scott, B. M. (2008). Tundra lake changes from 1978 to 2001 on the Tuktoyaktuk Peninsula, western Canadian Arctic. *Geophysical Research Letters*, 35(3). <https://doi.org/10.1029/2007GL032303>
- Pohl, S., Marsh, P., Onclin, C., & Russell, M. (2009). The summer hydrology of a small upland tundra thaw lake: Implications to lake drainage. *Hydrological Processes*, 23(17), 2536–2546. <https://doi.org/10.1002/hyp.7238>
- Roach, J. K., Griffith, B., & Verbyla, D. (2013). Landscape influences on climate-related lake shrinkage at high latitudes. *Global Change Biology*, 19(7), 2276–2284. <https://doi.org/10.1111/gcb.12196>
- Schuur, E. a. G., McGuire, A. D., Schädel, C., Grosse, G., Harden, J. W., Hayes, D. J., Hugelius, G., Koven, C. D., Kuhry, P., Lawrence, D. M., Natali, S. M., Olefeldt, D., Romanovsky, V. E., Schaefer, K., Turetsky, M. R., Treat, C. C., & Vonk, J. E. (2015). Climate change and the permafrost carbon feedback. *Nature*, 520(7546), 171–179. <https://doi.org/10.1038/nature14338>
- Serreze, M. C., Barrett, A. P., Stroeve, J. C., Kindig, D. N., & Holland, M. M. (2009). The emergence of surface-based Arctic amplification. *The Cryosphere*, 9.
- Smith, L. C., Sheng, Y., MacDonald, G., M., & Hinzman, L. D. (2005). Disappearing Arctic Lakes. *Science*, 208, 1429–1431.
- Smol, J. P., & Douglas, M. S. V. (2007). Crossing the final ecological threshold in high Arctic ponds. *Proceedings of the National Academy of Sciences*, 104(30), 12395–12397. <https://doi.org/10.1073/pnas.0702777104>

- Swanson, D. K. (2019). Thermokarst and precipitation drive changes in the area of lakes and ponds in the National Parks of northwestern Alaska, 1984–2018. *Arctic, Antarctic, and Alpine Research*, 51(1), 265–279. <https://doi.org/10.1080/15230430.2019.1629222>
- Turner, K. W., Wolfe, B. B., Edwards, T. W. D., Lantz, T. C., Hall, R. I., & Larocque, G. (2014). Controls on water balance of shallow thermokarst lakes and their relations with catchment characteristics: A multi-year, landscape-scale assessment based on water isotope tracers and remote sensing in Old Crow Flats, Yukon (Canada). *Global Change Biology*, 20(5), 1585–1603. <https://doi.org/10.1111/gcb.12465>
- Walter Anthony, K. M., Schneider von Deimling, T., Nitze, I., Frolking, S., Emond, A., Daanen, R., Anthony, P., Lindgren, P., Jones, B., & Grosse, G. (2018). 21st-century modeled permafrost carbon emissions accelerated by abrupt thaw beneath lakes. *Nature Communications*, 9(1), 1–11. <https://doi.org/10.1038/s41467-018-05738-9>
- Wang, L., Jolivel, M., Marzahn, P., Bernier, M., & Ludwig, R. (2018). Thermokarst pond dynamics in subarctic environment monitoring with radar remote sensing. *Permafrost and Periglacial Processes*, 29(4), 231–245. <https://doi.org/10.1002/ppp.1986>
- Watts, J. D., Kimball, J. S., Jones, L. A., Schroeder, R., & McDonald, K. C. (2012). Satellite Microwave remote sensing of contrasting surface water inundation changes within the Arctic–Boreal Region. *Remote Sensing of Environment*, 127, 223–236. <https://doi.org/10.1016/j.rse.2012.09.003>
- Wood, S. N. (2017). *Generalized Additive Models: An Introduction with R* (2nd ed.). Chapman and Hall.
- Yoshikawa, K., Bolton, W. R., Romanovsky, V. E., Fukuda, M., & Hinzman, L. D. (2002). Impacts of wildfire on the permafrost in the boreal forests of Interior Alaska. *Journal of Geophysical Research: Atmospheres*, 107(D1), FFR 4-1-FFR 4-14. <https://doi.org/10.1029/2001JD000438>
- Yoshikawa, K., & Hinzman, L. D. (2003). Shrinking thermokarst ponds and groundwater dynamics in discontinuous permafrost near council, Alaska. *Permafrost and Periglacial Processes*, 14(2), 151–160. <https://doi.org/10.1002/ppp.451>
- Zeileis, A. (2004). Implementing a Class of Structural Change Tests: An Econometric Computing Approach. *Computational Statistics & Data Analysis*, 50, 2987–3008.
- Zipper, S. C., Lamontagne-Hallé, P., McKenzie, J. M., & Rocha, A. V. (2018). Groundwater Controls on Postfire Permafrost Thaw: Water and Energy Balance Effects. *Journal of Geophysical Research: Earth Surface*, 123(10), 2677–2694. <https://doi.org/10.1029/2018JF004611>

## Appendix 1: Sub-pixel water fraction method

We applied a method developed by Olthof et al. (2015) to map surface water using data from the Landsat satellite image archive. Low SWIR reflectance generally corresponds to water, while moderate to high reflectance generally corresponds to land. Thresholds in SWIR reflectance representing pure land and water pixels were defined using breakpoints in the histogram of SWIR reflectance values. Pixels with reflectance greater than the land threshold were classified as 100% land, and pixels with reflectance less than the water threshold were classified as 100% water. Between these thresholds, the fraction of each pixel covered by water is estimated by linear interpolation between the pure water and land SWIR thresholds. This method assumes that as SWIR reflectance increases above the pure water threshold, sub-pixel water fraction decreases at a constant rate until reflectance values are equal to the land threshold. Olthof et al. (2015) show that this method outperforms binary classifications of land and water as well as linear un-mixing techniques. To apply this method, we defined pure land and water thresholds using mean threshold values from a random subset of 12 scenes used in this analysis. We also checked for linear trends in threshold values over time and detected no significant trend. We applied a pure water threshold of 0.024 and a pure land threshold of 0.079 to all images in the study area.

High resolution air photos from the Mackenzie Valley Air Photo Project acquired in 2004 at 1:30000 scale were used to assess the accuracy of lake area derived from Landsat scenes (Schwarz et al., 2007). Sub-pixel water fraction was calculated using a Landsat scene acquired the same month and year as the air photos. The area of 114 lakes larger than 100m<sup>2</sup> was manually digitized in ArcGIS while viewing the air photos at approximately 1:500 scale. The lake mask created using the sub-pixel water fraction method was buffered by 30m and lake area was calculated by multiplying the sum of all SWF pixels within the mask by a pixel area of 900m<sup>2</sup>. We calculated relative error for water bodies as:  $(Area_{SWF} - Area_{AF})/Area_{AF}$ . Where  $Area_{SWF}$  is the area obtained from the SWF method and  $Area_{AF}$  is the area based on air photo digitization. The SWF method underestimated total surface water area by 6%, but error for individual lakes varied substantially depending on the size of the lake. Smaller lakes showed higher error, and little error was observed from lakes greater than 0.1km<sup>2</sup> (Figure A1.1). The SWF method was not able to consistently detect lakes smaller than 1500m<sup>2</sup> (0.001km<sup>2</sup>).

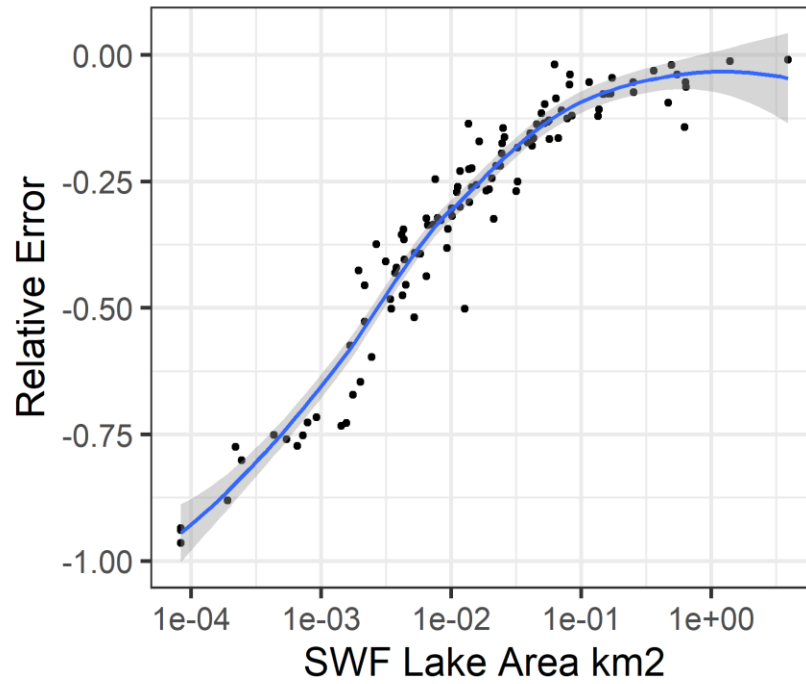


Figure A.10: Relative error in lake area calculated as:  $(Area_{SWF} - Area_{AF})/Area_{AF}$ . The x-axis is displayed on a logarithmic scale and the shaded area around the fitted line represents the 95% confidence interval for the slope parameter.

## Appendix 2: Lake area trend classification

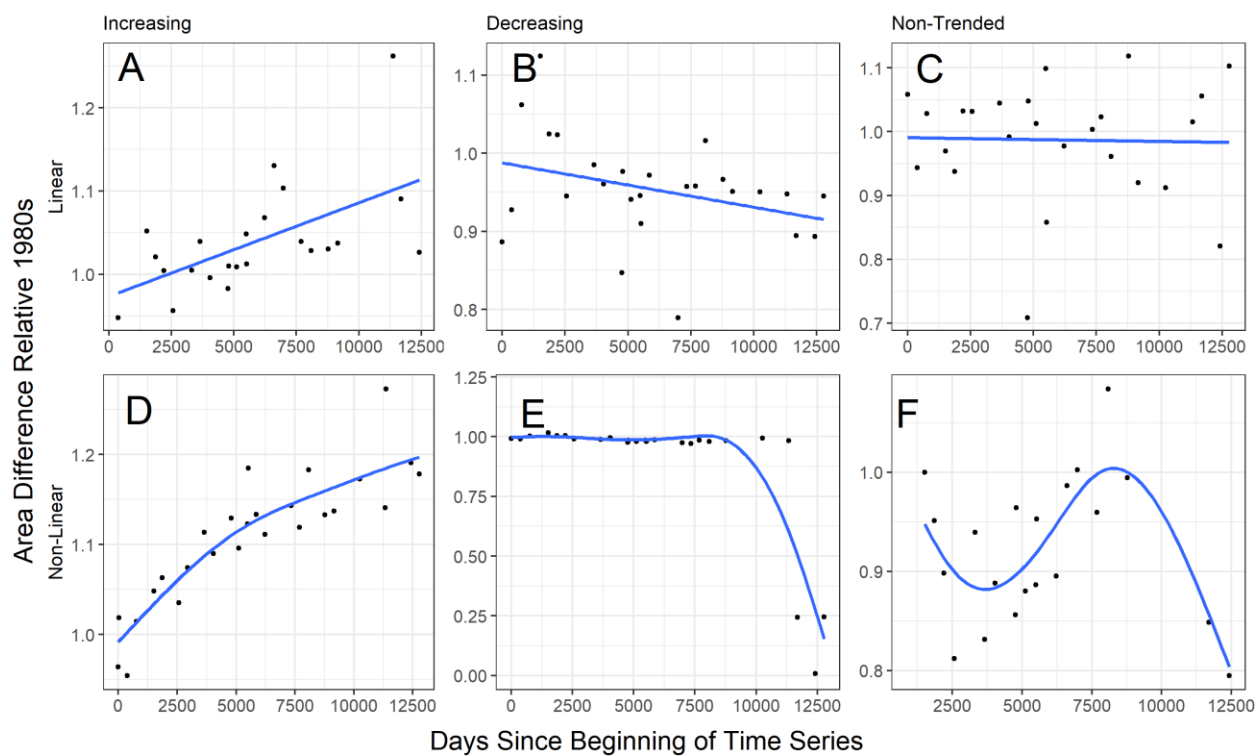


Figure A.2: Example times series showing the categories used to classify changes in lake area depending on the direction of change and whether change over time was linear or non-linear. Plots A-C show different linear trends and plots D-F show different non-linear patterns. The blue line shows the fitted model using Ordinary Least Squares (OLS) regression for the linear class and a Generalized Additive Model (GAM) with a smooth term for time for the non-linear class. Note that the range of the y-axis varies among plots.

### **3. Drivers of surface water change across the western Canadian Arctic and Sub-Arctic**

Hana Travers-Smith<sup>1</sup>, Trevor C. Lantz<sup>1</sup>, Robert H. Fraser<sup>2</sup>

1. School of Environmental Studies, University of Victoria

2. Canada Centre of Remote Sensing

### 3.1 Introduction

Rising air temperatures and increasing precipitation are driving changes in surface water across Arctic and boreal ecosystems (Nitze et al., 2017; Pastick et al., 2019; Smith et al., 2005; Watts et al., 2012). The direction and magnitude of these changes have been associated with terrain factors including ground-ice content (Jones et al., 2020; Swanson, 2019; Yoshikawa & Hinzman, 2003), permafrost distribution (Nitze et al., 2017; Smith et al., 2005), surficial geology (Carroll & Loboda, 2018; Nitze et al., 2017; Wang et al., 2018) and vegetation cover (K. W. Turner et al., 2014). Understanding factors influencing the trajectory of change in surface water is important because lakes can cover over 40% of the land surface at high latitudes, and have a significant impact on the climate system and carbon cycle (Grosse et al., 2013; Hinkel et al., 2003; E. a. G. Schuur et al., 2015; Tarnocai et al., 2009). Trends in the number and size of lakes have been investigated using medium (30m) and high (<1m) resolution remote sensing imagery (Bouchard et al., 2013; Cooley et al., 2019; Jones et al., 2011; Nitze et al., 2017) and recent research showing high year to year variation and non-linear changes in lake area highlights the need for analyses with high temporal and spatial resolution (Carroll & Loboda, 2017; S. W. Cooley et al., 2019).

A number of recent studies suggest that patterns in lake expansion and drainage are influenced by permafrost zonation (Kokelj & Jorgenson, 2013; Nitze et al., 2020). Continuous permafrost has generally been associated with increases in the area of surface water (Nitze et al., 2017; Olthof et al., 2015; Walter et al., 2006), and discontinuous permafrost has been associated with decreases in surface water (Rover et al., 2012; Smith et al., 2005; Smol & Douglas, 2007).

However, reports of decreases in lake area in the continuous permafrost zone driven by the rapid drainage of large lakes (Jones et al., 2011; Lantz & Turner, 2015; Lindgren et al., 2021; Travers-

Smith et al., In Review), and evaporative drying (Campbell et al., 2018), suggest that regional controls of lake area are also important. Previous remote sensing analyses in the western Canadian Arctic have focused primarily on regions with continuous permafrost (S. V. Kokelj et al., 2005; Labrecque et al., 2009; Lantz & Turner, 2015; Olthof et al., 2015; Plug et al., 2008; Pohl et al., 2009), and despite recent research showing substantial seasonal variation in the area of surface water area in shield dominated areas (S. W. Cooley et al., 2019), lake dynamics in bedrock landscapes remain understudied.

In regions that have high-levels of ground ice, thermokarst processes can also have a significant impact on the area of lakes and ponds (Grosse et al., 2013; S. V. Kokelj & Jorgenson, 2013; Lantz & Turner, 2015; Nitze et al., 2020a). Rising air temperatures, changes in the intensity of precipitation, and more frequent wildfire are also increasing the frequency of thermokarst disturbances across the circumpolar (Fraser et al., 2018; Hu et al., 2015; Kasischke & Turetsky, 2006; Segal et al., 2016). Wildfire is an especially important driver of permafrost dynamics in boreal regions (Jones et al., 2015a; Narita et al., 2015; Yoshikawa et al., 2002; Zipper et al., 2018), where it can initiate a range of thermokarst processes including the formation of thermokarst bogs, fens and high and low-centre polygons (Gibson et al., 2018; Jones et al., 2015a; Zipper et al., 2018). Surface water in lake-rich regions of the boreal is also impacted by fire; but these effects have not been studied in detail (Roach et al., 2013).

In this study we examined the influence of terrain and climate factors on net changes in the area of surface water across the western Canadian Arctic and sub-Arctic. Our goal was to quantify landscape level drivers of change and predict areas that may be susceptible to ongoing climate warming. To accomplish this, we used the Global Surface Water Change dataset developed by Pickens et al. (2020) to summarize change in total permanent water across the NWT and Yukon.

We also trained a Random Forests model to predict changes in surface water using a range of broad-scale terrain and climate variables. To investigate regional drivers of change we selected six regions in both continuous and discontinuous permafrost zones representing a range of climatic and geologic conditions. In each study area we used the Landsat satellite archive to map trends in the area of individual lakes from 1985 to 2020, and examined the potential drivers of change. Based on recent findings in the Lower Mackenzie Plain (Travers-Smith et al., In Review), we also examined the role of fire in initiating abrupt non-linear decreases in lake area within upland and lowland boreal sites.

## **3.2 Methods**

### **3.2.1 Study Domain**

Our study domain covers approximately 1.4 million km<sup>2</sup> of western Canada, including the Northwest Territories, Yukon and Nunavut (Figure 3.1). Average annual temperature across this area decreases with increasing latitude with temperatures of -4.3°C at Yellowknife (62° 27' 46") and -10.1°C at Tuktoyaktuk (69° 26' 00"). The southern part of the study area is within the discontinuous permafrost zone and the northern part of the study area is underlain by continuous permafrost (Figure 3.1). Vegetation and surficial geology vary across the study area, which includes four ecozones: the Southern Arctic, the Taiga Plains, the Taiga Shield and the Taiga Cordillera.

The Southern Arctic extends northward from the limit of continuous forest to the coast of the Beaufort Sea and Amundsen Gulf. It is characterized by dwarf and low-shrub tundra and is underlain by glaciofluvial, lacustrine and marine sediments (Ecosystem Classification Group, 2012). This region experiences short, cold summers and long winters with 130-300mm of annual precipitation (Table 3.1). Annual temperature and precipitation are slightly higher in the southern

portion of this ecozone. The Taiga Plains covers the central portion of the study area and is characterized by spruce and pine forests (Ecosystem Classification Group, 2009). Forest fire is an important driver of vegetation change in this ecoregion and extensive peatlands and lake complexes are also common (Ecosystem Classification Group, 2009). Temperature and precipitation vary considerably across this ecoregion, with the northernmost area experiencing conditions similar to the Southern Arctic and the southernmost part of this ecoregion experiencing warm, moist summers with over 300-500mm of annual precipitation (Ecosystem Classification Group, 2009). The Taiga Shield is located in the northeastern part of the study domain and is characterized by a mosaic of Precambrian bedrock and glacial till. Much of this region was once covered by glacial Lake McConnell, which drained approximately 8.3ka depositing fine-grained lacustrine sediments (Smith, 1994). Vegetation in this region varies from closed spruce, pine and aspen forests in the south to isolated spruce stands in the north (Ecosystem Classification Group, 2010). Climate across this ecozone depends on latitude, with northernmost areas experiencing short, cool summer and very cold winters and the southernmost portion with warm, moist summers and mean annual temperatures above 0°C (Ecosystem Classification Group, 2010). The Boreal Cordillera and Taiga Cordillera ecozones occupy the south western portion of the study domain and includes large areas of alpine terrain underlain by colluvial deposits. Lakes in this region are generally small and sparsely distributed (Ecosystem Classification Group, 2010).

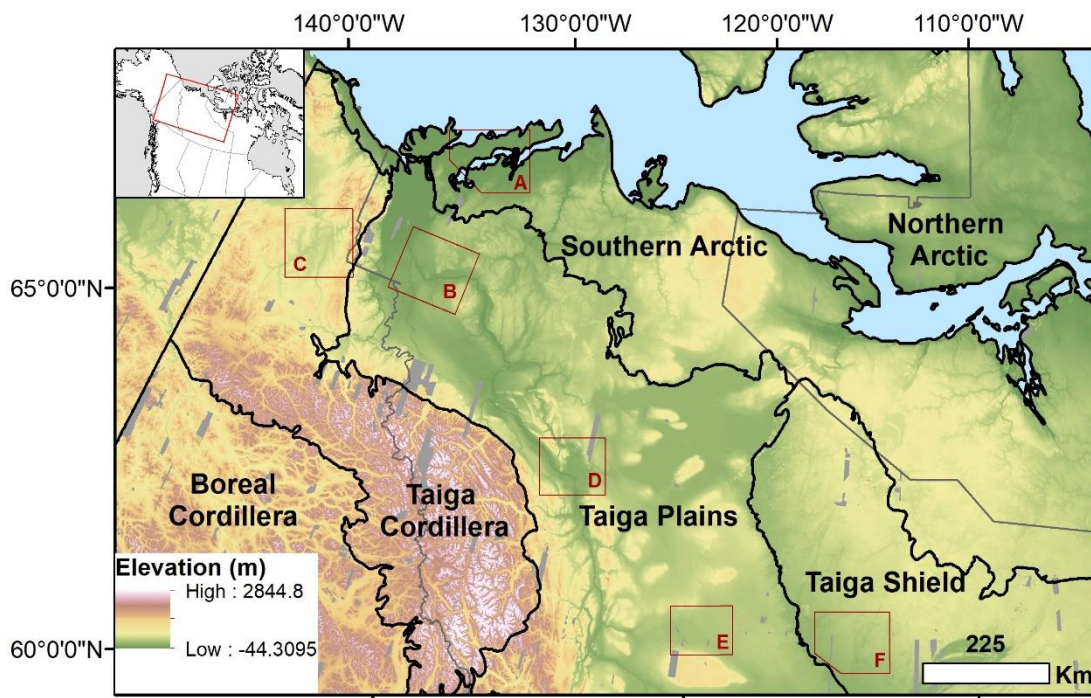


Figure 3.11: Map of the study domain in the western Canadian Arctic showing the major ecozones and elevation from Arctic DEM (Porter et al., 2018). Study areas used to explore regional controls of surface water are shown with red boxes: A) Tuktoyaktuk Coastal Plain, B) Lower Mackenzie Plain, C) Eagle Plains, D) Central Mackenzie Valley, E) Bulmer Plain and F) Great Slave Upland. The inset map in the upper left shows the location of the study domain within Canada.

Table 3.1: Climate normals (1981-2010) across the study domain in the western Canadian arctic. Data is from ECCC and can be found at: [https://climate.weather.gc.ca/climate\\_normals/index\\_e.html](https://climate.weather.gc.ca/climate_normals/index_e.html)

Station	Latitude	Longitude	Mean Annual Temperature (°C)	Total Rainfall (mm)	Total Snowfall (mm)
Tuktoyaktuk	69° 26' 00"	133° 01' 35"	-10.1	74	103
Old Crow	67° 34' 14"	139° 59' 21"	-8.3	154	141
Fort McPherson	67° 24' 28"	134° 51' 37"	-7.3	145	152
Norman Wells	65° 16' 57"	126° 48' 01"	-5.1	171	161
Yellowknife	62° 27' 46"	114° 26' 25"	-4.3	170	157

### 3.2.2 Net Change in Surface Water

We used the Global Surface Water Dynamics (1999-2020) data product developed by the Global Land Analysis and Discovery group to summarize changes in the area of permanent water across the study domain (Pickens et al., 2020). This dataset was developed using the Landsat satellite archive to classify global changes in surface water at 30m resolution (Pickens et al., 2020). Inter and intra-annual water dynamics were classified per-pixel based on variation in annual water percent, which was defined as the percent of annual observations flagged as water for a given pixel. Pixels consistently flagged as water were classified as permanent water, while pixels showing variation in annual water percent were classified based on the direction of change and the number of transitions from water to land. The classification system includes permanent water, seasonal water, permanent water gains, permanent water losses and bi-directional trends. Data covering the study domain were downloaded from the GLAD Surface Water Dynamics dataset online portal (<https://glad.umd.edu/dataset/global-surface-water-dynamics>), and projected to the Lambert Conformal Conic coordinate system. Using a grid of 100km<sup>2</sup> cells, we calculated the number of pixels classified as 1) permanent water, 2) probable water, 3) water gain and 4) water loss within each grid cell. The area of total permanent water per grid cell was calculated as the number of permanent water pixels and probable water pixels multiplied by the pixel area (~272m<sup>2</sup>). Net change in the area of permanent water in each grid cell was calculated as the difference between the number of pixels showing gains in surface water and the number of pixels representing losses, multiplied by the pixel resolution. To reduce noise in cells with low water area, we removed cells with less than 5km<sup>2</sup> of total permanent water (n=5528/12691). To calculate relative change in the area of surface water in each grid cell, we divided net change in the area of surface water by the area of total permanent water and multiplied by 100. Next, we classified net change in each grid cell as either stable, increasing or decreasing. To establish

thresholds to classify grid cells, we took the absolute value of the percent change per grid cell and used the median value of 0.7% as the positive and negative thresholds. Cells with relative change greater than 0.7% were classified as increasing, and cells with relative change less than -0.7% were classified as decreasing, all other cells were classified as stable (Appendix 1).

To predict increasing and decreasing trends in total permanent water we used a classification Random Forests model (Breiman, 2001). Explanatory variables used in this model are described in Table 3.2. Random forests were created in R using the randomforests package (Liaw & Wiener, 2002). Each tree was trained on a balanced sample of change classes to account for class imbalance in the data. Cells completely covered by water were excluded from analysis. We estimated the relative impact of terrain and climate variables on surface water dynamics using the unscaled mean decrease in accuracy to calculate variable importance. We also plotted partial dependence plots showing the marginal probability of a cell belonging to the increasing or decreasing classes across the range of the explanatory variables and using the pdp package in R (Greenwell, 2017).

Table 3.2: Explanatory variables used in the Random Forests classifier to predict increasing and decreasing change in total permanent water within 10x10km grid cells.

<b>Variable</b>	<b>Description</b>	<b>Resolution - Calculation</b>	<b>Reference</b>
Average temperature	Average annual temperature 1970-2000	2.5min resolution – value at cell centroid	Fink & Hijmans, 2017
Total precipitation	Total annual precipitation 1970-2000	2.5min resolution – value at cell centroid	Fink & Hijmans, 2017
Snow water equivalent	Change in annual maximum snow water equivalent 1981-2016	0.25x0.25° resolution - Mann-Kendall slope of annual max SWE	Mudryk et al., 2018
Vegetation zone	Major vegetation zones of Canada	Majority class per cell	Baldwin, 2019
Fire history	Fire perimeters below treeline in NWT and Yukon	Percent coverage of fire affected area per cell	Geomatics Yukon, 2019; NWT Centre for Geomatics, 2020
Surficial geology	National scale surficial geology	Majority class per cell	Fulton, 1989
Ground ice content	Percent ground ice content classified on a 5 point scale	Median per cell	O’Neill et al., 2020
Permafrost zonation	Zones defined based on extent of frozen ground: discontinuous, continuous, sporadic	Majority class per cell	O’Neill et al., 2020

### 3.2.3 Regional Change in Surface Water

We selected six study areas across the NWT and Yukon to investigate the regional controls of surface water (Figure 3.3). Study areas were selected in areas showing stable and dynamic patterns in net surface water across a range of climatic, geologic and permafrost conditions (Table 3.3). Detailed descriptions of each study area are presented in Appendix 2.

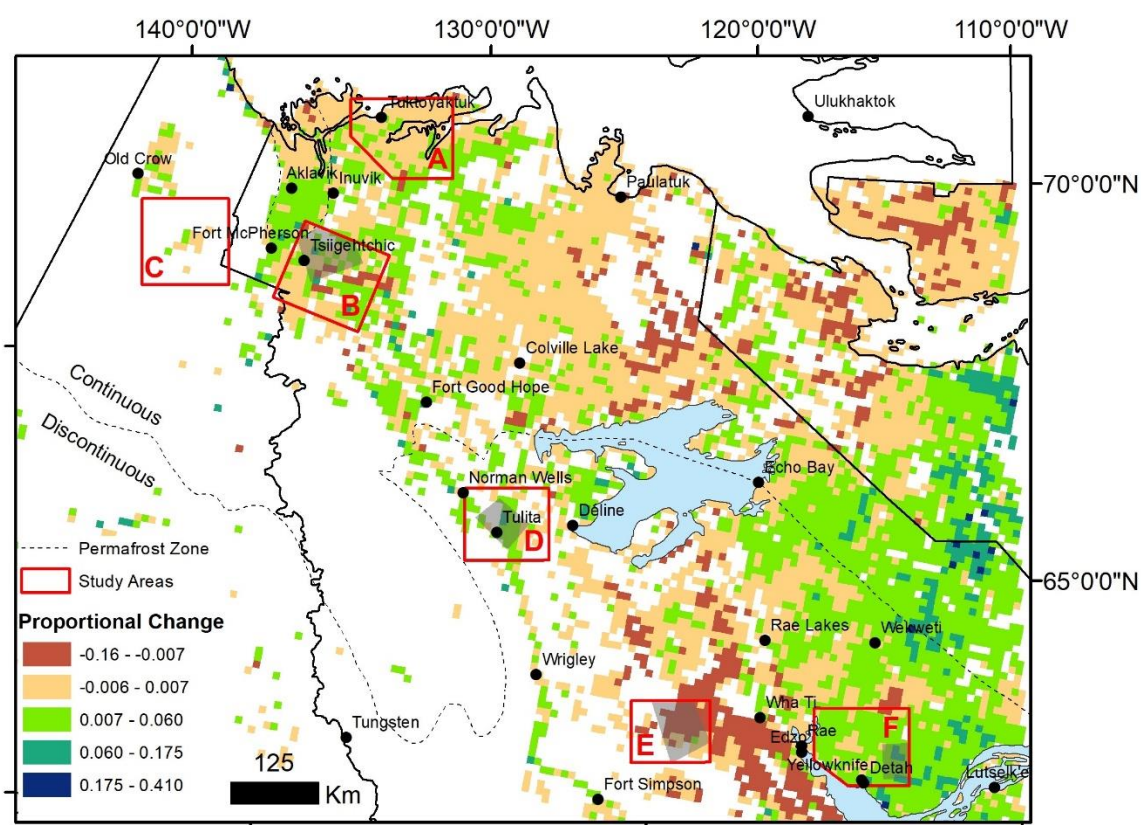


Figure 3.2: Map of the study domain showing proportional change in total permanent water between 1999 and 2020 derived from the GLAD Global Surface Water Dataset (Pickens et al., 2020). Only cells with over 5km of total permanent water are shown. Study areas used to explore regional controls of surface water are shown with red boxes: A) Tuktoyaktuk Coastal Plain, B) Lower Mackenzie Plain, C) Eagle Plains, D) Central Mackenzie Valley, E) Bulmer Plain and F) Great Slave Upland. The dashed line shows the boundary between continuous and discontinuous permafrost (O’Neil, 2019) and the grey boxes show the extent of the fire boundaries shown in Figure 3.7.

Table 3.3: Summary table showing the physical parameters within the six regional study areas.

<b>Study Area</b>	<b>Dominant Surficial Deposit</b>	<b>Ecoregion</b>	<b>Number of water bodies</b>	<b>Maximum lake area*</b>	<b>Permafrost Zone</b>
<b>Tuktoyaktuk Coastal Plain</b>	Glaciofluvial, glaciolacustrine	Southern Arctic	7848	2781km <sup>2</sup>	Continuous
<b>Lower Mackenzie Plain</b>	Till blanket	Taiga Plains	5379	1623km <sup>2</sup>	Continuous
<b>Eagle Plain</b>	Colluvial	Taiga Cordillera	883	197km <sup>2</sup>	Continuous
<b>Central Mackenzie Valley</b>	Till veneer, lacustrine	Taiga Plains	2642	628km <sup>2</sup>	Discontinuous
<b>Bulmer Plain</b>	Till blanket	Taiga Plains	3000	675km <sup>2</sup>	Discontinuous
<b>Great Slave Upland</b>	Bedrock, lacustrine	Taiga Shield	8003	2449km <sup>2</sup>	Discontinuous

### 3.2.4 Landsat Processing

In each of the six study areas we acquired all available July and August Landsat scenes from 1985 to 2020 with less than 30% cloud cover (Dwyer, 2019). We restricted our acquisitions to Tier 1 Collection 1 Top of Atmosphere (TOA) images that are most suitable for time series analysis (Dwyer, 2019). These images have minimal geometric error and have been radiometrically calibrated across different Landsat for use in time-series analysis (Dwyer, 2019). We used the Quality Assessment Band to mask clouds and cloud shadows and each scene was visually inspected and discarded if smoke or clouds remained in the study area.

We used the histogram breakpoint method developed by Olthof et al., (2015) to map annual surface water. This method uses thresholds in the shortwave infrared reflectance band (SWIR1) to quantify the proportion of a pixel covered by water (sub-pixel water fraction). Breakpoints in the histogram of SWIR reflectance were used to define a lower threshold representing pure water pixels and an upper threshold representing pure land pixels. Pixels with reflectance lower than

the water threshold were classified as 100% water and pixels with reflectance greater than the land threshold were classified as 100% land. For pixels with values between the water and land thresholds, we estimated sub-pixel water fraction using linear interpolation between the two thresholds. To apply this method, we calculated separate water and land thresholds for each study area using mean thresholds calculated from a subset of images across all Landsat sensors. We created masks of maximum water area in each study area by classifying pixels where sub-pixel water fraction was greater than 0.5 in at least two scenes as water. Individual lake objects were created by transforming the maximal water area raster to polygon features in ArcMap 10.7.1 (Table 2). We removed ponds smaller than  $0.03\text{km}^2$  and water bodies that were not completely inside the study area. The lake mask was buffered by 30m and the lake area in each scene was calculated as the sum of the sub-pixel water fraction (ranging from 0 to 1) within the lake mask multiplied by the pixel resolution ( $900\text{m}^2$ ). This method has been previously validated for a boreal region (Travers-Smith et al., In Review) and a tundra site (Olthof et al., 2015).

### **3.2.5 Mapping Trends in Lake Area**

To compare changes in surface water dynamics among study areas, we performed the following analysis in each area. For each water body, we calculated annual change relative to the average lake area during a reference period from 1985 to 1990. Lakes were also grouped into the following size classes based on average area during the reference period: 1) large lakes ( $>0.5\text{km}^2$ ), medium lakes ( $0.05\text{-}0.5\text{km}^2$ ), and small lakes ( $<0.05\text{km}^2$ ). To test for trends in the area of individual lakes we used the Kendall package in R to calculate Kendall's Tau statistic and associated p-value (McLeod, 2011). Using a p-value threshold of 0.1, lakes were classified as either significantly increasing, significantly decreasing or not significantly trended in area. The

proportion of lakes exhibiting significant trends in surface area in each study area are shown in Table 5.

To explore interannual changes in total lake area we used a subset of lakes where Landsat imagery allowed estimates of area in more than half of the available Landsat acquisitions between 1985 and 2020. To minimize the impact of missing data in the time-series, we calculated a five-point rolling mean for each lake and estimated total lake area and lake area by size class using the sum of lake area within each time-period. To calculate relative change over time we compared lake area in each time-period to the average area in the first time-period. These results were also compared with the change in total lake area between the beginning and end of the time-series, which was calculated as  $(Area_{t1} - Area_{tn}) / Area_1$ , where  $Area_{t1}$  is lake area in the first time period and  $Area_{tn}$  is lake area in the last time period.

### **3.2.6 Rapid Lake Drainage and Wildfire**

Data on the area of surface water in individual lakes was also used to identify rapid lake drainage events, which we defined as permanent loss of at least 30% lake area that occurred in a single year. We used the breakpoint regression function in the R package `strucchange` to identify large ( $>0.05\text{km}^2$ ) lakes exhibiting rapid declines in surface water (Zeileis, 2004). We also examined the time series for all lakes showing a decrease in relative area of more than 30%, and at least one significant breakpoint. Visual inspection of each time series allowed us to distinguish rapidly drained lakes from lakes exhibiting gradual water loss or bi-directional trends (Appendix 3). In each study site we also calculated the lake area lost via rapid drainage events and compared this to the overall change in surface water.

To explore the impact of fire on non-linear decreases in lake area in regions affected by forest fire (Lower Mackenzie Plain, Central Mackenzie Valley, Bulmer Plain, Great Slave Upland regions), we used chi-square analysis to test if there were a larger number of lakes with increasing or decreasing trends in area impacted by recent fires. In each study area we selected one fire that burned between 1985 and 2020 and was at least 10,000m<sup>2</sup> in area (Figure 4) and used boxplots compare changes in median area for lakes inside burned areas and unburned areas within 10km of each fire boundary.

### **3.3 Results**

#### **3.3.1 Random Forests**

Across the entire study domain the area of total permanent surface water increased by 1158km<sup>2</sup> (1.2%) between 1999 and 2020. Unscaled variable importance from the Random Forests classification shows that the most important predictors of the direction of change in surface water (increasing or decreasing), were mean annual air temperature, surficial geology, ground ice content and total annual precipitation (Figure 3.3). Partial dependence plots for temperature shows that the probability of observing increasing surface water is greatest when temperature is low and precipitation is high (Figure 3.4). Partial dependence plots also show that increases in surface water were more likely to occur in areas underlain by fine-colluvial sediment, Precambrian bedrock and in regions with low ground ice content, representative of much of the Taiga Shield ecoregion. Conversely, regions underlain by till blanket and moderate to high ground ice content were most likely to show decreases in the area of surface water (Figure 3.5). The Random Forests classification showed an out of bag error rate of 9.26% and a Kappa score

of 0.70, indicating substantial agreement between predicted and actual change classes (Landis & Koch, 1977).

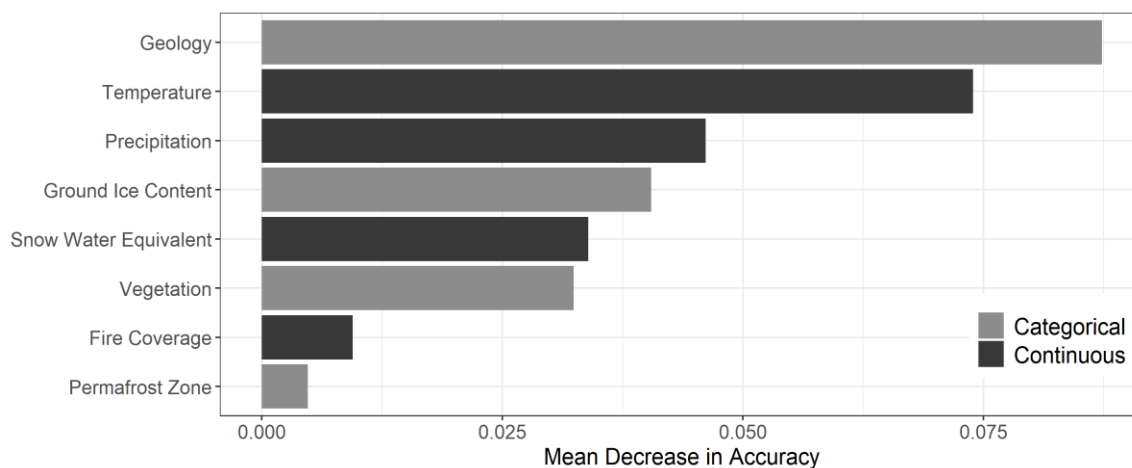


Figure 3.3: Variable importance plot from the Random Forests Model of lake-trend type (increasing, decreasing, stable). Unscaled variable importance shows the mean decrease in model accuracy if that variable is removed.

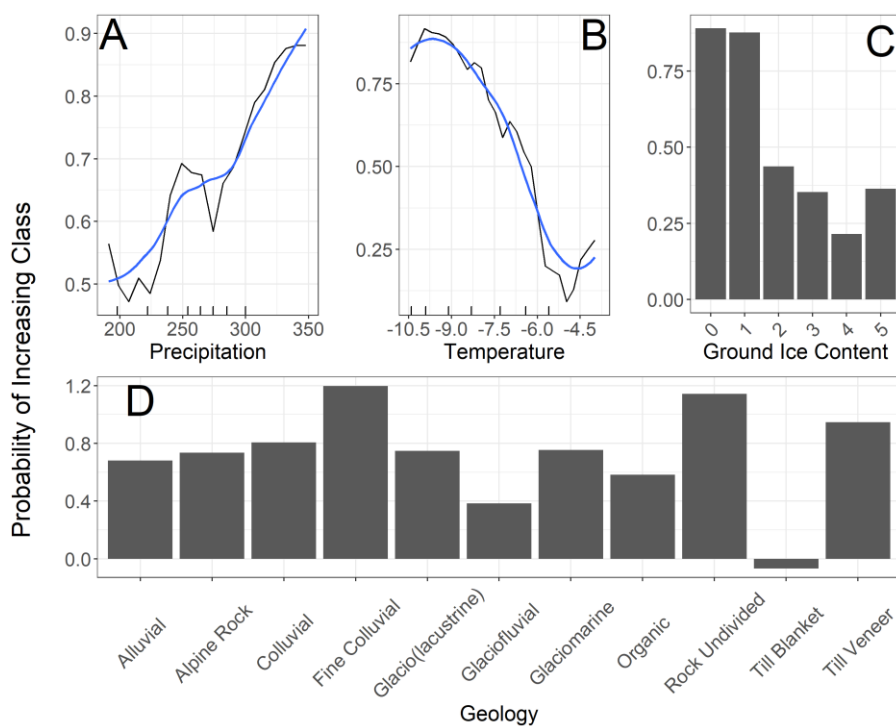


Figure 3.4: Partial dependence plots showing the probability of observing increasing surface water area as a function of the four most important independent variables in the random forests model: (A)

precipitation, (B) temperature (C) ground ice content (ranked on a 5 point scale, with 5 representing high ice content) and (D) surficial geology. Negative probability values indicate that increases in area were less likely at that value of the independent variable. Note that the x-axis has been scaled to avoid plotting partial dependence at levels not characteristic of the study domain. Rug marks show the deciles of the precipitation and temperature data. The blue line in A and B shows the smoothed trend.

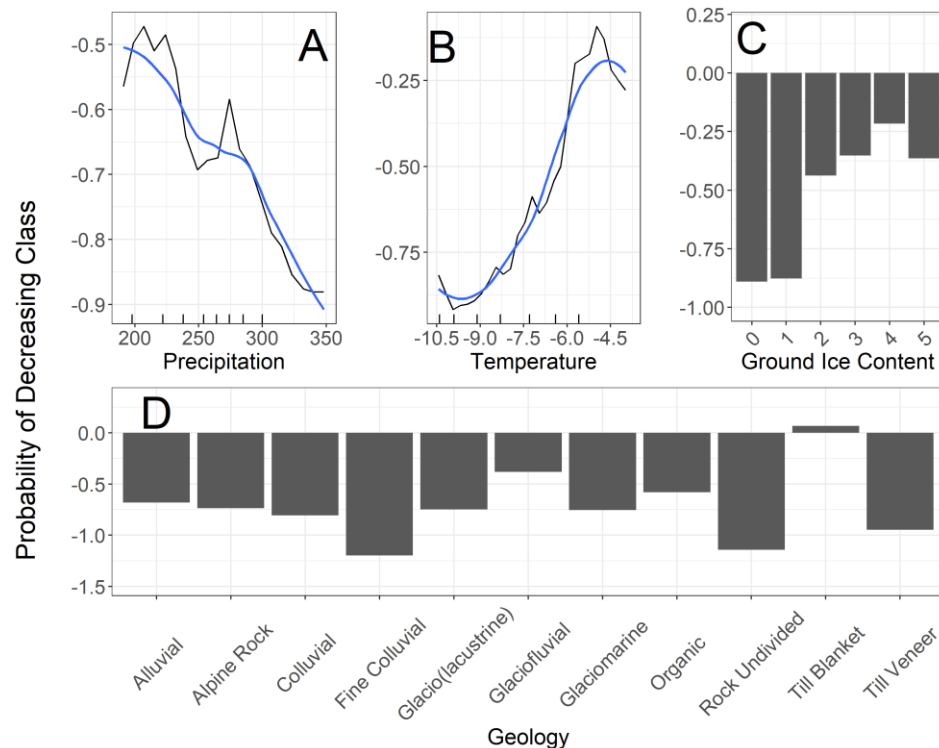


Figure 3.5: Partial dependence plots showing the probability of observing decreasing surface water area as a function of the four most important independent variables in the random forests model: (A) precipitation, (B) temperature and (C) ground ice content (ranked on a 5 point scale, with 5 representing high ice content) and (D) surficial geology. Negative probability values indicate that decreases in area were less likely at that value of the independent variable. Note that the x-axis has been scaled to avoid plotting partial dependence at levels not characteristic of the study domain. Rug marks show the deciles of the precipitation and temperature data. The blue line in A and B shows the smoothed trend.

### 3.3.2 Regional Lake Change

Overall, the direction of change in surface water across the entire study domain was consistent with changes observed in the smaller study areas. Four of the six study areas showed increasing surface water with an average change of 1.3%, consistent with the 1.2% increase observed across the larger study domain (Table 3.4). Within these smaller areas we observed the greatest percent

increase in surface water in the Tuktoyaktuk Coastal Plain (2.7%). All study areas had a greater proportion of lakes showing significant increasing trends compared to decreasing trends (Figure 3.8). The Tuktoyaktuk Coastal Plain showed the greatest proportion of lakes with significant increases (74%) and the Bulmer Plain site exhibited the least (17%). The Bulmer Plain study area showed negligible change between the beginning and end of the time series (0.00%), but the area of small lakes fluctuated considerably during the time series (Figure 3.6).

The magnitude of change also varied by lake size in all study areas (Figure 3.6). Small lakes generally showed the largest change, but in most study areas, the overall trend in small lakes was mirrored in larger lakes. For example, in the Eagle Plains, total lake area increased by 2.4% and the area of small lakes increased by approximately a 10% (Figure 3.6). Conversely, in the Lower Mackenzie Plain, the total area of small lakes increased by approximately 5%, while the area of large and medium sized lakes decreased by 1% (Figure 3.6). There was also no consistent difference in relative change between areas of continuous versus discontinuous permafrost. We observed similar responses for lakes located in both continuous and discontinuous permafrost. Average relative change in the continuous permafrost zone was +1.38% (n=3), and average relative change in the regions in the discontinuous permafrost zone was +1.23% (n=3). The study areas with the greatest increase and greatest decrease in surface water (Tuktoyaktuk Coastal Plain and Lower Mackenzie Plain, respectively) were both in the zone of continuous permafrost.

Table 3.4: Absolute and relative change in total lake area in each study area. Absolute change in area was calculated as the difference between total lake area in the first and last five years of the time series and relative change was calculated as absolute change divided by total area in the first time period.

<b>Site</b>	<b>Permafrost Zone</b>	<b>Absolute Change km<sup>2</sup> = Area<sub>t<sub>n</sub></sub> - Area<sub>t<sub>1</sub></sub></b>	<b>Relative Change = (Area<sub>t<sub>n</sub></sub> - Area<sub>t<sub>1</sub></sub>) / Area<sub>t<sub>1</sub></sub></b>
Tuktoyaktuk Coastal Plain	Continuous	+51.68km <sup>2</sup>	+2.7%
Central Mackenzie Valley	Discontinuous	+12.42km <sup>2</sup>	+2.4%
Eagle Plain	Continuous	+2.99km <sup>2</sup>	+2.4%
Great Slave Upland	Discontinuous	+23.79km <sup>2</sup>	+1.3%
Bulmer Plain	Discontinuous	+0.72km <sup>2</sup>	0.00%
Lower Mackenzie Plain	Continuous	-5.18km <sup>2</sup>	-0.96%

Table 3.5: Proportion of lakes showing non-trended and significant increasing and decreasing patterns in each study area.

<b>Site</b>	<b>Proportion Increasing</b>	<b>Proportion Decreasing</b>	<b>Proportion Non-Trended</b>
Tuktoyaktuk Coastal Plain	0.74	0.04	0.22
Eagle Plain	0.34	0.09	0.57
Lower Mackenzie Plain	0.29	0.14	0.57
Great Slave Upland	0.39	0.12	0.49
Central Mackenzie Valley	0.27	0.22	0.51
Bulmer Plain	0.17	0.16	0.67

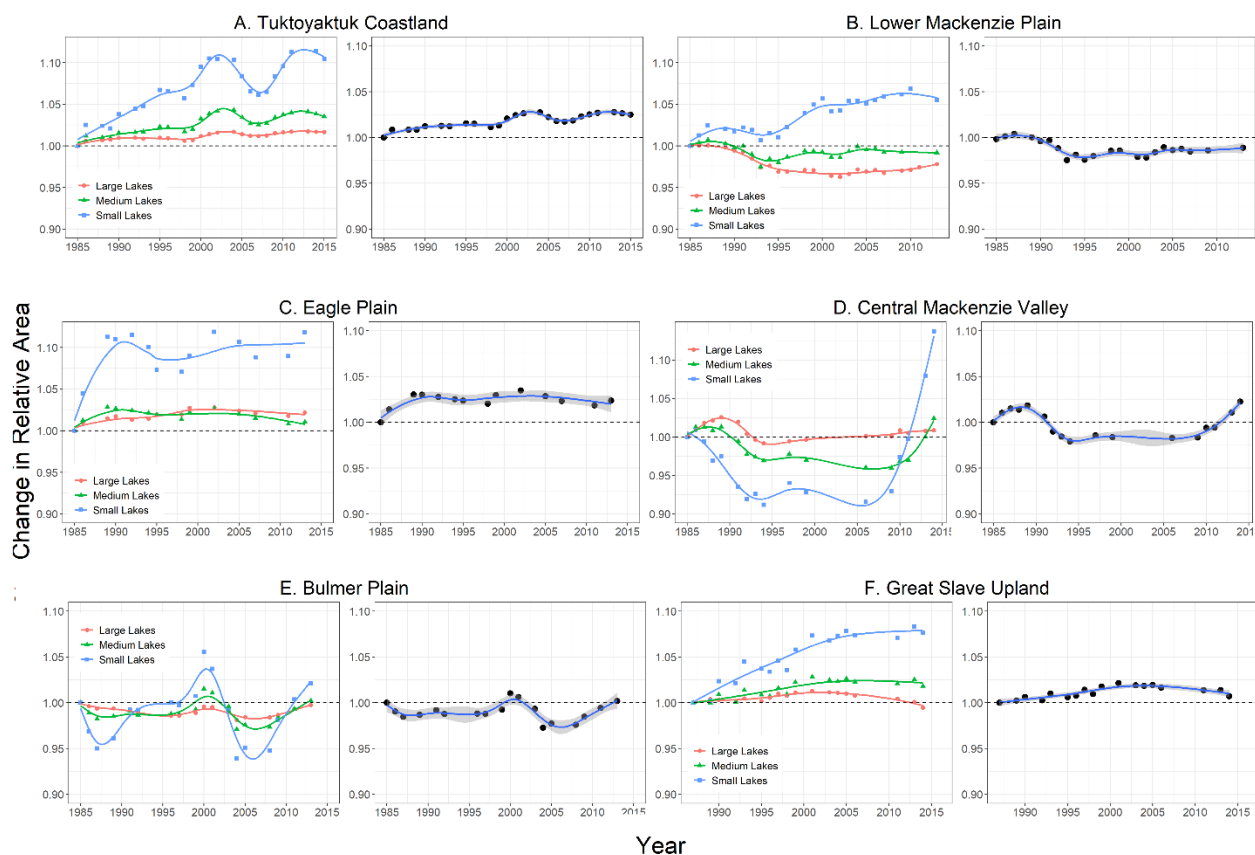


Figure 3.6: Changes in lake area in the six study areas relative to the average area in the first time period ( $t_1$ ). The left panel of each plot shows the change in lake area grouped by lake size and the right panel shows change in total lake area across all lakes. Each point represents the average relative area for a rolling 5-point period and the shaded area represents a 95% confidence interval.

### 3.2.3 Rapid Drainage

The frequency and relative importance of rapid lake drainage events varied by study area (Table 3.6). The Great Slave Upland had few rapid drainage events and minimal contributions to overall lake area change compared to sites in the Taiga Plains and Southern Arctic. The Tuktoyaktuk Coastal Plain and Lower Mackenzie Plain showed the largest number of rapid drainage events. In the Lower Mackenzie Plain, 27% of the total losses in surface water were associated with rapid drainage events. While the Eagle Plains study area only showed 2 rapid drainage events, water losses associated with these events accounted for 31% of overall change in surface water.

Table 3.6: The number of rapid drainage events per study site and the lake area losses associated with these events. The last column in the table shows the percent of the absolute change in lake area attributable to rapid drainage.

<b>Site</b>	<b>Rapid Drainage Events</b>	<b>Lake area loss km<sup>2</sup></b>	<b>Water loss km<sup>2</sup> / Absolute Change km<sup>2</sup>*100</b>
Tuktoyaktuk Coastal Plain	9	1.186	2%
Central Mackenzie Valley	4	1.197	11%
Great Slave Upland	1	0.046	0.2%
Bulmer Plain	1	0.073	10%
Eagle Plain	2	0.161	31%
Lower Mackenzie Plain	5	1.41	27%

Chi-square tests show that all lakes exhibiting decreasing trends were more likely to occur within fire scars (Table 3.5; Figure 3.7). Boxplots from the four sites where we assessed the impact of wildfire on lake area also show a consistent trajectory of change in lake area after fire (Figure 3.8). Declines in lake area typically followed a 1-3 year lag after the year of the fire (Figure 3.8) and in all cases were apparent for at least 10 years after the fire.

Table 3.7: Standardized residuals from Chi-square tests comparing lake area trends and the presence of fire. Standardized residuals were calculated as: observed count – expected count / sqrt(expected count). Residuals with an asterisk (\*) indicate a significant deviation ( $p < 0.01$ ) from expected counts with positive values indicating more lakes than expected in that category and negative values indicating fewer lakes than expected.

Site		Decreasing	Increasing	Non-trended
<b>Central Mackenzie Valley</b>	Outside Fire	-6.677*	3.320*	1.999
	Within Fire	11.252*	-5.595*	-3.369*
<b>Lower Mackenzie Plain</b>	Outside Fire	-10.475*	3.816*	2.404
	Within Fire	9.923*	-3.615*	-2.277
<b>Bulmer Plain</b>	Outside Fire	-4.612*	7.818*	-0.673
	Within Fire	2.093	-3.548*	0.305
<b>Great Slave Upland</b>	Outside Fire	-12.9668*	14.949*	-6.850*
	Within Fire	17.263*	-19.904*	9.120*

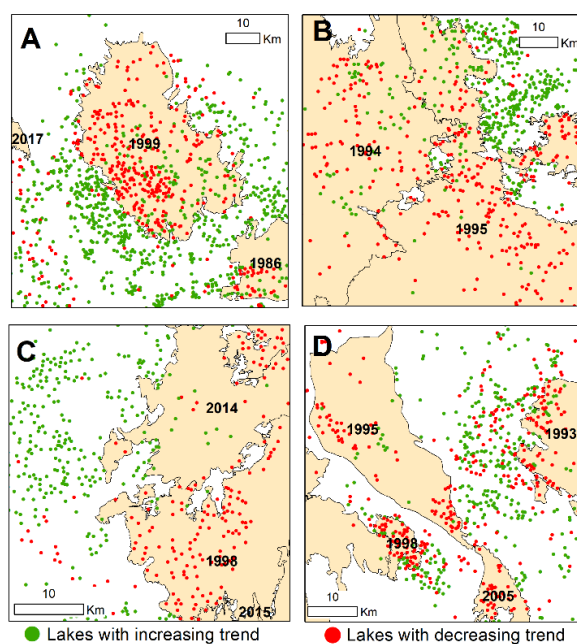


Figure 3.7: Lake area trends and fire history in A) Lower Mackenzie Plain, B) Bulmer Plain, C) Great Slave Upland and D) Central Mackenzie Valley study areas. Fire history data is from the NWT Centre for Geomatics (2019). Dates indicate the timing of each fire within the study area and points show lake centroids, with green points showing lakes with increasing trends in area and red points showing decreasing trends. The extent of the fires within each study area are shown in Figure 3.

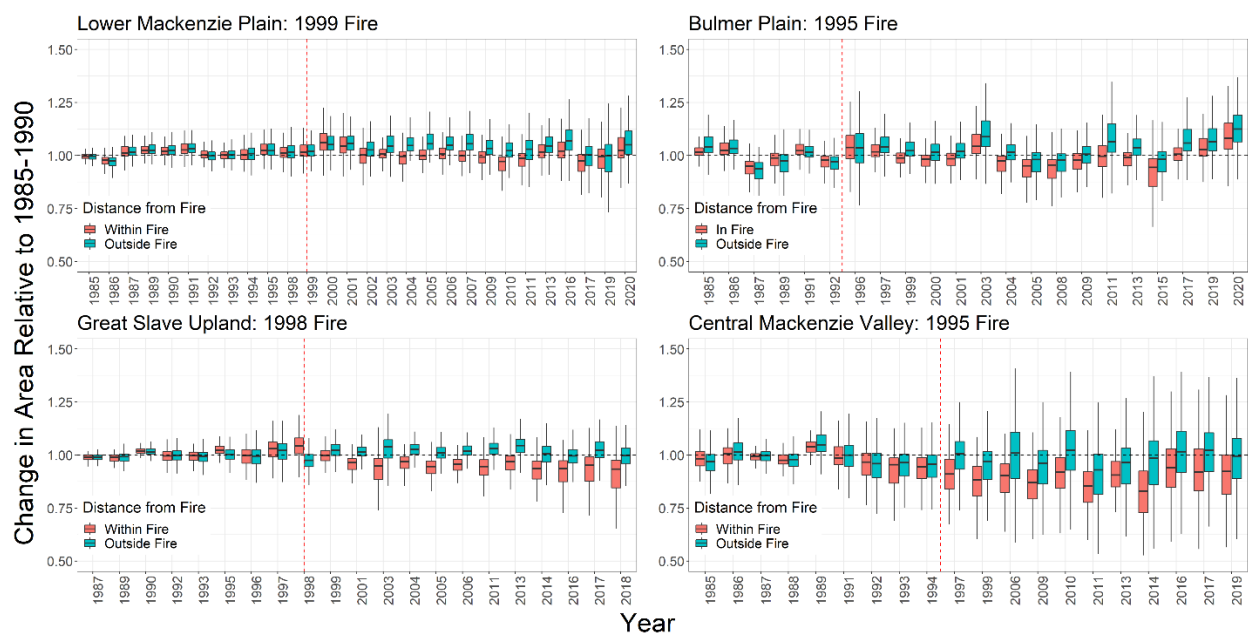


Figure 3.8: Boxplots showing change in the relative area of lakes within fire affected areas and outside fires (within 10km of fire boundaries) for the four study sites in forested study areas. The dashed red lines show the year the fire occurred. Note that the x-axis is not continuous because it does not show years with missing data.

### 3.4 Discussion

Our analysis shows that climate driven changes in surface water across the western Canadian Arctic are mediated by terrain factors. Total surface water area increased by approximately 1.3% across the entire study domain. This widespread increase in surface water area likely reflects increases in precipitation observed across the circumpolar (ACIA, 2004; Box et al., 2019). Between 1970 and 2017, Box et al. (2019) reported a 6.2 % increase in total annual precipitation across the pan-Arctic and increasing trends in precipitation have been observed at several sites across the Yukon and Northwest Territories (Lantz & Turner, 2015; Segal et al., 2016; Travers-Smith et al., In Review). Increases in surface water area were more likely to occur in regions with less permeable substrates and low ground ice, including regions underlain by bedrock and fine-colluvium. This is likely caused by the lower permeability of these substrates which can isolate lakes from groundwater systems and potentially make them more responsive to increases

in temperature and precipitation (Carroll & Loboda, 2018; Nitze et al., 2017; Wang et al., 2018). This conclusion is consistent with findings reported by Carroll and Loboda (2018), where shrinking tundra ponds in a bedrock-dominant region of the Southern Arctic ecoregion were associated with increased air temperatures and evaporation.

We also observed more decreases in surface water area in regions with moderate to high ground ice content. This could be caused by more frequent thermokarst leading to rapid lake drainage (Jones et al., 2020; Jones & Arp, 2015; Lantz & Turner, 2015; Mackay, 1988; Nitze et al., 2020). Previous studies have demonstrated that increasing precipitation in ice-rich permafrost regions can drive catastrophic drainage of large lakes and overall declines in lake area (Lantz & Turner, 2015; Lindgren et al., 2021; Nitze et al., 2020a; Travers-Smith et al., In Review). This conclusion is also supported by the fact that we observed more rapid drainage events, and a greater contribution of these events to overall surface water change in study areas with higher ground ice content (ie Lower Mackenzie Plain and Tuktoyaktuk Coastal Plain versus Great Slave Upland).

Our findings differ from previous studies suggesting that lake area is increasing in the zone of continuous permafrost and decreasing in the zone of discontinuous permafrost (Smith et al., 2005; Smol & Douglas, 2007; Walter et al., 2006), and emphasizes the importance of regional variation in surficial geology. Across our study domain we observed increases in surface water in areas of continuous and discontinuous permafrost, and the only study area with declining surface water area was in the zone of continuous permafrost. This finding is similar to Lindgren et al., (2021) who also observed widespread declines in surface water in three permafrost zones (continuous, discontinuous and isolated) in Alaska.

Our analysis also shows that wildfire can cause persistent declines in surface water. In all four of the boreal study areas (Lower Mackenzie Plains, Central Mackenzie Valley, Bulmer Plain and Great Slave Upland) lakes impacted by wildfire were more likely to show decreases in area. These changes were likely driven by changes in permafrost conditions (i.e. active layer deepening, ground ice degradation, terrain subsidence) which can impact surface hydrology (Connon et al., 2014; Haynes et al., 2019; Liljedahl et al., 2007; Roach et al., 2013). Our observation is also consistent with declines in lake area following fire in Alaska (Roach et al., 2013). We were unable to assess the impact of fire in tundra study areas as few large fires were recorded above the treeline in the data we used. However, larger and more frequent tundra fires demonstrates the need for additional research (Hu et al., 2015; Kasischke & Turetsky, 2006).

Our work highlights the importance of fine scale lake-based studies to understanding regional controls on surface water and intrannual change. Regional factors can play a significant role in lake dynamics; Turner et al., (2014) show that surrounding vegetation coverage determines whether water levels within individual lakes are more influenced by rain, snowmelt or evaporation. Lake dynamics can also vary considerably over the course of a single year. Cooley et al., (2019) show that sub seasonal changes in lake area can vary considerably. We also observed differences in the magnitude and direction of change between the analyses using the GLAD Surface Water dataset (Pickens et al., 2019), and the datasets we compiled within individual study areas. These discrepancies likely reflect differences in the seasonality of the data and the precision of surface water change detection. The GLAD Surface Water dataset considers per-pixel changes across all snow and ice-free Landsat scenes in a given year, while our datasets reflect sub-pixel changes and conditions in July and August. This also highlights the need for future work to examine seasonal as well as interannual lake dynamics. To better understand

broad-scale spatial patterns in surface water change, future work should consider regional controls driving lake expansion and drainage.

## Bibliography

ACIA. (2004). *Impacts of a Warming Arctic: Arctic Climate Impact Assessment*. Cambridge University Press.

Bouchard, F., Turner, K. W., MacDonald, L. A., Deakin, C., White, H., Farquharson, N., Medeiros, A. S., Wolfe, B. B., Hall, R. I., Pienitz, R., & Edwards, T. W. D. (2013). Vulnerability of shallow subarctic lakes to evaporate and desiccate when snowmelt runoff is low. *Geophysical Research Letters*, *40*(23), 6112–6117. <https://doi.org/10.1002/2013GL058635>

Box, J. E., Colgan, W. T., Christensen, T. R., Schmidt, N. M., Lund, M., Parmentier, F.-J. W., Brown, R., Bhatt, U. S., Euskirchen, E. S., Romanovsky, V. E., Walsh, J. E., Overland, J. E., Wang, M., Corell, R. W., Meier, W. N., Wouters, B., Mernild, S., Mård, J., Pawlak, J., & Olsen, M. S. (2019). Key indicators of Arctic climate change: 1971–2017. *Environmental Research Letters*, *14*(4), 045010. <https://doi.org/10.1088/1748-9326/aafc1b>

Breiman, L. (2001). Random Forests. *Machine Learning*, *45*, 5–32.

Campbell, T. K. F., Lantz, T. C., & Fraser, R. H. (2018). Impacts of Climate Change and Intensive Lesser Snow Goose (*Chen caerulescens caerulescens*) Activity on Surface Water in High Arctic Pond Complexes. *Remote Sensing*, *10*(12), 1892. <https://doi.org/10.3390/rs10121892>

Carroll, M. L., & Loboda, T. V. (2017). Multi-Decadal Surface Water Dynamics in North American Tundra. *Remote Sensing*, *9*(5), 497. <https://doi.org/10.3390/rs9050497>

Carroll, M. L., & Loboda, T. V. (2018). The sign, magnitude and potential drivers of change in surface water extent in Canadian tundra. *Environmental Research Letters*, *13*(4), 045009. <https://doi.org/10.1088/1748-9326/aab794>

Connon, R. F., Quinton, W. L., Craig, J. R., & Hayashi, M. (2014). Changing hydrologic connectivity due to permafrost thaw in the lower Liard River valley, NWT, Canada. *Hydrological Processes*, *28*(14), 4163–4178. <https://doi.org/10.1002/hyp.10206>

Cooley, S. W., Smith, L. C., Ryan, J. C., Pitcher, L. H., & Pavelsky, T. M. (2019). Arctic-Boreal Lake Dynamics Revealed Using CubeSat Imagery. *Geophysical Research Letters*, *46*(4), 2111–2120. <https://doi.org/10.1029/2018GL081584>

Dwyer, J. L. (2019). *Landsat Collection 1 Level 1 Product Definition*. Department of the Interior US Geological Survey; LSDS-1656 Version 2.0.

Fink, S. E., & Hijmans, R. J. (2017). WorldClim 2: New 1km spatial resolution climate surfaces for global land areas. *International Journal of Climatology*, *37*(12), 4302–4315.

Fraser, R., Kokelj, S., Lantz, T., McFarlane-Winchester, M., Olthof, I., & Lacelle, D. (2018). Climate Sensitivity of High Arctic Permafrost Terrain Demonstrated by Widespread Ice-Wedge Thermokarst on Banks Island. *Remote Sensing*, *10*(6), 954. <https://doi.org/10.3390/rs10060954>

Fulton, R. J. (1989). *Quaternary Geology of Canada and Greenland* [Map]. Geological Survey of Canada, Geology of Canada Series no. 1, 1989, 839 pages (5 sheets),. <https://doi.org/10.4095/127905>

Geomatics Yukon. (2019). *Fire History*. <https://open.yukon.ca/data/datasets/fire-history>

Gibson, C. M., Chasmer, L. E., Thompson, D. K., Quinton, W. L., Flannigan, M. D., & Olefeldt, D. (2018). Wildfire as a major driver of recent permafrost thaw in boreal peatlands. *Nature Communications*, *9*(1), 3041. <https://doi.org/10.1038/s41467-018-05457-1>

Greenwell, B. M. (2017). pdp: An R Package for Constructing Partial Dependence Plots. *The R Journal*, *9*(1), 421–436.

Grosse, G., Jones, B. M., & Arp, C. D. (2013). Thermokarst lakes, drainage, and drained basins. In J. F. Shroder (Ed.), *Treatise on Geomorphology*. 8. (pp. 325–353). Academic Press, San Diego, CA. <https://doi.org/10.1016/B978-0-12-374739-6.00216-5>

Haynes, K. M., Connon, R. F., & Quinton, W. L. (2019). Hydrometeorological measurements in peatland-dominated, discontinuous permafrost at Scotty Creek, Northwest Territories, Canada. *Geoscience Data Journal*, *6*(2), 85–96. <https://doi.org/10.1002/gdj3.69>

Hinkel, K. M., Eisner, W. R., Bockheim, J. G., Nelson, F. E., Peterson, K. M., & Dai, X. (2003). Spatial Extent, Age, and Carbon Stocks in Drained Thaw Lake Basins on the Barrow Peninsula, Alaska. *Arctic, Antarctic, and Alpine Research*, *35*(3), 291–300. [https://doi.org/10.1657/1523-0430\(2003\)035\[0291:SEAACS\]2.0.CO;2](https://doi.org/10.1657/1523-0430(2003)035[0291:SEAACS]2.0.CO;2)

Hu, F. S., Higuera, P. E., Duffy, P., Chipman, M. L., Rocha, A. V., Young, A. M., Kelly, R., & Dietze, M. C. (2015). Arctic tundra fires: Natural variability and responses to climate change. *Frontiers in Ecology and the Environment*, *13*(7), 369–377. <https://doi.org/10.1890/150063>

Jones, B. M., & Arp, C. D. (2015). Observing a Catastrophic Thermokarst Lake Drainage in Northern Alaska. *Permafrost and Periglacial Processes*, *26*(2), 119–128. <https://doi.org/10.1002/ppp.1842>

Jones, B. M., Arp, C. D., Grosse, G., Nitze, I., Lara, M. J., Whitman, M. S., Farquharson, L. M., Kanevskiy, M., Parsekian, A. D., Breen, A. L., Ohara, N., Rangel, R. C., & Hinkel, K. M. (2020). Identifying historical and future potential lake drainage events on the western Arctic coastal plain of Alaska. *Permafrost and Periglacial Processes*, *31*(1), 110–127. <https://doi.org/10.1002/ppp.2038>

- Jones, B. M., Grosse, G., Arp, C. D., Jones, M. C., Anthony, K. M. W., & Romanovsky, V. E. (2011). Modern thermokarst lake dynamics in the continuous permafrost zone, northern Seward Peninsula, Alaska. *Journal of Geophysical Research: Biogeosciences*, 116(G2). <https://doi.org/10.1029/2011JG001666>
- Jones, B. M., Grosse, G., Arp, C. D., Miller, E., Liu, L., Hayes, D. J., & Larsen, C. F. (2015). Recent Arctic tundra fire initiates widespread thermokarst development. *Scientific Reports*, 5(1), 15865. <https://doi.org/10.1038/srep15865>
- Kasischke, E. S., & Turetsky, M. R. (2006). Recent changes in the fire regime across the North American boreal region—Spatial and temporal patterns of burning across Canada and Alaska. *Geophysical Research Letters*, 33(9). <https://doi.org/10.1029/2006GL025677>
- Kokelj, S. V., Jenkins, R. E., Milburn, D., Burn, C. R., & Snow, N. (2005). The influence of thermokarst disturbance on the water quality of small upland lakes, Mackenzie Delta region, Northwest Territories, Canada. *Permafrost and Periglacial Processes*, 16(4), 343–353. <https://doi.org/10.1002/ppp.536>
- Kokelj, S. V., & Jorgenson, M. T. (2013). Advances in Thermokarst Research. *Permafrost and Periglacial Processes*, 24(2), 108–119. <https://doi.org/10.1002/ppp.1779>
- Labrecque, S., Lacelle, D., Duguay, C. R., Lauriol, B., & Hawkings, J. (2009). Contemporary (1951–2001) Evolution of Lakes in the Old Crow Basin, Northern Yukon, Canada: Remote Sensing, Numerical Modeling, and Stable Isotope Analysis. *ARCTIC*, 62(2), 225–238. <https://doi.org/10.14430/arctic134>
- Landis, J. R., & Koch, G. G. (1977). The Measurement of Observer Agreement for Categorical Data. *Biometrics*, 33(1), 159–174. <https://doi.org/10.2307/2529310>
- Lantz, T. C., & Turner, K. W. (2015). Changes in lake area in response to thermokarst processes and climate in Old Crow Flats, Yukon. *Journal of Geophysical Research: Biogeosciences*, 120(3), 513–524. <https://doi.org/10.1002/2014JG002744>
- Liaw, A., & Wiener, M. (2002). Classification and Regression by randomForest. *R News*, 2(3), 18–22.
- Liljedahl, A., Hinzman, L., Busey, R., & Yoshikawa, K. (2007). Physical short-term changes after a tussock tundra fire, Seward Peninsula, Alaska. *Journal of Geophysical Research: Earth Surface*, 112(F2). <https://doi.org/10.1029/2006JF000554>
- Lindgren, P. R., Farquharson, L. M., Romanovsky, V. E., & Grosse, G. (2021). Landsat-based lake distribution and changes in western Alaska permafrost regions between the 1970s and 2010s. *Environmental Research Letters*, 16(2), 025006. <https://doi.org/10.1088/1748-9326/abd270>

- Mackay, J. R. (1988). Catastrophic lake drainage, Tuktoyaktuk Peninsula area, District of Mackenzie. *Geological Survey of Canada*, 88-1D.
- McLeod, A. I. (2011). *Kendall: Kendall rank correlation and Mann-Kendall trend test. R package version 2.2*. <https://CRAN.R-project.org/package=Kendall>
- Mudryk, L. R., Derksen, C., Howell, S., Laliberté, F., Thackeray, C., Sospedra-Alfonso, R., Vionnet, V., Kushner, P. J., & Brown, R. (2018). Canadian snow and sea ice: Historical trends and projections. *The Cryosphere*, 12(4), 1157–1176. <https://doi.org/10.5194/tc-12-1157-2018>
- Narita, K., Harada, K., Saito, K., Sawada, Y., Fukuda, M., & Tsuyuzaki, S. (2015). Vegetation and Permafrost Thaw Depth 10 Years after a Tundra Fire in 2002, Seward Peninsula, Alaska. *Arctic, Antarctic, and Alpine Research*, 47(3), 547–559. <https://doi.org/10.1657/AAAR0013-031>
- Nitze, I., Cooley, S., Duguay, C., Jones, B. M., & Grosse, G. (2020). The catastrophic thermokarst lake drainage events of 2018 in northwestern Alaska: Fast-forward into the future. *The Cryosphere Discussions*, 1–33. <https://doi.org/10.5194/tc-2020-106>
- Nitze, I., Grosse, G., Jones, B., Arp, C., Ulrich, M., Fedorov, A., & Veremeeva, A. (2017). Landsat-Based Trend Analysis of Lake Dynamics across Northern Permafrost Regions. *Remote Sensing*, 9(7), 640. <https://doi.org/10.3390/rs9070640>
- NWT Centre for Geomatics. (2020). *Fire history: Fire History Data of the NWT*. <http://www.geomatics.gov.nt.ca/Downloads/Vector/Biota/FireHistory.zip>
- Olthof, I., Fraser, R. H., & Schmitt, C. (2015). Landsat-based mapping of thermokarst lake dynamics on the Tuktoyaktuk Coastal Plain, Northwest Territories, Canada since 1985. *Remote Sensing of Environment*, 168, 194–204. <https://doi.org/10.1016/j.rse.2015.07.001>
- O'Neill, H. B., Wolfe, S. A., & Duchesne, C. (2020). *Ground ice map of Canada* [Map]. Geological Survey of Canada, Open File 8713, (ed. version 1). <https://doi.org/10.4095/326885>
- Pastick, N. J., Jorgenson, M. T., Goetz, S. J., Jones, B. M., Wylie, B. K., Minsley, B. J., Genet, H., Knight, J. F., Swanson, D. K., & Jorgenson, J. C. (2019). Spatiotemporal remote sensing of ecosystem change and causation across Alaska. *Global Change Biology*, 25(3), 1171–1189. <https://doi.org/10.1111/gcb.14279>
- Pickens, A. H., Hansen, M. C., Hancher, M., Stehman, S. V., Tyukavina, A., Potapov, P., Marroquin, B., & Sherani, Z. (2020). Mapping and sampling to characterize global inland water dynamics from 1999 to 2018 with full Landsat time-series. *Remote Sensing of Environment*, 243, 111792. <https://doi.org/10.1016/j.rse.2020.111792>
- Plug, L. J., Walls, C., & Scott, B. M. (2008). Tundra lake changes from 1978 to 2001 on the Tuktoyaktuk Peninsula, western Canadian Arctic. *Geophysical Research Letters*, 35(3). <https://doi.org/10.1029/2007GL032303>

- Pohl, S., Marsh, P., Onclin, C., & Russell, M. (2009). The summer hydrology of a small upland tundra thaw lake: Implications to lake drainage. *Hydrological Processes*, 23(17), 2536–2546. <https://doi.org/10.1002/hyp.7238>
- Porter, C., Morin, P., Howat, I., Noh, M. J., Bates, B., Peterman, K., Scott, K., & Schlenk, M. (2018). *ArcticDEM*. Harvard Dataverse, V1. <https://doi.org/10.7910/DVN/OHHUKH>
- Roach, J. K., Griffith, B., & Verbyla, D. (2013). Landscape influences on climate-related lake shrinkage at high latitudes. *Global Change Biology*, 19(7), 2276–2284. <https://doi.org/10.1111/gcb.12196>
- Rover, J., Ji, L., Wylie, B. K., & Tieszen, L. L. (2012). Establishing water body areal extent trends in interior Alaska from multi-temporal Landsat data. *Remote Sensing Letters*, 3(7), 595–604. <https://doi.org/10.1080/01431161.2011.643507>
- Schuur, E. a. G., McGuire, A. D., Schädel, C., Grosse, G., Harden, J. W., Hayes, D. J., Hugelius, G., Koven, C. D., Kuhry, P., Lawrence, D. M., Natali, S. M., Olefeldt, D., Romanovsky, V. E., Schaefer, K., Turetsky, M. R., Treat, C. C., & Vonk, J. E. (2015). Climate change and the permafrost carbon feedback. *Nature*, 520(7546), 171–179. <https://doi.org/10.1038/nature14338>
- Segal, R. A., Lantz, T. C., & Kokelj, S. V. (2016). Acceleration of thaw slump activity in glaciated landscapes of the Western Canadian Arctic. *Environmental Research Letters*, 11(3), 034025. <https://doi.org/10.1088/1748-9326/11/3/034025>
- Smith, L. C., Sheng, Y., MacDonald, G., M., & Hinzman, L. D. (2005). Disappearing Arctic Lakes. *Science*, 208, 1429–1431.
- Smol, J. P., & Douglas, M. S. V. (2007). Crossing the final ecological threshold in high Arctic ponds. *Proceedings of the National Academy of Sciences*, 104(30), 12395–12397. <https://doi.org/10.1073/pnas.0702777104>
- Swanson, D. K. (2019). Thermokarst and precipitation drive changes in the area of lakes and ponds in the National Parks of northwestern Alaska, 1984–2018. *Arctic, Antarctic, and Alpine Research*, 51(1), 265–279. <https://doi.org/10.1080/15230430.2019.1629222>
- Tarnocai, C., Canadell, J. G., Schuur, E. a. G., Kuhry, P., Mazhitova, G., & Zimov, S. (2009). Soil organic carbon pools in the northern circumpolar permafrost region. *Global Biogeochemical Cycles*, 23(2). <https://doi.org/10.1029/2008GB003327>
- Travers-Smith, H., Lantz, T. C., & Fraser, R. H. (In Review). Surface Water Dynamics and Rapid Lake Drainage in the Western Canadian Subarctic. *Journal of Geophysical Research: Biogeosciences*.
- Turner, K. W., Wolfe, B. B., Edwards, T. W. D., Lantz, T. C., Hall, R. I., & Larocque, G. (2014). Controls on water balance of shallow thermokarst lakes and their relations with catchment characteristics: A multi-year, landscape-scale assessment based on water isotope tracers and

remote sensing in Old Crow Flats, Yukon (Canada). *Global Change Biology*, 20(5), 1585–1603. <https://doi.org/10.1111/gcb.12465>

Walter, K. M., Zimov, S. A., Chanton, J. P., Verbyla, D., & Chapin, F. S. (2006). Methane bubbling from Siberian thaw lakes as a positive feedback to climate warming. *Nature*, 443(7107), 71–75. <https://doi.org/10.1038/nature05040>

Wang, L., Jolivel, M., Marzahn, P., Bernier, M., & Ludwig, R. (2018). Thermokarst pond dynamics in subarctic environment monitoring with radar remote sensing. *Permafrost and Periglacial Processes*, 29(4), 231–245. <https://doi.org/10.1002/ppp.1986>

Watts, J. D., Kimball, J. S., Jones, L. A., Schroeder, R., & McDonald, K. C. (2012). Satellite Microwave remote sensing of contrasting surface water inundation changes within the Arctic–Boreal Region. *Remote Sensing of Environment*, 127, 223–236. <https://doi.org/10.1016/j.rse.2012.09.003>

Yoshikawa, K., Bolton, W. R., Romanovsky, V. E., Fukuda, M., & Hinzman, L. D. (2002). Impacts of wildfire on the permafrost in the boreal forests of Interior Alaska. *Journal of Geophysical Research: Atmospheres*, 107(D1), FFR 4-1-FFR 4-14. <https://doi.org/10.1029/2001JD000438>

Yoshikawa, K., & Hinzman, L. D. (2003). Shrinking thermokarst ponds and groundwater dynamics in discontinuous permafrost near council, Alaska. *Permafrost and Periglacial Processes*, 14(2), 151–160. <https://doi.org/10.1002/ppp.451>

Zeileis, A. (2004). Implementing a Class of Structural Change Tests: An Econometric Computing Approach. *Computational Statistics & Data Analysis*, 50, 2987–3008.

Zipper, S. C., Lamontagne-Hallé, P., McKenzie, J. M., & Rocha, A. V. (2018). Groundwater Controls on Postfire Permafrost Thaw: Water and Energy Balance Effects. *Journal of Geophysical Research: Earth Surface*, 123(10), 2677–2694. <https://doi.org/10.1029/2018JF004611>

- ACIA. (2004). *Impacts of a Warming Arctic: Arctic Climate Impact Assessment*. Cambridge University Press.
- Bouchard, F., Turner, K. W., MacDonald, L. A., Deakin, C., White, H., Farquharson, N., Medeiros, A. S., Wolfe, B. B., Hall, R. I., Pienitz, R., & Edwards, T. W. D. (2013). Vulnerability of shallow subarctic lakes to evaporate and desiccate when snowmelt runoff is low. *Geophysical Research Letters*, *40*(23), 6112–6117. <https://doi.org/10.1002/2013GL058635>
- Box, J. E., Colgan, W. T., Christensen, T. R., Schmidt, N. M., Lund, M., Parmentier, F.-J. W., Brown, R., Bhatt, U. S., Euskirchen, E. S., Romanovsky, V. E., Walsh, J. E., Overland, J. E., Wang, M., Corell, R. W., Meier, W. N., Wouters, B., Mernild, S., Mård, J., Pawlak, J., & Olsen, M. S. (2019). Key indicators of Arctic climate change: 1971–2017. *Environmental Research Letters*, *14*(4), 045010. <https://doi.org/10.1088/1748-9326/aafc1b>
- Breiman, L. (2001). Random Forests. *Machine Learning*, *45*, 5–32.
- Burn, C. R., & Kokelj, S. V. (2009). The environment and permafrost of the Mackenzie Delta area. *Permafrost and Periglacial Processes*, *20*(2), 83–105. <https://doi.org/10.1002/ppp.655>
- Campbell, T. K. F., Lantz, T. C., & Fraser, R. H. (2018). Impacts of Climate Change and Intensive Lesser Snow Goose (*Chen caerulescens caerulescens*) Activity on Surface Water in High Arctic Pond Complexes. *Remote Sensing*, *10*(12), 1892. <https://doi.org/10.3390/rs10121892>
- Carroll, M. L., & Loboda, T. V. (2017). Multi-Decadal Surface Water Dynamics in North American Tundra. *Remote Sensing*, *9*(5), 497. <https://doi.org/10.3390/rs9050497>
- Carroll, M. L., & Loboda, T. V. (2018). The sign, magnitude and potential drivers of change in surface water extent in Canadian tundra. *Environmental Research Letters*, *13*(4), 045009. <https://doi.org/10.1088/1748-9326/aab794>
- Chander, G., Markham, B. L., & Helder, D. L. (2009). Summary of current radiometric calibration coefficients for Landsat MSS, TM, ETM+, and EO-1 ALI sensors. *Remote Sensing of Environment*, *113*(5), 893–903. <https://doi.org/10.1016/j.rse.2009.01.007>
- Connon, R. F., Quinton, W. L., Craig, J. R., & Hayashi, M. (2014). Changing hydrologic connectivity due to permafrost thaw in the lower Liard River valley, NWT, Canada. *Hydrological Processes*, *28*(14), 4163–4178. <https://doi.org/10.1002/hyp.10206>
- Cooley, S. W., Smith, L. C., Ryan, J. C., Pitcher, L. H., & Pavelsky, T. M. (2019). Arctic-Boreal Lake Dynamics Revealed Using CubeSat Imagery. *Geophysical Research Letters*, *46*(4), 2111–2120. <https://doi.org/10.1029/2018GL081584>
- Dowle, M., & Srinivasan, A. (2019). *Data.table: Extension of `data.frame`*. R package version 1.12.8. <https://CRAN.R-project.org/package=data.table>
- Dwyer, J. L. (2019). *Landsat Collection 1 Level 1 Product Definition*. Department of the Interior US Geological Survey; LSDS-1656 Version 2.0.

- Ecosystem Classification Group. (2009). *Ecological Regions of the Northwest Territories – Taiga Plains*. (viii + 173 pp. + folded insert map.). Department of Environment and Natural Resources, Government of the Northwest Territories.
- Ecosystem Classification Group. (2012). *Ecological Regions of the Northwest Territories-Southern Arctic* (x + 170pp + insert map). Department of Environment and Natural Resources, Government of the Northwest Territories.
- Ecosystem Classification Group, & Northwest Territories (Eds.). (2010). *Ecological regions of the Northwest Territories: Cordillera*. Dept. of Environment and Natural Resources, Govt. of the Northwest Territories.
- Fink, S. E., & Hijmans, R. J. (2017). WorldClim 2: New 1km spatial resolution climate surfaces for global land areas. *International Journal of Climatology*, 37(12), 4302–4315.
- Fraser, R., Kokelj, S., Lantz, T., McFarlane-Winchester, M., Olthof, I., & Lacelle, D. (2018). Climate Sensitivity of High Arctic Permafrost Terrain Demonstrated by Widespread Ice-Wedge Thermokarst on Banks Island. *Remote Sensing*, 10(6), 954. <https://doi.org/10.3390/rs10060954>
- French, H. M. (2017). The Northern Interior Yukon: An Example of Periglaciation. In O. Slaymaker (Ed.), *Landscapes and Landforms of Western Canada* (pp. 257–266). Springer International Publishing. [https://doi.org/10.1007/978-3-319-44595-3\\_18](https://doi.org/10.1007/978-3-319-44595-3_18)
- Fulton, R. J. (1989). *Quaternary Geology of Canada and Greenland* [Map]. Geological Survey of Canada, Geology of Canada Series no. 1, 1989, 839 pages (5 sheets),. <https://doi.org/10.4095/127905>
- Fulton, R. J. (1995). *Surficial materials of Canada. “A” Series Map 1880A, 1995, 1 sheet* [Map]. Geological Survey of Canada. [doi.org/10.4095/205040](https://doi.org/10.4095/205040)
- Geomatics Yukon. (2019). *Fire History*. <https://open.yukon.ca/data/datasets/fire-history>
- Gibson, C. M., Chasmer, L. E., Thompson, D. K., Quinton, W. L., Flannigan, M. D., & Olefeldt, D. (2018). Wildfire as a major driver of recent permafrost thaw in boreal peatlands. *Nature Communications*, 9(1), 3041. <https://doi.org/10.1038/s41467-018-05457-1>
- Gibson, C., Morse, P. D., Kelly, J. M., Turetsky, M. R., Baltzer, J. L., Gingras-Hill, T., & Kokelj, S. V. (n.d.). *Thermokarst Mapping Collective: Protocol for organic permafrost terrain and preliminary inventory from the Taiga Plains test area, Northwest Territories*. 29.
- Greenwell, B. M. (2017). pdp: An R Package for Constructing Partial Dependence Plots. *The R Journal*, 9(1), 421–436.
- Grosse, G., Jones, B. M., & Arp, C. D. (2013). Thermokarst lakes, drainage, and drained basins. In J. F. Shroder (Ed.), *Treatise on Geomorphology*. 8. (pp. 325–353). Academic Press, San Diego, CA. <https://doi.org/10.1016/B978-0-12-374739-6.00216-5>

- Haynes, K. M., Connon, R. F., & Quinton, W. L. (2019). Hydrometeorological measurements in peatland-dominated, discontinuous permafrost at Scotty Creek, Northwest Territories, Canada. *Geoscience Data Journal*, 6(2), 85–96. <https://doi.org/10.1002/gdj3.69>
- Hinkel, K. M., Eisner, W. R., Bockheim, J. G., Nelson, F. E., Peterson, K. M., & Dai, X. (2003). Spatial Extent, Age, and Carbon Stocks in Drained Thaw Lake Basins on the Barrow Peninsula, Alaska. *Arctic, Antarctic, and Alpine Research*, 35(3), 291–300. [https://doi.org/10.1657/1523-0430\(2003\)035\[0291:SEAACS\]2.0.CO;2](https://doi.org/10.1657/1523-0430(2003)035[0291:SEAACS]2.0.CO;2)
- Hu, F. S., Higuera, P. E., Duffy, P., Chipman, M. L., Rocha, A. V., Young, A. M., Kelly, R., & Dietze, M. C. (2015). Arctic tundra fires: Natural variability and responses to climate change. *Frontiers in Ecology and the Environment*, 13(7), 369–377. <https://doi.org/10.1890/150063>
- Hughes, O. L., Hodgson, D. J., & Pilon, J. (1972). *Surficial geology maps of part of the Mackenzie Valley, District of Mackenzie, Northwest Territories. 106-I, 106 M, 106 N.* [Map]. Geological Survey of Canada.
- Jones, Benjamin M., & Arp, C. D. (2015). Observing a Catastrophic Thermokarst Lake Drainage in Northern Alaska. *Permafrost and Periglacial Processes*, 26(2), 119–128. <https://doi.org/10.1002/ppp.1842>
- Jones, Benjamin M., Arp, C. D., Grosse, G., Nitze, I., Lara, M. J., Whitman, M. S., Farquharson, L. M., Kanevskiy, M., Parsekian, A. D., Breen, A. L., Ohara, N., Rangel, R. C., & Hinkel, K. M. (2020). Identifying historical and future potential lake drainage events on the western Arctic coastal plain of Alaska. *Permafrost and Periglacial Processes*, 31(1), 110–127. <https://doi.org/10.1002/ppp.2038>
- Jones, Benjamin M., Grosse, G., Arp, C. D., Miller, E., Liu, L., Hayes, D. J., & Larsen, C. F. (2015). Recent Arctic tundra fire initiates widespread thermokarst development. *Scientific Reports*, 5(1), 15865. <https://doi.org/10.1038/srep15865>
- Jones, B.M, Grosse, G., Arp, C. D., Jones, M. C., Anthony, K. M. W., & Romanovsky, V. E. (2011). Modern thermokarst lake dynamics in the continuous permafrost zone, northern Seward Peninsula, Alaska. *Journal of Geophysical Research: Biogeosciences*, 116(G2). <https://doi.org/10.1029/2011JG001666>
- Kasischke, E. S., & Turetsky, M. R. (2006). Recent changes in the fire regime across the North American boreal region—Spatial and temporal patterns of burning across Canada and Alaska. *Geophysical Research Letters*, 33(9). <https://doi.org/10.1029/2006GL025677>
- Kokelj, S. V., Jenkins, R. E., Milburn, D., Burn, C. R., & Snow, N. (2005). The influence of thermokarst disturbance on the water quality of small upland lakes, Mackenzie Delta region, Northwest Territories, Canada. *Permafrost and Periglacial Processes*, 16(4), 343–353. <https://doi.org/10.1002/ppp.536>
- Kokelj, S. V., & Jorgenson, M. T. (2013). Advances in Thermokarst Research. *Permafrost and Periglacial Processes*, 24(2), 108–119. <https://doi.org/10.1002/ppp.1779>

- Labrecque, S., Lacelle, D., Duguay, C. R., Lauriol, B., & Hawkings, J. (2009). Contemporary (1951–2001) Evolution of Lakes in the Old Crow Basin, Northern Yukon, Canada: Remote Sensing, Numerical Modeling, and Stable Isotope Analysis. *ARCTIC*, 62(2), 225–238. <https://doi.org/10.14430/arctic134>
- Landis, J. R., & Koch, G. G. (1977). The Measurement of Observer Agreement for Categorical Data. *Biometrics*, 33(1), 159–174. <https://doi.org/10.2307/2529310>
- Lantz, T. C., & Turner, K. W. (2015). Changes in lake area in response to thermokarst processes and climate in Old Crow Flats, Yukon. *Journal of Geophysical Research: Biogeosciences*, 120(3), 513–524. <https://doi.org/10.1002/2014JG002744>
- Liaw, A., & Wiener, M. (2002). Classification and Regression by randomForest. *R News*, 2(3), 18–22.
- Liljedahl, A., Hinzman, L., Busey, R., & Yoshikawa, K. (2007). Physical short-term changes after a tussock tundra fire, Seward Peninsula, Alaska. *Journal of Geophysical Research: Earth Surface*, 112(F2). <https://doi.org/10.1029/2006JF000554>
- Lindgren, P. R., Farquharson, L. M., Romanovsky, V. E., & Grosse, G. (2021). Landsat-based lake distribution and changes in western Alaska permafrost regions between the 1970s and 2010s. *Environmental Research Letters*, 16(2), 025006. <https://doi.org/10.1088/1748-9326/abd270>
- Mackay, J. R. (1988). Catastrophic lake drainage, Tuktoyaktuk Peninsula area, District of Mackenzie. *Geological Survey of Canada*, 88-1D.
- McLeod, A. I. (2011). *Kendall: Kendall rank correlation and Mann-Kendall trend test. R package version 2.2*. <https://CRAN.R-project.org/package=Kendall>
- Mudryk, L. R., Derksen, C., Howell, S., Laliberté, F., Thackeray, C., Sospedra-Alfonso, R., Vionnet, V., Kushner, P. J., & Brown, R. (2018). Canadian snow and sea ice: Historical trends and projections. *The Cryosphere*, 12(4), 1157–1176. <https://doi.org/10.5194/tc-12-1157-2018>
- Narita, K., Harada, K., Saito, K., Sawada, Y., Fukuda, M., & Tsuyuzaki, S. (2015). Vegetation and Permafrost Thaw Depth 10 Years after a Tundra Fire in 2002, Seward Peninsula, Alaska. *Arctic, Antarctic, and Alpine Research*, 47(3), 547–559. <https://doi.org/10.1657/AAAR0013-031>
- Nitze, I., Cooley, S., Duguay, C., Jones, B. M., & Grosse, G. (2020). The catastrophic thermokarst lake drainage events of 2018 in northwestern Alaska: Fast-forward into the future. *The Cryosphere Discussions*, 1–33. <https://doi.org/10.5194/tc-2020-106>
- Nitze, I., Grosse, G., Jones, B., Arp, C., Ulrich, M., Fedorov, A., & Veremeeva, A. (2017). Landsat-Based Trend Analysis of Lake Dynamics across Northern Permafrost Regions. *Remote Sensing*, 9(7), 640. <https://doi.org/10.3390/rs9070640>
- Norris, D. (1984). *Geology Northern Yukon and Northwestern District of Mackenzie. 1581A* [Map]. Geological Survey of Canada.

- NWT Centre for Geomatics. (2020). *Fire history: Fire History Data of the NWT*. <http://www.geomatics.gov.nt.ca/Downloads/Vector/Biota/FireHistory.zip>
- Olthof, I., Fraser, R. H., & Schmitt, C. (2015). Landsat-based mapping of thermokarst lake dynamics on the Tuktoyaktuk Coastal Plain, Northwest Territories, Canada since 1985. *Remote Sensing of Environment*, 168, 194–204. <https://doi.org/10.1016/j.rse.2015.07.001>
- O'Neill, H. B., Wolfe, S. A., & Duchesne, C. (2020). *Ground ice map of Canada* [Map]. Geological Survey of Canada, Open File 8713, (ed. version 1). <https://doi.org/10.4095/326885>
- Pastick, N. J., Jorgenson, M. T., Goetz, S. J., Jones, B. M., Wylie, B. K., Minsley, B. J., Genet, H., Knight, J. F., Swanson, D. K., & Jorgenson, J. C. (2019). Spatiotemporal remote sensing of ecosystem change and causation across Alaska. *Global Change Biology*, 25(3), 1171–1189. <https://doi.org/10.1111/gcb.14279>
- Paul, J. R., Kokelj, S. V., & Baltzer, J. L. (2021). Spatial and stratigraphic variation of near-surface ground ice in discontinuous permafrost of the taiga shield. *Permafrost and Periglacial Processes*, 32(1), 3–18. <https://doi.org/10.1002/ppp.2085>
- Pickens, A. H., Hansen, M. C., Hancher, M., Stehman, S. V., Tyukavina, A., Potapov, P., Marroquin, B., & Sherani, Z. (2020). Mapping and sampling to characterize global inland water dynamics from 1999 to 2018 with full Landsat time-series. *Remote Sensing of Environment*, 243, 111792. <https://doi.org/10.1016/j.rse.2020.111792>
- Plug, L. J., Walls, C., & Scott, B. M. (2008). Tundra lake changes from 1978 to 2001 on the Tuktoyaktuk Peninsula, western Canadian Arctic. *Geophysical Research Letters*, 35(3). <https://doi.org/10.1029/2007GL032303>
- Pohl, S., Marsh, P., Onclin, C., & Russell, M. (2009). The summer hydrology of a small upland tundra thaw lake: Implications to lake drainage. *Hydrological Processes*, 23(17), 2536–2546. <https://doi.org/10.1002/hyp.7238>
- Porter, C., Morin, P., Howat, I., Noh, M. J., Bates, B., Peterman, K., Scott, K., & Schlenk, M. (2018). *ArcticDEM*. Harvard Dataverse, V1. <https://doi.org/10.7910/DVN/OHHUKH>
- Rampton, V. N. (1987). *Surficial geology, Tuktoyaktuk Coastlands, District of Mackenzie, Northwest Territories*. Geological Survey of Canada, Map 1647A, scale 1:500,000, 1 sheet [Map]. doi:10.4095/125160
- Roach, J. K., Griffith, B., & Verbyla, D. (2013). Landscape influences on climate-related lake shrinkage at high latitudes. *Global Change Biology*, 19(7), 2276–2284. <https://doi.org/10.1111/gcb.12196>
- Rover, J., Ji, L., Wylie, B. K., & Tieszen, L. L. (2012). Establishing water body areal extent trends in interior Alaska from multi-temporal Landsat data. *Remote Sensing Letters*, 3(7), 595–604. <https://doi.org/10.1080/01431161.2011.643507>
- Schuur, E. a. G., McGuire, A. D., Schädel, C., Grosse, G., Harden, J. W., Hayes, D. J., Hugelius, G., Koven, C. D., Kuhry, P., Lawrence, D. M., Natali, S. M., Olefeldt, D., Romanovsky, V. E.,

- Schaefer, K., Turetsky, M. R., Treat, C. C., & Vonk, J. E. (2015). Climate change and the permafrost carbon feedback. *Nature*, *520*(7546), 171–179. <https://doi.org/10.1038/nature14338>
- Segal, R. A., Lantz, T. C., & Kokelj, S. V. (2016). Acceleration of thaw slump activity in glaciated landscapes of the Western Canadian Arctic. *Environmental Research Letters*, *11*(3), 034025. <https://doi.org/10.1088/1748-9326/11/3/034025>
- Smith, D. G. (1994). Glacial lake McConnell: Paleogeography, age, duration, and associated river deltas, mackenzie river basin, western Canada. *Quaternary Science Reviews*, *13*(9), 829–843. [https://doi.org/10.1016/0277-3791\(94\)90004-3](https://doi.org/10.1016/0277-3791(94)90004-3)
- Smith, L. C., Sheng, Y., MacDonald, G., M., & Hinzman, L. D. (2005). Disappearing Arctic Lakes. *Science*, *208*, 1429–1431.
- Smol, J. P., & Douglas, M. S. V. (2007). Crossing the final ecological threshold in high Arctic ponds. *Proceedings of the National Academy of Sciences*, *104*(30), 12395–12397. <https://doi.org/10.1073/pnas.0702777104>
- Swanson, D. K. (2019). Thermokarst and precipitation drive changes in the area of lakes and ponds in the National Parks of northwestern Alaska, 1984–2018. *Arctic, Antarctic, and Alpine Research*, *51*(1), 265–279. <https://doi.org/10.1080/15230430.2019.1629222>
- Tarnocai, C., Canadell, J. G., Schuur, E. a. G., Kuhry, P., Mazhitova, G., & Zimov, S. (2009). Soil organic carbon pools in the northern circumpolar permafrost region. *Global Biogeochemical Cycles*, *23*(2). <https://doi.org/10.1029/2008GB003327>
- Travers-Smith, H., Lantz, T. C., & Fraser, R. H. (In Review). Surface Water Dynamics and Rapid Lake Drainage in the Western Canadian Subarctic. *Journal of Geophysical Research: Biogeosciences*.
- Turner, K. W., Wolfe, B. B., Edwards, T. W. D., Lantz, T. C., Hall, R. I., & Larocque, G. (2014). Controls on water balance of shallow thermokarst lakes and their relations with catchment characteristics: A multi-year, landscape-scale assessment based on water isotope tracers and remote sensing in Old Crow Flats, Yukon (Canada). *Global Change Biology*, *20*(5), 1585–1603. <https://doi.org/10.1111/gcb.12465>
- Walter, K. M., Zimov, S. A., Chanton, J. P., Verbyla, D., & Chapin, F. S. (2006). Methane bubbling from Siberian thaw lakes as a positive feedback to climate warming. *Nature*, *443*(7107), 71–75. <https://doi.org/10.1038/nature05040>
- Wang, L., Jolivel, M., Marzahn, P., Bernier, M., & Ludwig, R. (2018). Thermokarst pond dynamics in subarctic environment monitoring with radar remote sensing. *Permafrost and Periglacial Processes*, *29*(4), 231–245. <https://doi.org/10.1002/ppp.1986>
- Warnes, G. R., Bolker, B. M., Lumley, T., & Johnson, R. C. (2018). *Gmodels: Various R Programming Tools for Model Fitting. R package version 2.18.1*. <https://CRAN.R-project.org/package=gmodels>

- Watts, J. D., Kimball, J. S., Jones, L. A., Schroeder, R., & McDonald, K. C. (2012). Satellite Microwave remote sensing of contrasting surface water inundation changes within the Arctic–Boreal Region. *Remote Sensing of Environment*, *127*, 223–236.  
<https://doi.org/10.1016/j.rse.2012.09.003>
- Wickham, H. (2016). *ggplot2: Elegant Graphics for Data Analysis* (3rd ed.). Springer-Verlag.
- Wickham, H., François, R., Henry, L., & Kirill, M. (2020). *Dplyr: A Grammar of Data Manipulation. R package version 0.8.5*. <https://CRAN.R-project.org/package=dplyr>
- Wickham, H., & Henry, L. (2020). *Tidyr: Tidy Messy Data. R package version 1.0.2*. <https://CRAN.R-project.org/package=tidyr>
- Wolfe, S. A., & Kerr, D. E. (2014). *Surficial geology, Yellowknife area, Northwest Territories, parts of NTS 85-J/7, NTS 85-J/8, NTS 85-J/9 and NTS 85-J/10* [Map]. Natural Resources Canada. doi.org/10.4095/293725
- Wolfe, Stephen A., Morse, P. D., Kokelj, S. V., & Gaanderse, A. J. (2017). Great Slave Lowland: The Legacy of Glacial Lake McConnell. In O. Slaymaker (Ed.), *Landscapes and Landforms of Western Canada* (pp. 87–96). Springer International Publishing.  
[https://doi.org/10.1007/978-3-319-44595-3\\_5](https://doi.org/10.1007/978-3-319-44595-3_5)
- Yoshikawa, K., Bolton, W. R., Romanovsky, V. E., Fukuda, M., & Hinzman, L. D. (2002). Impacts of wildfire on the permafrost in the boreal forests of Interior Alaska. *Journal of Geophysical Research: Atmospheres*, *107*(D1), FFR 4-1-FFR 4-14.  
<https://doi.org/10.1029/2001JD000438>
- Yoshikawa, K., & Hinzman, L. D. (2003). Shrinking thermokarst ponds and groundwater dynamics in discontinuous permafrost near council, Alaska. *Permafrost and Periglacial Processes*, *14*(2), 151–160. <https://doi.org/10.1002/ppp.451>
- Yukon Ecoregions Working Group. (2004). *Eagle Plains*. Agriculture and Agri-Food Canada, PARC Technical Bulletin No. 04-01,.
- Zeileis, A., & Grothendieck, G. (2005). zoo: S3 Infrastructure for Regular and Irregular Time Series. *Journal of Statistical Software*, *14*(6), 1–27.
- Zeileis, Achim. (2004). Implementing a Class of Structural Change Tests: An Econometric Computing Approach. *Computational Statistics & Data Analysis*, *50*, 2987–3008.
- Zipper, S. C., Lamontagne-Hallé, P., McKenzie, J. M., & Rocha, A. V. (2018). Groundwater Controls on Postfire Permafrost Thaw: Water and Energy Balance Effects. *Journal of Geophysical Research: Earth Surface*, *123*(10), 2677–2694.  
<https://doi.org/10.1029/2018JF004611>

## **Appendix 3: Regional Study Areas**

### **A. Tuktoyaktuk Coastal Plain**

This study area is located in the Southern Arctic in the upland tundra to the east of the Mackenzie River Delta. This landscape has low relief and is covered by thousands of lakes, small ponds and wetlands (Ecosystem Classification Group, 2012). The entire study area is underlain by continuous permafrost with relatively high ice-content, and thermokarst features such as pingos, thermokarst lakes and ice-wedge polygons are common (Burn & Kokelj, 2009). Surficial deposits consist primarily of glaciolacustrine and glaciofluvial sediments (Rampton, 1987). Regional vegetation is dominated by upright and dwarf shrub tundra and sedge-moss wetlands with isolated stands of white spruce located at the southern edge of this ecoregion (Ecosystem Classification Group, 2012).

### **B. Lower Mackenzie Plain**

The Lower Mackenzie Plain is located southeast of the Mackenzie Delta near the community of Tsiigehtchic. This study area is composed of two distinct ecoregions: the Arctic Red Plain and the Travaillant Uplands (Ecosystem Classification Group, 2009). The low-lying Arctic Red Plain is located adjacent to the Mackenzie River and is characterized by dense black spruce forest and upright shrublands interspersed with extensive peatlands (Ecosystem Classification Group, 2009). Surficial deposits in this area a patchwork of till blanket, with silty fluvial deposits and organic peatlands adjacent to the Mackenzie River (Hughes et al., 1972). The Travaillant Uplands are located at higher elevations and are characterized by white spruce forests underlain by bedrock with a thin veneer of glacial till (Ecosystem Classification Group, 2009). Forest fire is also common in this area and 41% of the study area has burned since 1965.

### **C. Eagle Plains**

This study area is located in the Yukon Territory to the west of the maximal extent of the Laurentide ice sheet and is dominated by sandstone and siltstone deposits (Norris, 1984). The Eagle Plains are located in an intermontane basin bordered by the Richardson Mountains to the east and north and the Ogilvie Mountains to the south and west. Lakes are common in the floodplains of the Whitestone, Porcupine and eagle rivers (Yukon Ecoregions Working Group, 2004). Active layer thickness in this area varies depending on soil conditions, ranging from 30-

50cm in vegetated colluvial deposits to 2.5-3m beneath exposed bedrock (French, 2017).

Vegetation in this area is characterized by black and white spruce woodlands at low elevation and shrub tundra at higher elevations (French, 2017; Yukon Ecoregions Working Group, 2004).

#### **D. Central Mackenzie Valley**

This study area is located in the Central Mackenzie Valley at the intersection of the Taiga Plains and Taiga Cordillera. It is within the discontinuous permafrost zone and consists of low-elevation plains in the centre of the study site and upland terrain in the northern and southern parts of the study area. The majority of the lakes in this region are located within the North Mackenzie Plain ecoregion, but smaller ponds are also scattered in the Mackenzie Foothills ecoregion to the southwest, and the Great Bear Upland ecoregion to the northeast (Ecosystem Classification Group, 2009). The North Mackenzie Plain ecoregion is strongly influenced by the Mackenzie River and surficial deposits consist primarily of lacustrine, alluvial and glaciofluvial deposits (Fulton, 1995). Vegetation in this region is strongly influenced by fire, and regenerating shrub tundra dominated by dwarf birch and green alder is common (Ecosystem Classification Group, 2009).

#### **E. Bulmer Plain**

This study area is located to the west of Yellowknife and Great Slave Lake and is within the Taiga Plains. The majority of this area is within the Bulmer Plain ecoregion and is underlain by discontinuous permafrost. This region is characterized by low elevation plains and numerous lakes, limestone deposits in the eastern part of the study area create a dense network of shallow ponds high in calcium carbonate (Ecosystem Classification Group, 2009). Analysis of satellite imagery shows that thermokarst terrain including peat plateaus, collapse scars and bogs are common in this area (Gibson et al., n.d.). Forest fires are extensive and 76% of the study area was burned in two fires in 1994 and 1995. Vegetation cover across the study area is dominated by regenerating white spruce, black spruce and jackpine forests (Ecosystem Classification Group, 2009).

#### **F. Great Slave Upland**

This study area is located in the Taiga Shield north of Yellowknife and Great Slave Lake. The majority of this area is within the Great Slave Upland ecoregion and is characterized by low-relief and poorly drained bedrock (Paul et al., 2021). Lithalás, a permafrost feature formed from

aggrading ice-rich permafrost, are also common in lowland areas (Wolfe et al., 2017). Much of this region was glaciated and subsequently inundated by Lake McConnell between 13,000 and 9500 years ago (Wolfe et al., 2017). As a result, pockets of fine-grained glaciolacustrine and lacustrine sediments are common between rocky outcrops (Wolfe & Kerr, 2014; Wolfe et al., 2017). Vegetation in this region consists primarily of scattered stands of black spruce in hummocky terrain and birch and white spruce forests in warmer, well-drained soils (Paul et al., 2021). Permafrost in this area is discontinuous and located primarily in forested areas (Paul et al., 2021).

#### Appendix 4: Change in permanent surface water

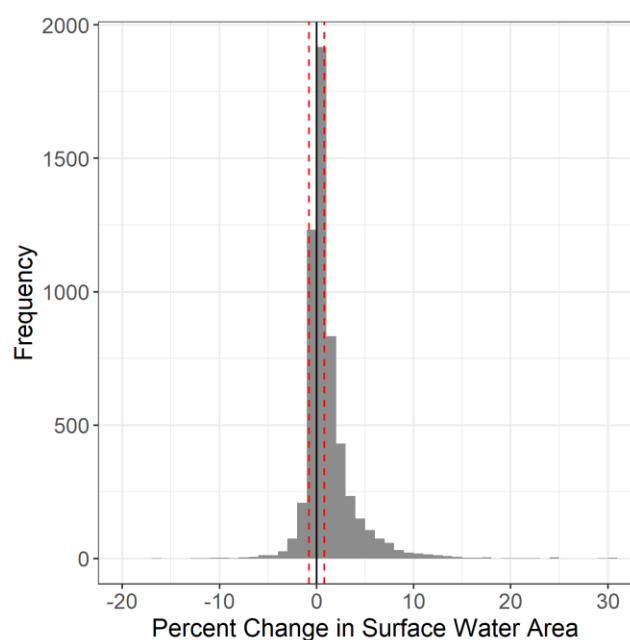


Figure 12: Histogram of net change in permanent surface water within 10x10km grid cells. Increasing and decreasing classes were defined using the median absolute percent change in surface water area. Thresholds for increasing and decreasing classes are shown as red dashed lines.

### Appendix 5: Rapid Lake Drainage

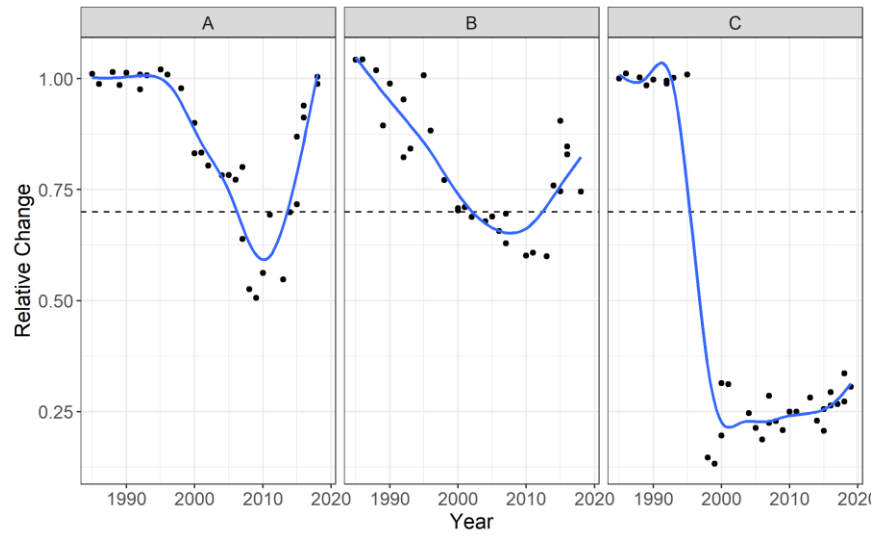


Figure 13 Examples of annual lake area time series showing gradual drainage followed by expansion (ie bi-directional change shown in A and B) and rapid permanent drainage (C). The horizontal line shows a 30% decrease in lake area relative to average lake area between 1985 and 1990.

## 4. Conclusion

### 4.1 Study Synthesis

Rising temperatures and increasing precipitation are driving a range of biophysical changes at high latitudes (ACIA, 2004). In particular, climate change can facilitate widespread change in the number and size of northern lakes and ponds (Jones et al., 2011; Lantz & Turner, 2015; Lindgren et al., 2021; Nitze et al., 2017, 2020). The direction and magnitude of change in northern lakes likely depends on the interaction between climate change and fine-scale terrain characteristics (Carroll & Loboda, 2017; Roach et al., 2013; Travers-Smith et al., In Review; Wang et al., 2018) The objectives of my MSc thesis were to better understand how northern lakes and ponds are responding to climate change and how these effects are mediated by terrain factors. In Chapters 2 and 3 of this thesis I completed two research projects to explore climatic and terrain drivers of change in surface water dynamics across the western Canadian Arctic.

In Chapter 2, I focused my analysis on the Lower Mackenzie Plains, Northwest Territories, Canada. This study area is located within the Gwich'in Settlement Area and includes the Gwichya Gwich'in community of Tsiigehtchic. In my analysis I used the Landsat satellite archive to map interannual changes in 5328 lakes between 1985 and 2020. Generalized Additive Models were used to test the effects of spring and summer climate variables on lake area and Chi-Square tests were employed to assess links between increasing and decreasing trends and lake properties and terrain factors. Despite significant increases in summer precipitation, I observed a 1% decrease in total lake area, which was driven by the rapid drainage of large lakes. My analysis also shows that 27% of lake area losses can be attributed to rapid drainage events in five large lakes and suggests that thermokarst processes are an important contributor to lake area change in this region. In particular, lakes located in fire scars were 3.8x more likely to show a

decreasing trend in area. Analysis of a large fire that burned in 1999 also indicates that lakes within the burned area exhibited declines in area that persisted for 20 years after the fire. These findings highlight the importance of rapid non-linear changes in northern lakes and provides a detailed account of the timing and magnitude of lake area changes associated with wildfire in a Sub-Arctic ecosystem.

In Chapter 3 I analyzed changes in surface water across the western Canadian Arctic and Sub-Arctic. I used the Global Surface Water dataset developed by the GLAD research group to map changes in total permanent water from 1999 to 2020 across a 1.4million km<sup>2</sup> study domain covering five distinct ecoregions: the Taiga Plains, the Taiga Cordillera, the Southern Arctic, the Taiga Shield and the Boreal Cordillera. I trained a Random Forests model to analyze the relative importance and impact of several terrain and climate variables in predicting the direction of change. Next, I selected six smaller study regions and analyzed changes within individual lakes using the methods developed in Chapter 2. I also identified the frequency and impact of rapid lake drainage events on overall surface water change and explored the effects of wildfire on lake area within four boreal study areas. Overall, I found that the area of total permanent water increased by approximately 1% between 1999 and 2020 across the entire study domain and that the direction of change in surface water was largely determined by surficial geology and ground ice content. Regional analyses corroborate these findings, with increasing surface water area observed in five of the six study areas. My analysis also shows that the presence of wildfire is strongly associated with persistent declines in lake area across in the four Boreal study areas, consistent with results from Chapter 2.

Overall, my research shows that the effects of climate change on surface water depend on complex interactions between lake size, terrain controls and wildfire. Changes in surface water

are concerning because they have the potential to impact local livelihoods (GRRB, 2018). For example, lake drainage can result in a loss of habitat for lake fish and waterfowl and drained basins develop different vegetation communities compared to the surrounding landscape (Harris et al., 2012; Lantz, 2017; Roach & Griffith, 2015). Lake expansion through shoreline erosion and lake drainage also impacts lake chemistry and water quality (Tondu et al., 2016). Understanding the terrain and climate drivers of lake surface area is important to identify areas that are more vulnerable to change and will contribute to our understanding of the impacts that changes in lake area will have on wildlife habitat and freshwater resources.

## **4.2 Limitations and Future Research Opportunities**

My thesis provides several important insights about the impact of climate change on lakes and ponds in the Arctic and Sub-Arctic, but additional research is needed to identify fine-scale biophysical processes driving lake area change, and understand the contributions of seasonal precipitation, groundwater hydrology, and within-year variation in lake area.

Results from Chapters 2 and 3 show that fire is an important driver of non-linear decreases in lake area, but additional research is needed to explore the mechanisms of change and interactions between fire, permafrost conditions and change in lake area. In particular, our analysis was limited to remotely sensed data, and did not include any measurements taken in the field. To better understand lake area responses to wildfire, future research could pair remote sensing with measurements of ground temperature and active layer depth within drained lake basins and adjacent to lakes impacted by wildfire. Other forms of remote sensing data such as repeated LIDAR surveys and thermal imaging would also help map changes in permafrost conditions and ground temperature following fire. Kokelj et al., (2009) show that active layer deepening following wildfire can increase the concentration of ions in nearby lakes. In the Old

Crow Flats, the rapid drainage of Zelma Lake lead to increased nutrient and ion concentrations and a different composition of algal pigments in the residual water body (Tondu et al., 2016). Additional research on the relationship between fire, thermokarst processes and lake water quality will also contribute to our understanding of changes in wildlife habitat and freshwater supply.

Additional field-based studies are also needed to link remote sensing observations with hydrological processes. In Chapter 3 I showed that regions with greater precipitation were more likely to exhibit an increase in surface water area, and regions with warmer annual temperatures were more likely to show decreases in surface water. However, the response of individual lakes to precipitation and temperature is mediated by regional vegetation characteristics (Turner et al., 2014), and connectivity to other lakes (Woo & Guan, 2006). Changes in land-cover due to permafrost thaw can also impact runoff and moisture inputs into water bodies (Connon et al., 2014; Haynes et al., 2019).

Other limitations of this research stem from the temporal and spatial resolution of the Landsat remote sensing data. Lake area can change significantly within a single year in response to periods of drought or increased precipitation (Cooley et al., 2019; Pohl et al., 2009; Turner et al., 2014). Recent research by Cooley et al. (2019) shows that within a single year lake area can decline significantly from May to September, making interannual time-series data sensitive to differences in data acquisition dates between years. To account for seasonal variation in water levels in Chapters 2 and 3 I restricted Landsat scenes to those acquired in July and August, and preferentially selected scenes from July 15 to August 15. I also used a 5-point rolling mean to investigate long-term patterns in total lake area, further minimizing the impact of within-year variation. The revisit time for Landsat acquisitions is approximately every 16 days, however

smoke and clouds can reduce data availability considerably, making it challenging to maintain a balanced sample of Landsat acquisition dates. As the accessibility of very high temporal resolution data increases (i.e. CubeSat with 5-day revisit time) there will be greater opportunities to investigate within-year water dynamics that are not possible to capture with Landsat data.

Although the 30m spatial resolution of Landsat data is advantageous for mapping over large regions, lake area can also vary at fine-spatial scales. As such, it is possible to miss the contributions of smaller water bodies to overall change. In Chapter 2 our validation of the sub-pixel water fraction method showed that mapping error increases as lake area decreases, and that the sub-pixel water fraction method was not able to consistently detect lakes smaller than 1500m<sup>2</sup> (approximately two Landsat pixels). Similarly, Muster et al., (2013) show that 30m Landsat data consistently underestimates the number of water bodies and total surface water area compared to data of 2m resolution, or finer. Due to this limitation, the early stages of lake development and initial ponding within low-centre polygons are not likely to be captured. The 30m resolution of the Landsat satellite archive also contributes to uncertainties in water fraction along lake margins where pixels cover both land and water. The sub-pixel water fraction method attempts to map the fractional coverage of water within a pixel using a linear interpolation between shortwave infrared reflectance (SWIR) values representing 100% land and water. While the sub-pixel water fraction method has been shown to outperform binary land/water classifications (Olthof et al., 2015), this is likely an overly simplified model as SWIR reflectance can vary depending on vegetation and soil moisture content (Roach et al., 2012). Interannual differences in moisture content in vegetation along lake margins may contribute to mapping error. These issues can be addressed by validating lake area estimates using higher resolution imagery or by using ancillary weather data to avoid selecting Landsat scenes during periods of

drought or intense precipitation. Emergent vegetation along lake margins and floating vegetation within the lake can also obscure the underlying water and lead to smaller estimates of lake area. Lakes impacted by emergent vegetation could be identified using the green or near-infrared bands to mask out vegetation and remotely sensed radar data could be used to validate estimates of lake area as the longer radar wavelengths are better able to penetrate vegetation (Whitcomb et al., 2009).

It is also possible that beaver activity contributed to observed changes in lake area in the areas explored in my thesis. Recent studies show that beaver range expansion in the Arctic can drive significant changes in surface water (Jones, et al., 2020; Jung et al., 2016; Tape et al., 2018). Beaver dams can increase surface water by flooding drained lake basins and damming lake outlets and beaded streams (Jones et al., 2020). On the Baldwin Peninsula, Alaska 66% of increases in surface water area were attributed to beaver dams (Jones et al., 2020). Other studies have associated beaver dams with thermokarst processes including the formation and degradation of palsas mounds (Lewkowicz & Coultish, 2004) as well as lake expansion and drainage (Tape et al., 2018). Local observations indicate that beaver populations in the Mackenzie Delta are increasing (Turner et al., 2018). To explore the possible influence of beavers on surface water in more detail, future studies should compile ground-based and aerial observations of beaver activity in other parts of the western Canadian Arctic.

## Bibliography

- ACIA. (2004). *Impacts of a Warming Arctic: Arctic Climate Impact Assessment*. Cambridge University Press.
- Carroll, M. L., & Loboda, T. V. (2017). Multi-Decadal Surface Water Dynamics in North American Tundra. *Remote Sensing*, 9(5), 497. <https://doi.org/10.3390/rs9050497>
- Connon, R. F., Quinton, W. L., Craig, J. R., & Hayashi, M. (2014). Changing hydrologic connectivity due to permafrost thaw in the lower Liard River valley, NWT, Canada. *Hydrological Processes*, 28(14), 4163–4178. <https://doi.org/10.1002/hyp.10206>
- Cooley, S. W., Smith, L. C., Ryan, J. C., Pitcher, L. H., & Pavelsky, T. M. (2019). Arctic-Boreal Lake Dynamics Revealed Using CubeSat Imagery. *Geophysical Research Letters*, 46(4), 2111–2120. <https://doi.org/10.1029/2018GL081584>
- GRRB. (2018). *Research and Management Interests for the GSA*. [http://www.grrb.nt.ca/pdf/Public%20registry/research/Research%20Interests\\_2018.pdf](http://www.grrb.nt.ca/pdf/Public%20registry/research/Research%20Interests_2018.pdf)
- Harris, L. N., Loewen, T. N., Reist, J. D., Halden, N. M., Babaluk, J. A., & Tallman, R. F. (2012). Migratory Variation in Mackenzie River System Broad Whitefish: Insights from Otolith Strontium Distributions. *Transactions of the American Fisheries Society*, 141(6), 1574–1585. <https://doi.org/10.1080/00028487.2012.713885>
- Haynes, K. M., Connon, R. F., & Quinton, W. L. (2019). Hydrometeorological measurements in peatland-dominated, discontinuous permafrost at Scotty Creek, Northwest Territories, Canada. *Geoscience Data Journal*, 6(2), 85–96. <https://doi.org/10.1002/gdj3.69>
- Jones, B. M., Grosse, G., Arp, C. D., Jones, M. C., Anthony, K. M. W., & Romanovsky, V. E. (2011). Modern thermokarst lake dynamics in the continuous permafrost zone, northern Seward Peninsula, Alaska. *Journal of Geophysical Research: Biogeosciences*, 116(G2). <https://doi.org/10.1029/2011JG001666>
- Jones, B. M., Tape, K. D., Clark, J. A., Nitze, I., Grosse, G., & Disbrow, J. (2020). Increase in beaver dams controls surface water and thermokarst dynamics in an Arctic tundra region, Baldwin Peninsula, northwestern Alaska. *Environmental Research Letters*, 15(7), 075005. <https://doi.org/10.1088/1748-9326/ab80f1>
- Jung, T. S., Frandsen, J., Gordon, D. C., & Mossop, D. H. (2016). Colonization of the Beaufort Coastal Plain by Beaver (*Castor canadensis*): A Response to Shrubification of the Tundra? *The Canadian Field-Naturalist*, 130(4), 332–335. <https://doi.org/10.22621/cfn.v130i4.1927>
- Kokelj, S. V., Zajdlik, B., & Thompson, M. S. (2009). The impacts of thawing permafrost on the chemistry of lakes across the subarctic boreal-tundra transition, Mackenzie Delta region, Canada. *Permafrost and Periglacial Processes*, 20(2), 185–199. <https://doi.org/10.1002/ppp.641>

- Lantz, T. C. (2017). Vegetation Succession and Environmental Conditions following Catastrophic Lake Drainage in Old Crow Flats, Yukon. *ARCTIC*, 70(2), 177. <https://doi.org/10.14430/arctic4646>
- Lantz, T. C., & Turner, K. W. (2015). Changes in lake area in response to thermokarst processes and climate in Old Crow Flats, Yukon. *Journal of Geophysical Research: Biogeosciences*, 120(3), 513–524. <https://doi.org/10.1002/2014JG002744>
- Lewkowicz, A. G., & Coultish, T. L. (2004). Beaver Damming and Palsa Dynamics in a Subarctic Mountainous Environment, Wolf Creek, Yukon Territory, Canada. *Arctic, Antarctic, and Alpine Research*, 36(2), 208–218. [https://doi.org/10.1657/1523-0430\(2004\)036\[0208:BDAPDI\]2.0.CO;2](https://doi.org/10.1657/1523-0430(2004)036[0208:BDAPDI]2.0.CO;2)
- Lindgren, P. R., Farquharson, L. M., Romanovsky, V. E., & Grosse, G. (2021). Landsat-based lake distribution and changes in western Alaska permafrost regions between the 1970s and 2010s. *Environmental Research Letters*, 16(2), 025006. <https://doi.org/10.1088/1748-9326/abd270>
- Muster, S., Heim, B., Abnizova, A., & Boike, J. (2013). Water Body Distributions Across Scales: A Remote Sensing Based Comparison of Three Arctic Tundra Wetlands. *Remote Sensing*, 5(4), 1498–1523. <https://doi.org/10.3390/rs5041498>
- Nitze, I., Cooley, S., Duguay, C., Jones, B. M., & Grosse, G. (2020). The catastrophic thermokarst lake drainage events of 2018 in northwestern Alaska: Fast-forward into the future. *The Cryosphere Discussions*, 1–33. <https://doi.org/10.5194/tc-2020-106>
- Nitze, I., Grosse, G., Jones, B., Arp, C., Ulrich, M., Fedorov, A., & Veremeeva, A. (2017). Landsat-Based Trend Analysis of Lake Dynamics across Northern Permafrost Regions. *Remote Sensing*, 9(7), 640. <https://doi.org/10.3390/rs9070640>
- Pohl, S., Marsh, P., Onclin, C., & Russell, M. (2009). The summer hydrology of a small upland tundra thaw lake: Implications to lake drainage. *Hydrological Processes*, 23(17), 2536–2546. <https://doi.org/10.1002/hyp.7238>
- Roach, J. K., & Griffith, B. (2015). Climate-induced lake drying causes heterogeneous reductions in waterfowl species richness. *Landscape Ecology*, 30(6), 1005–1022. <https://doi.org/10.1007/s10980-015-0207-3>
- Roach, J. K., Griffith, B., & Verbyla, D. (2012). Comparison of three methods for long-term monitoring of boreal lake area using Landsat TM and ETM+ imagery. *Canadian Journal of Remote Sensing*, 38(4), 427–440. <https://doi.org/10.5589/m12-035>
- Roach, J. K., Griffith, B., & Verbyla, D. (2013). Landscape influences on climate-related lake shrinkage at high latitudes. *Global Change Biology*, 19(7), 2276–2284. <https://doi.org/10.1111/gcb.12196>

Tape, K. D., Jones, B. M., Arp, C. D., Nitze, I., & Grosse, G. (2018). Tundra be dammed: Beaver colonization of the Arctic. *Global Change Biology*, *24*(10), 4478–4488. <https://doi.org/10.1111/gcb.14332>

Tondu, J. M. E., Turner, K. W., Wiklund, J. A., Wolfe, B. B., Hall, R. I., & McDonald, I. (2016). Limnological evolution of Zelma Lake, a recently drained thermokarst lake in Old Crow Flats (Yukon, Canada). *Arctic Science*. <https://doi.org/10.1139/as-2016-0012>

Travers-Smith, H., Lantz, T. C., & Fraser, R. H. (In Review). Surface Water Dynamics and Rapid Lake Drainage in the Western Canadian Subarctic. *Journal of Geophysical Research: Biogeosciences*.

Turner, C. K., Lantz, T. C., & Gwich'in Tribal Council Department of Cultural Heritage. (2018). Springtime in the Delta: The Socio-Cultural Importance of Muskrats to Gwich'in and Inuvialuit Trappers through Periods of Ecological and Socioeconomic Change. *Human Ecology*, *46*(4), 601–611. <https://doi.org/10.1007/s10745-018-0014-y>

Turner, K. W., Wolfe, B. B., Edwards, T. W. D., Lantz, T. C., Hall, R. I., & Larocque, G. (2014). Controls on water balance of shallow thermokarst lakes and their relations with catchment characteristics: A multi-year, landscape-scale assessment based on water isotope tracers and remote sensing in Old Crow Flats, Yukon (Canada). *Global Change Biology*, *20*(5), 1585–1603. <https://doi.org/10.1111/gcb.12465>

Wang, L., Jolivel, M., Marzahn, P., Bernier, M., & Ludwig, R. (2018). Thermokarst pond dynamics in subarctic environment monitoring with radar remote sensing. *Permafrost and Periglacial Processes*, *29*(4), 231–245. <https://doi.org/10.1002/ppp.1986>

Whitcomb, J., Moghaddam, M., McDonald, K. C., Kellndorfer, J., & Podest, E. (2009). Mapping vegetated wetlands of Alaska using L-band radar satellite imagery. *Canadian Journal of Remote Sensing*, *35*(1), 54–72.

Woo, M.-K., & Guan, X. J. (2006). Hydrological connectivity and seasonal storage change of tundra ponds in a polar oasis environment, Canadian High Arctic. *Permafrost and Periglacial Processes*, *17*(4), 309–323. <https://doi.org/10.1002/ppp.565>